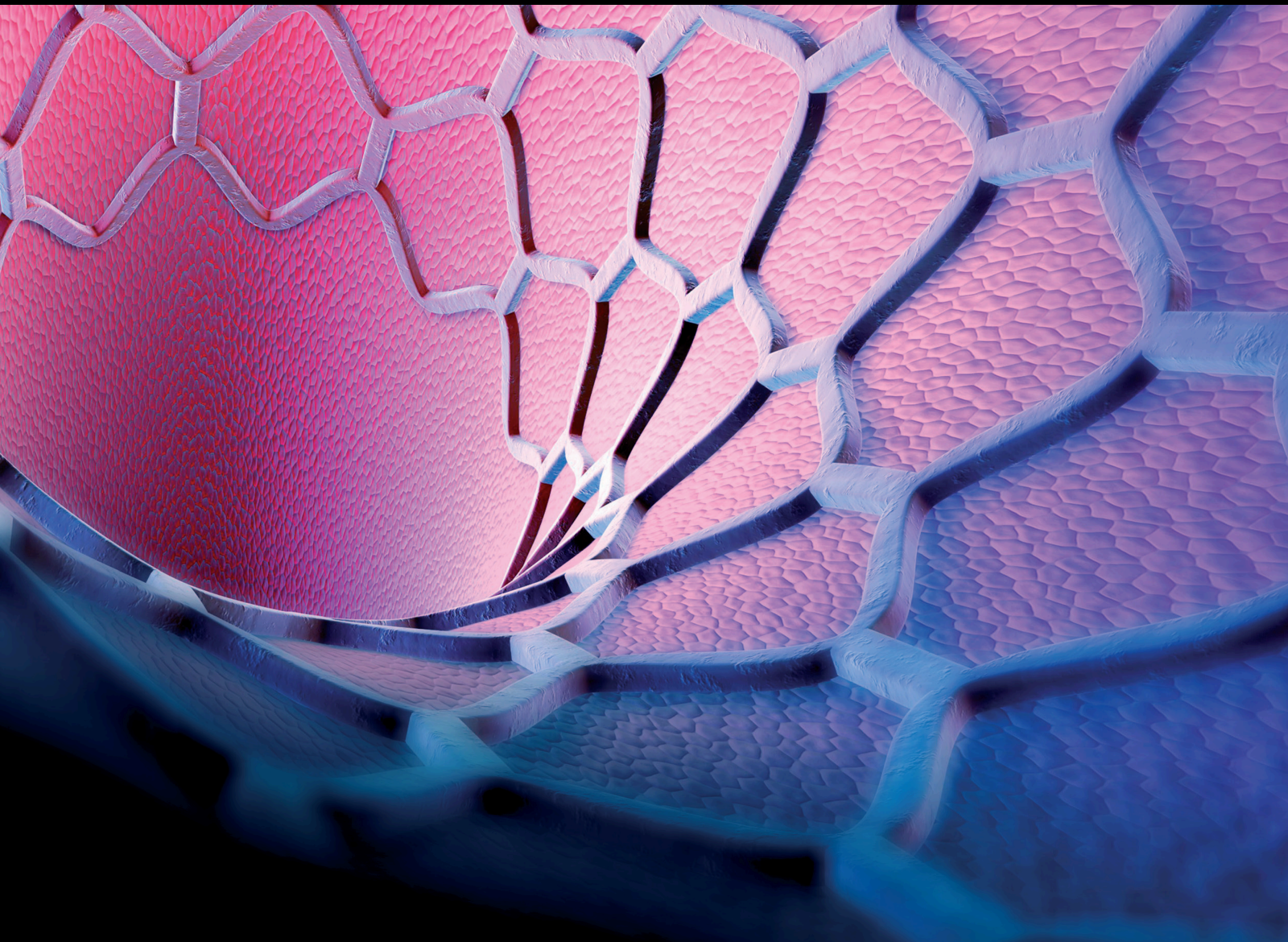
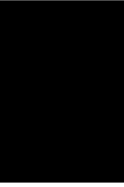


# Myocardial Microvascular Physiology in Acute and Chronic Coronary Syndromes, Aortic Stenosis, and Heart Failure

Lead Guest Editor: Alf Inge Larsen

Guest Editors: William Fearon, Todd J. Anderson, and Nico Pijls





---

**Myocardial Microvascular Physiology in Acute  
and Chronic Coronary Syndromes, Aortic  
Stenosis, and Heart Failure**



Journal of Interventional Cardiology

---

**Myocardial Microvascular Physiology  
in Acute and Chronic Coronary  
Syndromes, Aortic Stenosis, and Heart  
Failure**

Lead Guest Editor: Alf Inge Larsen

Guest Editors: William Fearon, Todd J. Anderson,  
and Nico Pijls



---

Copyright © 2022 Hindawi Limited. All rights reserved.

This is a special issue published in "Journal of Interventional Cardiology." All articles are open access articles distributed under the Creative Commons Attribution License, which permits unrestricted use, distribution, and reproduction in any medium, provided the original work is properly cited.



# Chief Editor

Patrizia Presbitero, Italy



---

## Editorial Board


Amr E. Abbas, USA  
Antonio Abbate, USA  
Konstantinos Dean Boudoulas, USA  
Jeremiah Brown, USA  
Fausto Castriota, Italy  
Periklis Davlouros, Greece  
Leonardo De Luca, Italy  
Salvatore De Rosa, Italy  
Joseph Dens, Belgium  
Seif S. El-Jack, New Zealand  
Cristina Giannini, Italy  
Paul M. Grossman, USA  
Ziyad M. Hijazi, Qatar  
William B. Hillegass, USA  
David G. Iosseliani, Russia  
Michael C. Kim, USA  
Viktor Kočka, Czech Republic  
Faisal Latif, USA  
Yuichiro Maekawa, Japan  
Piotr Musiałek, Poland  
Christian J. Mussap, Australia  
Toshiko Nakai, Japan  
Thach N. Nguyen, USA  
Vasileios Panoulas, United Kingdom  
Stefano Rigattieri, Italy  
Andrea Rubboli, Italy  
Kintur Sanghvi, USA  
Alessandro Sciahbasi, Italy  
Amit Segev, Israel  
Magnus Settergren, Sweden  
Martin J. Swaans, The Netherlands  
Matteo Tebaldi, Italy  
Leo Timmers, The Netherlands  
Jan-Peter van Kuijk, The Netherlands  
Luigi Vignali, Italy  
Jochen Wöhrle, Germany  
Ming-Ming Wu, China  
Shenghua Zhou, China

# Contents




## **Myocardial Microvascular Physiology in Acute and Chronic Coronary Syndromes, Aortic Stenosis, and Heart Failure**

Alf I. Larsen , William F. Fearon, Todd J. Anderson , and Nico Pijls  
Editorial (7 pages), Article ID 9846391, Volume 2022 (2022)


## **Transthoracic Assessment of Coronary Flow Velocity Reserve: A Practical Approach to Diagnostic Testing in Patients with Angina and No Obstructive Coronary Artery Disease**

Daria Frestad Bechsgaard  and Eva Prescott  
Review Article (8 pages), Article ID 6689312, Volume 2021 (2021)

## **Thermodilution-Based Invasive Assessment of Absolute Coronary Blood Flow and Microvascular Resistance: Quantification of Microvascular (Dys)Function?**

Daniëlle C. J. Keulards , Mohamed El Farissi , Pim A. L. Tonino , Koen Teeuwen, Pieter-Jan Vlaar, Eduard van Hagen, Inge. F. Wijnbergen, Annemiek de Vos, Guus R. G. Brueren, Marcel van't Veer, and Nico H. J. Pijls  
Review Article (7 pages), Article ID 5024971, Volume 2020 (2020)

## **Coronary Microcirculation in Aortic Stenosis: Pathophysiology, Invasive Assessment, and Future Directions**

Jo M. Zelis, Pim A. L. Tonino, Nico H. J. Pijls, Bernard De Bruyne, Richard L. Kirkeeide, K. Lance Gould, and Nils P. Johnson   
Review Article (13 pages), Article ID 4603169, Volume 2020 (2020)



## **Rate Pressure Products Affect the Relationship between the Fractional Flow Reserve and Instantaneous Wave-Free Ratio**

Suguru Ebihara, Hisao Otsuki, Hiroyuki Arashi , Junichi Yamaguchi, and Nobuhisa Hagiwara  
Research Article (8 pages), Article ID 6230153, Volume 2020 (2020)



## Editorial

# Myocardial Microvascular Physiology in Acute and Chronic Coronary Syndromes, Aortic Stenosis, and Heart Failure

Alf I. Larsen <sup>1</sup>, William F. Fearon,<sup>2</sup> Todd J. Anderson <sup>3</sup> and Nico Pijls<sup>4</sup>

<sup>1</sup>Department of Cardiology, Stavanger University Hospital, University of Bergen, Stavanger, Norway

<sup>2</sup>Stanford University, Stanford, CA, USA

<sup>3</sup>Libin Cardiovascular Institute, Cumming School of Medicine, University of Calgary, Calgary, Canada

<sup>4</sup>Catharina Hospital, Eindhoven, Netherlands

Correspondence should be addressed to Alf I. Larsen; [alf.inge.larsen@sus.no](mailto:alf.inge.larsen@sus.no)

Received 28 July 2021; Accepted 28 July 2021; Published 22 January 2022

Copyright © 2022 Alf I. Larsen et al. This is an open access article distributed under the Creative Commons Attribution License, which permits unrestricted use, distribution, and reproduction in any medium, provided the original work is properly cited.

Myocardial ischemia occurs when myocardial oxygen demand exceeds the coronary blood supply. The etiology is usually atherosclerotic obstructive epicardial coronary artery disease (CAD) presenting with the features of chronic coronary syndrome (CCS). Fractional flow reserve (FFR) has become the gold standard for assessing myocardial ischemia due to coronary artery stenosis. As demonstrated in the DEFER study, long-term prognosis after deferral of PCI of an intermediate coronary stenosis based on  $\text{FFR} \geq 0.75$  is excellent. The risk of cardiac death or myocardial infarction related to this stenosis is <1% per year and not decreased by stenting [1]. In the FAME study, it was shown that routine guidance of revascularization with measurement of FFR in patients with multivessel coronary artery disease, who are undergoing PCI with drug-eluting stents, significantly reduced the rate of the composite endpoint of death, nonfatal myocardial infarction, and repeat revascularization at 1 year [2]. In the FAME 2 trial, the investigators extended their findings by showing that in patients with stable coronary artery disease, FFR-guided PCI, as compared with medical therapy alone, improved the outcome. Furthermore, patients without ischemia had a favorable outcome with medical therapy alone [3].

These studies are dependent on the use of full hyperemia using vasodilating agents like adenosine. As a non-hyperemic surrogate to FFR, the so-called instantaneous wave-free ratio (iFR) and a number of comparable non-hyperemic pressure indices have been proposed [4]. Although these indices have been demonstrated to be noninferior to FFR in

studies in relatively low-risk patients (Define Flair [5] and Swede Heart [6]), these are not as well validated and lack the clinical outcome data existing for FFR [7]. In the current issue of the journal, Ebihara et al. explored the effect of rate pressure product (RPP) on instantaneous wave-free ratio (iFR) [8]. By adding these extra parameters, the values might be more accurate and reproducible. They found that the best cutoff value of the iFR for predicting an FFR of 0.8 was 0.90 for all lesions. However, when the study population was divided into the low-RPP and high-RPP groups according to the median RPP, they found different iFR values predicting an FFR of 0.8, 0.93 for the low-RPP group and 0.82 for the high-RPP group. Consequently, the RPP has been demonstrated to affect the relationship between the FFR and iFR. With FFR as the gold standard, the iFR may underestimate and overestimate the functionality of ischemia in the low- and high-RPP groups, respectively.

However, with this being said, the angiographic evidence of “normal” or mildly diseased epicardial coronary arteries, usually defined as the absence of a luminal diameter reduction of <50% (or <70% of the luminal area reduction), is a common finding. This condition is usually defined as ischemia with no obstructive coronary artery (INOCA) disease and is likely related to the so-called coronary microcirculatory or microvascular dysfunction (CMD). Angina with no obstructive coronary arteries (ANOCAs) is the clinical term when a clinical diagnosis of ischemia is made in a patient without significant obstructive coronary artery disease, without the necessity of having demonstrated

inducible ischemia. In reported studies on ANOCA, ischemia has been demonstrated in approximately 50% of the patients. Nevertheless, the two terms INOCA and ANOCA are often interchangeably used.

## 1. Epidemiology

Up to 40% of patients undergoing coronary angiography with signs and symptoms of angina pectoris are characterized with INOCA [9]. In the American College of Cardiology National Cardiovascular Data Registry from January 2004 through April 2008, at 663 hospitals, slightly more than one-third of patients without known disease who underwent elective cardiac catheterization had obstructive coronary artery disease. The authors of this report suggested better strategies for risk stratification to inform decisions and to increase the diagnostic yield of cardiac catheterization in routine clinical practice [7]. Moreover, estimates from the WISE database indicate that there are at least 3-4 million patients in the USA with signs and symptoms of ischemia despite no evidence of obstructive CAD [10]. However, this might be an old fashion approach to the problem of recurrent angina. In patients with residual angina or recurrence of angina after percutaneous coronary intervention (PCI), functional mechanisms are responsible for the vast majority of cases [11]. The large proportion of patients with angina and near-normal or normal coronary angiogram is thus a large challenge for the cardiology society because a vast number of patients are not appropriately diagnosed. Recently, a large study using intracoronary flow wires in 151 patients with INOCA demonstrated microvascular dysfunction in approximately 75% of the patients [12].

## 2. Definition

In 1988, Cannon and Epstein proposed that dysfunction of small intramural prearteriolar coronary arteries might be the pathogenic cause of a syndrome introduced as “microvascular angina” (MVA) in this patient population. This condition was characterized by heightened sensitivity of the coronary microcirculation to vasoconstrictor stimuli and a limited microvascular vasodilator capacity [13], mainly caused by dysfunction of small intramural prearteriolar coronary arteries [14]. Tests to identify this syndrome are typically performed using mediators of full hyperemia—adenosine or dipyridamole. However, functional etiology for angina also comprises endothelial dysfunction-associated vasospasm of large epicardial arteries. In 1959, Prinzmetal and his colleagues described a syndrome characterized by angina at rest, with transient ST-segment elevation, in patients with diseased coronary arteries [15].

This might be diagnosed during provocation tests with acetylcholine during coronary angiography. Acetylcholine binds vascular muscarinic acetylcholine receptors inducing endothelial NO release with subsequent arterial dilatation when endothelial function is intact. However, in the presence of endothelial dysfunction, acetylcholine induces conduit vessel arterial constriction due to direct smooth muscle cell constriction.

Reproduction of typical symptoms, ECG changes, and angiographically verified vasospasm is diagnostic [16]. Unlike the focal spasm and ST elevation seen with classic Prinzmetal’s angina, diffuse vasospasm is the usual pattern with endothelial dysfunction detected with acetylcholine. In the CorMica study, a vasospastic pattern was seen in about ¼ of the INOCA cohort [17]. Many subjects will have both microvascular and conduit vessel abnormalities. Finally, typical symptoms and ECG alterations might also occur without obvious changes of the coronary angiogram in response to acetylcholine indicating small-vessel vasospasm. All of these conditions are more or less associated with the progressive process of coronary atherosclerosis initiated by endothelial dysfunction. It is also important for clinicians to be aware that the vast majority of patients presenting with chest pain and minimal CAD do have an underlying abnormality of coronary vasomotion even if they do not have manifest ischemia on noninvasive testing. This is still not widely recognized amongst the cardiology community. Interventional cardiologists doing diagnostic procedures are critical in conveying this message to patients and referring physicians.

In addition, in a substantial proportion of patients with acute coronary syndromes, normal or near-normal coronary angiograms are found [18]. This condition is known as myocardial infarction with no obstructive coronary arteries (MINOCAs). Moreover, microvascular dysfunction is a major player in the no-reflow phenomenon in primary percutaneous coronary intervention (PCI) for STEMI [19]. However, in this issue, we focus on the microvascular dysfunction described above.

## 3. Etiology

Risk factors for MVD are the same as for CCS. Endothelial dysfunction is the first step in this process, and inflammation is central in the progression of the disease. Patients with coronary endothelial dysfunction are recognized to have significant health service use and morbidity as well as an increased risk of developing flow-limiting coronary artery disease and myocardial events, including death [20].

Additionally, recent studies have shown that especially vasospastic angina is associated with an early inflammatory coronary artery condition documented with the presence of low-grade inflammation-related endothelial dysfunction with resulting diffuse intimal thickening and impaired nitric oxide production [21]. Endothelial dysfunction, the precursor for CAD, is associated with MVD [22]. However, also nonendothelial-dependent vascular dysfunction is associated with the typical risk factors for atherosclerosis like aging [23], hypertension [24], diabetes [25], dyslipidemia, and insulin resistance [26]. The mechanisms underlying the development of MVD are thus multifactorial and only partly explained by current research.

In a small mechanistic study following PCI, both large- and small-vessel vasoconstriction were seen as manifested by a reduction in coronary conduit vessel diameter and in CBF. These effects were reversed by NTG. Serum levels of LDL were modestly related to the reduction of CBF and to the



degree of NTG-induced vasodilatation of the coronary microvasculature [27].

#### 4. Classification

In 2007, Camici and Crea presented a clinical classification with 4 subtypes of coronary microvascular dysfunction on the basis of the clinical settings in which it occurs: dysfunction occurring in the absence of CAD and myocardial diseases, dysfunction in the presence of myocardial diseases, dysfunction in the presence of obstructive epicardial CAD, and iatrogenic dysfunction [28].

The paper by Zelis et al. in the current issue sheds light on the coronary microvascular dysfunction in the presence of myocardial disease, i.e., aortic stenosis (AS) [29]. They describe the disadvantages of secondary cardiomyopathy in AS: diastolic dysfunction, insufficient capillary density, and diffuse fibrosis.

They refer to the area under the aortic (or, in situations of aortic stenosis, LV) curve during systole (systolic pressure time integral (SPTI)), which has been shown in animal models to have a very high and direct correlation with myocardial oxygen demand, even superior to the rate pressure product [30]. Furthermore, they refer to the diastolic pressure time integral (DPTI) which is an analog for "coronary perfusion pressure." The ratio of these DPTI/SPTI balances supply and demand into a single unitless ratio, although this formulation ignores other factors such as arterial oxygen content and relative LV mass and wall tension [31].

After reviewing the available literature, they found that existing data support an increase in hyperemic flow after TAVI due to a change in the myocardial load line. This change is due to a reduction in wedge pressure, largely "reflecting" LV filling pressures that fall after AS has been treated.

#### 5. Diagnosis and Methods

Established diagnostic tools for assessing microvascular disease are not readily available in most cath. labs, leaving many patients with no or a wrong diagnosis. Therefore, a growing part of the interventional cardiology community is looking for an available means to diagnose and quantify microvascular dysfunction to find the appropriate and accurate diagnosis for the individual patient.

For the last 2 decades, studies employing positron emission tomography (PET) have been used to describe the normal range of absolute myocardial blood flow (MBF, mL/min/g) and of coronary flow reserve (CFR). This is a measure of coronary circulatory capacity defined as the ratio of MBF during maximal coronary vasodilatation to baseline MBF [32].

The invasive methods presently used to assess microvascular function, CFR and Index of Microvascular Resistance (IMR), are operator dependent and are based on adenosine to induce hyperemia. In the current issue, Keullards et al. reviewed the new thermodilution-based method for the measurement of absolute coronary blood

flow and microvascular resistance [33]. The measurements are easy to perform using the Rayflow® infusion catheter and Coroventis® software. The method is accurate, reproducible, and completely operator independent and has been validated noninvasively against the current golden standard for flow assessment: PET-CT [34].

It has recently been shown that a comprehensive invasive assessment of these patients at the time of coronary angiography can be performed safely and provides important diagnostic information that may affect treatment and outcomes [35]. This should be integrated in modern invasive diagnostics in that conventional stress testing is insufficient for identifying occult coronary abnormalities that are frequently present in patients with angina in the absence of obstructive CAD. A normal noninvasive test for ischemia does not rule out a nonobstructive coronary etiology of angina, nor does it negate the need for comprehensive invasive testing [36].

In addition to PET, intracoronary Doppler measurements are considered close to the gold standard for determining CFR. However, both types of examinations are associated with a certain load of ionizing radiation in addition to the obvious invasive nature of intracoronary Doppler measurements. In the search for less-invasive methods, transthoracic Doppler echocardiography (TTDE) has emerged as a robust method to assess CRF [37].

In the current issue of the journal, Bechsgaard and Prescott described the method of TTDE for assessing coronary flow velocity reserve [38] as an established method of assessment of coronary microvascular function with a well-documented prognostic significance [39]. They review the use of adenosine infusion as a microvascular dilator by activation of A2A receptors yielding a 3- to 4-fold increase in coronary blood flow in a normal epicardial vessel [40]. Furthermore, they describe the ratio of hyperemic to resting coronary flow velocity, coronary flow velocity reserve (CFVR), as an established physiological estimate of coronary microvascular function, which is closely correlated with CFVR measured using an intracoronary Doppler guidewire in patients undergoing angiography for suspected obstructive CAD [41]. Dobutamine cMRI stress can yield useful information about wall motion abnormalities, and ischemia can be assessed using adenosine in INOCA subjects [42]. Due to the lack of radiation of both TTDE and cMRI, these methods might be particularly advantageous for young women with chest pain syndrome requiring diagnostic work-up.

#### 6. Prognosis

Patients with MVD show persistence and even worsening of symptoms over time [43], and they constitute a therapeutic problem with considerable residual morbidity associated with functional limitations and reduced quality of life in addition to the increasing economic burden of the health authority system [44]. Impaired CFR is associated with increased mortality in patients with INOCA [45, 46].

Furthermore, impaired CFR without any concomitant impairment of regional or global left ventricular function has additional prognostic significance [47]. In a large study evaluating the prognostic significance of both stress myocardial blood flow (MBF) and myocardial flow reserve (MFR) and the ratio of stress to rest MBF [48], the researchers found MFR to be substantially more consistent, regardless of the choice of input function derivation method and the extraction model used [49].

The link between MVD and flow-mediated vasodilation is further underlined in regard to prognosis in a study evaluating hyperemic velocity, the stimulus for flow-mediated dilation. Hyperemic velocity was a significant risk marker for adverse cardiovascular outcomes. The prognostic value is additive to traditional risk factors and carotid intima-media thickness [50]. This suggests that microvascular dysfunction may be systemic, and that peripheral testing may be useful in diagnosis and prognosis.

The size of the problem and the lack of therapeutic intervention justify the increasing efforts to develop diagnostic tools and to identify new treatment strategies when assessing patients with INOCA.

## 7. Treatment

Reduced physical activity is one of the major avoidance behaviours in patients with coronary heart disease [51]. On the other hand, several studies have documented the positive effect of exercise training (ET) in this population [52]. Psychological morbidity with great impact on daily living is well known in both patients with cardiovascular disease and in patients with chest pain with no obvious physical disease. This includes patients with INOCA. These patients constitute a relatively large proportion of patients taken care of by the health authority system, indicating that this issue has economic consequences for the society that is not neglectable [2].

Therefore, a major end point in the treatment of these patients is symptom control [53].

In patients with MVA, lifestyle modifications such as smoking cessation and weight loss, which are known to improve endothelial dysfunction, are as essential as in the prevention and treatment of CAD [54]. Notably, exercise training has been shown to improve symptoms in this population [55]. A small observational study also indicates that an improvement in  $VO_{2\text{ peak}}$  is associated with increased CFR and improved endothelial function. Importantly [56], these effects were followed by an improvement in quality of life [57].

Long-term treatment with carvedilol can significantly increase coronary flow reserve and reduce the occurrence of stress-induced perfusion defects, suggesting a favorable effect of the drug on coronary microvascular function in patients with IDC [58]. Additionally, Neglia and coworkers showed a beneficial effect of perindopril on coronary blood flow after 6 months of perindopril treatment. This treatment has also been shown to improve myocardial blood flow and reverse remodeling in myocardial arterioles in spontaneous hypertensive rats [59]. A large randomized multicentre,

prospective, randomized, blinded outcome study evaluating intensive medical therapy including high-intensity statins, ACE-Is or ARBs, and aspirin, vs. usual care in 4422 symptomatic women with INOCA will probably give the answer if patients with MVD should be treated as patients with CAD. A large randomized multicentre, prospective, randomized, blinded outcome study evaluating intensive medical therapy including high-intensity statins, ACE-Is or ARBs, and aspirin, vs. usual care in 4422 symptomatic women with INOCA, (Women's IschemiA TRial to Reduce Events In Non-Obstructive CAD, (WARRIOR)), will probably give the answer if patients with MVD should be treated as patients with CAD [60].

The purpose of the CorMica trial was to evaluate whether an interventional diagnostic procedure (IDP) linked to stratified medicine improves health status in patients with INOCA. Patients without angiographical obstructive CAD ( $n = 151-39\%$ ) were immediately randomized 1:1 to the intervention group (stratified medical therapy) or the control group (standard care, IDP sham procedure). The IDP consisted of guidewire-based assessment of coronary flow reserve, index of microcirculatory resistance, and fractional flow reserve, followed by vasoreactivity testing with acetylcholine. The primary endpoint was the mean difference in angina severity at 6 months. The authors concluded that stratified medical therapy, including an IDP with linked medical therapy, was routinely feasible and improved angina in patients with no obstructive CAD [17]. This strategy leads to marked and sustained angina improvement and better quality of life at 1 year following invasive coronary angiography [61]. The findings from this trial underline the need for an extended diagnostic framework when evaluating patients with INOCA. The correct diagnosis is a prerequisite for proper medical therapy and lifestyle intervention to increase quality of life in this population.

## 8. Conclusions

Microvascular dysfunction is responsible for angina in a substantial number of patients admitted for coronary angiogram. Diagnostic options are very limited in most centers, although these patients may have significant effects from cardiovascular risk reduction programs and tailored medical treatment, both in terms of symptoms and prognosis. Interventional cardiologists must lead the expansion of testing for microvascular angina so that the patients and the referring clinician have the correct diagnosis, which will aid in improved quality of life in these subjects.

## Conflicts of Interest

William Fearon receives institutional research support from Abbott, Boston, and Medtronic and have consulting relationships with CathWorks and HeartFlow. Nico Pijls receives institutional research grants from Abbott and Exacath. Nico Pijls has received consultancy fees from

Abbott and Opsons. Nico Pijls has minor equity in Philips, ASML, Heartflow, and General Electric. Todd Anderson and Alf Inge Larsen declare no conflicts of interest.

Alf I. Larsen  
William F. Fearon  
Todd J. Anderson  
Nico Pijls

## References

- [1] N. H. J. Pijls, P. van Schaardenburgh, G. Manoharan et al., "Percutaneous coronary intervention of functionally non-significant stenosis," *Journal of the American College of Cardiology*, vol. 49, no. 21, pp. 2105–2111, 2007.
- [2] P. A. L. Tonino, B. De Bruyne, N. H. J. Pijls et al., "Fractional flow reserve versus angiography for guiding percutaneous coronary intervention," *New England Journal of Medicine*, vol. 360, no. 3, pp. 213–224, 2009.
- [3] B. De Bruyne, W. F. Fearon, N. H. J. Pijls et al., "Fractional flow reserve-guided PCI for stable coronary artery disease," *New England Journal of Medicine*, vol. 371, no. 13, pp. 1208–1217, 2014.
- [4] S. Sen, J. Escaned, I. S. Malik et al., "Development and validation of a new adenosine-independent index of stenosis severity from coronary wave-intensity analysis," *Journal of the American College of Cardiology*, vol. 59, no. 15, pp. 1392–1402, 2012.
- [5] J. E. Davies, S. Sen, H. M. Dehbi et al., "Use of the instantaneous wave-free ratio or fractional flow reserve in PCI," *The New England Journal of Medicine*, vol. 376, pp. 1824–1834, 2017.
- [6] M. Götzberg, E. H. Christiansen, I. J. Gudmundsdottir, L. Sandhall, M. Danielewicz, and L. Jakobsen, "iFR-SWE-DEHEART investigators. Instantaneous wave-free ratio versus fractional flow reserve to guide PCI," *The New England Journal of Medicine*, vol. 37, no. 19, pp. 1813–1823, 2017.
- [7] M. R. Patel, J. H. Calhoun, G. J. Dehmer et al., "PKACC/AATS/AHA/ASE/ASNC/SCAI/SCCT/STS 2017 appropriate use criteria for coronary revascularization in patients with stable ischemic heart disease: a report of the American College of Cardiology appropriate use criteria task force, American Association for Thoracic Surgery, American Heart Association, American Society of Echocardiography, American Society of Nuclear Cardiology, Society for Cardiovascular Angiography and Interventions, Society of Cardiovascular Computed Tomography, and Society of Thoracic Surgeons, *J Am Coll Cardiol*, 2017, 69, 2212–2241," *Published Erratum Journal of the American College of Cardiology*, vol. 71, no. 19, pp. 2279–2280, 2018.
- [8] S. Ebihara, H. Otsuki, H. Arashi, J. Yamaguchi, and N. Hagiwara, "Rate pressure products affect the relationship between the fractional flow reserve and instantaneous wave-free ratio," *Journal of Interventional Cardiology*, vol. 21, Article ID 6230153, 2020.
- [9] M. R. Patel, E. D. Peterson, D. Dai et al., "Low diagnostic yield of elective coronary angiography," *New England Journal of Medicine*, vol. 362, no. 10, pp. 886–895, 2010.
- [10] N. B. Merz, B. D. Johnson, P. S. F. Kelsey et al., "Diagnostic, prognostic, and cost assessment of coronary artery disease in women," *The American Journal of Managed Care*, vol. 7, pp. 959–965, 2001.
- [11] G. Niccoli, R. A. Montone, G. A. Lanza, and F. Crea, "Angina after percutaneous coronary intervention: the need for precision medicine," *International Journal of Cardiology*, vol. 248, pp. 14–19, 2017.
- [12] T. J. Ford, E. Yü, N. Sidik et al., "Ischemia and no obstructive coronary artery disease: prevalence and correlates of coronary vasomotion disorders," *Circulation. Cardiovascular Interventions*, vol. 12, Article ID e008126, 2019.
- [13] R. O. Cannon 3rd and S. E. Epstein, "'Microvascular angina' as a cause of chest pain with angiographically normal coronary arteries," *The American Journal of Cardiology*, vol. 61, no. 15, pp. 1338–1343, 1988.
- [14] S. E. Epstein and R. O. Cannon, "Site of increased resistance to coronary flow in patients with angina pectoris and normal epicardial coronary arteries," *Journal of the American College of Cardiology*, vol. 8, no. 2, pp. 459–461, 1986.
- [15] M. Prinzmetal, M. Kenamer, R. Merliss et al., "Angina pectoris I. A variant form of angina pectoris," *The American Journal of Medicine*, vol. 27, no. 3, pp. 375–388, 1959.
- [16] D. S. Baim, "Coronary angiography," in *Grossman's Cardiac Catheterization, Angiography, and Intervention*, D. S. Baim, Ed., p. 215, 7th edition, Lippincott Williams & Wilkins, Philadelphia, PA, USA, 2006.
- [17] T. J. Ford, B. Stanley, R. Good et al., "Stratified medical therapy using invasive coronary function testing in angina," *Journal of the American College of Cardiology*, vol. 72, no. 23, pp. 2841–2855, 2018.
- [18] A. I. Larsen, P. D. Galbraith, W. A. Ghali, C. M. Norris, M. M. Graham, and M. L. Knudtson, "Characteristics and outcomes of patients with acute myocardial infarction and angiographically normal coronary arteries," *The American Journal of Cardiology*, vol. 95, no. 2, pp. 261–263, 2005.
- [19] S. H. Rezkalla and R. A. Kloner, "Coronary no-reflow phenomenon: from the experimental laboratory to the cardiac catheterization laboratory," *Catheterization and Cardiovascular Interventions*, vol. 72, no. 7, pp. 950–957, 2008.
- [20] J. Shaw and T. Anderson, "Coronary endothelial dysfunction in non-obstructive coronary artery disease: risk, pathogenesis, diagnosis and therapy," *Vascular Medicine*, vol. 21, no. 2, pp. 146–155, 2016.
- [21] K. Noma, Y. Kihara, and Y. Higashi, "Striking crosstalk of ROCK signaling with endothelial function," *Journal of Cardiology*, vol. 60, no. 1, pp. 1–6, 2012.
- [22] M. Long, Z. Huang, X. Zhuang et al., "Association of inflammation and endothelial dysfunction with coronary microvascular resistance in patients with cardiac syndrome X," *Arquivos brasileiros de cardiologia*, vol. 109, pp. 397–403, 2017.
- [23] P. Moreau, "Structure and reactivity of small arteries in aging," *Cardiovascular Research*, vol. 37, no. 1, pp. 247–253, 1998.
- [24] I. Antony, A. Nitenberg, J.-M. Foulst, and E. Aptekar, "Coronary vasodilator reserve in untreated and treated hypertensive patients with and without left ventricular hypertrophy," *Journal of the American College of Cardiology*, vol. 22, no. 2, pp. 514–520, 1993.
- [25] P. J. Nahser, R. E. Brown, H. Oskarsson, M. D. Winniford, and J. D. Rossen, "Maximal coronary flow reserve and metabolic coronary vasodilation in patients with diabetes mellitus," *Circulation*, vol. 91, no. 3, pp. 635–640, 1995.
- [26] N. Dages, B. Saller, M. Haude et al., "Insulin sensitivity and coronary vasoreactivity: insulin sensitivity relates to adenosine-stimulated coronary flow response in human subjects," *Clinical Endocrinology*, vol. 61, no. 6, pp. 724–731, 2004.
- [27] A. I. Larsen, R. Basran, T. Anderson, and D. Goodhart, "Large and small vessel vasoconstriction following coronary artery

- stenting," *International Journal of Cardiology*, vol. 113, no. 1, pp. 61–65, 2006.
- [28] P. G. Camici and F. Crea, "Coronary microvascular dysfunction," *New England Journal of Medicine*, vol. 356, no. 8, pp. 830–840, 2007.
- [29] J. M. Zelis, P. A. L. Tonino, N. H. J. Pijls et al., "Coronary microcirculation in aortic stenosis: pathophysiology, invasive assessment, and future directions," *Journal of Interventional Cardiology*, vol. 22, Article ID 4603169, 2020.
- [30] D. Baller, H. J. Bretschneider, and G. Hellige, "Validity of myocardial oxygen consumption parameters," *Clinical Cardiology*, vol. 2, no. 5, pp. 317–327, 1979.
- [31] J. I. Hoffman and G. D. Buckberg, "The myocardial oxygen supply:demand index revisited," *Journal of the American Heart Association*, vol. 3, p. e000285, 2014.
- [32] K. L. Gould and N. P. Johnson, "Quantitative coronary physiology for clinical management: the imaging standard," *Current Cardiology Reports*, vol. 18, no. 1, p. 9, 2016.
- [33] D. C. J. Keulards, M. El Farissi, P. A. L. Tonino et al., "Thermodilution-based invasive assessment of absolute coronary blood flow and microvascular resistance: quantification of microvascular (Dys) function?" *Journal of Interventional Cardiology*, vol. 2020, Article ID 5024971, 7 pages, 2020.
- [34] P. Xaplanteris, S. Fournier, D. C. J. Keulards et al., "Catheter-based measurements of absolute coronary blood flow and microvascular resistance: feasibility, safety, and reproducibility in humans," *Circulation. Cardiovascular Interventions*, vol. 11, Article ID e006194, 2018.
- [35] B.-K. Lee, H.-S. Lim, W. F. Fearon et al., "Invasive evaluation of patients with angina in the absence of obstructive coronary artery disease," *Circulation*, vol. 131, no. 12, pp. 1054–1060, 2015.
- [36] V. S. Pargaonkar, Y. Kobayashi, T. Kimura et al., "Accuracy of non-invasive stress testing in women and men with angina in the absence of obstructive coronary artery disease," *International Journal of Cardiology*, vol. 282, pp. 7–15, 2019.
- [37] P. Meimoun and C. Tribouilloy, "Non-invasive assessment of coronary flow and coronary flow reserve by transthoracic Doppler echocardiography: a magic tool for the real world," *European Journal of Echocardiography*, vol. 9, no. 4, pp. 449–457, 2008.
- [38] D. F. Bechsgaard and E. Prescott, "Transthoracic assessment of coronary flow velocity reserve; Practical approach to diagnostic testing in patients with angina and no obstructive coronary artery disease," *Interventional Journal of Cardiology*, vol. 2021, Article ID 6689312, 8 pages, 2021.
- [39] P. Brainin, D. Frestad, and E. Prescott, "The prognostic value of coronary endothelial and microvascular dysfunction in subjects with normal or non-obstructive coronary artery disease: a systematic review and meta-analysis," *International Journal of Cardiology*, vol. 254, pp. 1–9, 2018.
- [40] T. W. Hein, W. Wang, B. Zoghi, M. Muthuchamy, and L. Kuo, "Functional and molecular characterization of receptor subtypes mediating coronary microvascular dilation to adenosine," *Journal of Molecular and Cellular Cardiology*, vol. 33, no. 2, pp. 271–282, 2001.
- [41] C. Caiati, C. Montaldo, N. Zedda et al., "Validation of a new noninvasive method (contrast-enhanced transthoracic second harmonic echo Doppler) for the evaluation of coronary flow reserve," *Journal of the American College of Cardiology*, vol. 34, no. 4, pp. 1193–1200, 1999.
- [42] G. A. Lanza, A. Buffon, A. Sestito et al., "Relation between stress-induced myocardial perfusion defects on cardiovascular magnetic resonance and coronary microvascular dysfunction in patients with cardiac syndrome X," *Journal of the American College of Cardiology*, vol. 51, no. 4, pp. 466–472, 2008.
- [43] F. Crea and G. A. Lanza, "Angina pectoris and normal coronary arteries: cardiac syndrome X," *Heart*, vol. 90, no. 4, pp. 457–463, 2004.
- [44] R. Tyni-Lenne, S. Stryjan, B. Eriksson, M. Berglund, and C. Sylven, "Beneficial therapeutic effects of physical training and relaxation therapy in women with coronary syndrome X," *Physiotherapy Research International*, vol. 7, no. 1, pp. 35–43, 2002.
- [45] D. S. Marks, S. Gudapati, L. M. Prisant et al., "Mortality in patients with microvascular disease," *The Journal of Clinical Hypertension*, vol. 6, no. 6, pp. 304–309, 2004.
- [46] L. Jespersen, A. Hvelplund, S. Z. Abildstrom et al., "Stable angina pectoris with no obstructive coronary artery disease is associated with increased risks of major adverse cardiovascular events," *European Heart Journal*, vol. 33, no. 6, pp. 734–744, 2012.
- [47] R. Sicari, F. Rigo, L. Cortigiani, S. Gherardi, M. Galderisi, and E. Picano, "Additive prognostic value of coronary flow reserve in patients with chest pain syndrome and normal or near-normal coronary arteries," *The American Journal of Cardiology*, vol. 103, no. 5, pp. 626–631, 2009.
- [48] A. K. Tahari, A. Lee, M. Rajaram et al., "Absolute myocardial flow quantification with 82Rb PET/CT: comparison of different software packages and methods," *European Journal of Nuclear Medicine and Molecular Imaging*, vol. 41, no. 1, pp. 126–135, 2014.
- [49] V. L. Murthy, B. C. Lee, A. Sitek et al., "Comparison and prognostic validation of multiple methods of quantification of myocardial blood flow with 82Rb PET," *Journal of Nuclear Medicine*, vol. 55, no. 12, pp. 1952–1958, 2014.
- [50] T. J. Anderson, F. Charbonneau, L. M. Title et al., "Microvascular function predicts cardiovascular events in primary prevention," *Circulation*, vol. 123, no. 2, pp. 163–169, 2011.
- [51] B. H. Amundsen, U. Wisløff, and S. A. Slørdahl, "Exercise training in cardiovascular diseases," *The Journal of the Norwegian Medical Association*, vol. 127, pp. 446–448, 2007.
- [52] F. M. Wise and J. M. Patrick, "Resistance exercise in cardiac rehabilitation," *Clinical Rehabilitation*, vol. 25, no. 12, pp. 1059–1065, 2011.
- [53] J. Kaski and L. F. Valenzuela Garcia, "Therapeutic options for the management of patients with cardiac syndrome X," *European Heart Journal*, vol. 22, no. 4, pp. 283–293, 2001.
- [54] T. K. Lim, A. J. Choy, F. Khan, J. J. Belch, A. D. Struthers, and C. C. Lang, "Therapeutic development in cardiac syndrome X: a need to target the underlying pathophysiology," *Cardiovascular Therapeutics*, vol. 27, no. 1, pp. 49–58, 2009.
- [55] B. E. Eriksson, R. Tyni-Lenne, J. Svedenhag et al., "Physical training in syndrome X," *Journal of the American College of Cardiology*, vol. 36, no. 5, pp. 1619–1625, 2000.
- [56] A. I. Larsen, T. Valborgland, J. Vegsundvag et al., "Aerobic high-intensity exercise training improves coronary flow reserve velocity and endothelial function in individuals with chest pain and normal coronary angiogram," *European Heart Journal*, vol. 36, no. 1154, 2015.
- [57] I. O. Røysland, F. Friberg, B. Store Brinchmann, S. Nordeide Svello, T. Valborgland, and A. I. Larsen, "Confronting one's vulnerability - patients with chest pain participating in a high-intensity exercise programme," *Journal of Clinical Nursing*, vol. 26, pp. 2006–2015, 2017.
- [58] D. Neglia, R. De Maria, S. Masi et al., "Effects of long-term treatment with carvedilol on myocardial blood flow in

idiopathic dilated cardiomyopathy,” *Heart*, vol. 93, no. 7, pp. 808–813, 2007.

- [59] D. Neglia, E. Fommei, A. Varela-Carver et al., “Perindopril and indapamide reverse coronary microvascular remodelling and improve flow in arterial hypertension,” *Journal of Hypertension*, vol. 29, no. 2, pp. 364–372, 2011.
- [60] “Ischemia-Intensive Medical Treatment Reduces Events in Women with Non-Obstructive CAD,” 2021, <https://clinicaltrials.gov/ct2/show/NCT03417388>.
- [61] T. J. Ford, B. Stanley, N. Sidik et al., “1-Year outcomes of angina management guided by invasive coronary function testing (CorMicA),” *JACC: Cardiovascular Interventions*, vol. 13, no. 1, pp. 33–45, 2020.



## Review Article

# Transthoracic Assessment of Coronary Flow Velocity Reserve: A Practical Approach to Diagnostic Testing in Patients with Angina and No Obstructive Coronary Artery Disease

Daria Frestad Bechsgaard <sup>1</sup> and Eva Prescott<sup>2</sup>

<sup>1</sup>Department of Cardiology, North Zealand University Hospital, University of Copenhagen, Dyrehavevej 29, Hillerød 3400, Denmark

<sup>2</sup>Department of Cardiology, Bispebjerg University Hospital, University of Copenhagen, Bispebjerg Bakke 23, Copenhagen 2400, Denmark

Correspondence should be addressed to Daria Frestad Bechsgaard; [daria.frestad@gmail.com](mailto:daria.frestad@gmail.com)

Received 5 October 2020; Revised 16 February 2021; Accepted 18 March 2021; Published 29 March 2021

Academic Editor: Todd J. Anderson

Copyright © 2021 Daria Frestad Bechsgaard and Eva Prescott. This is an open access article distributed under the Creative Commons Attribution License, which permits unrestricted use, distribution, and reproduction in any medium, provided the original work is properly cited.

More than half of the patients with symptoms suggestive of myocardial ischemia presenting at invasive angiography have no obstructive coronary artery disease (CAD). A large proportion of these patients have ischemia caused by coronary microvascular dysfunction, a condition associated with adverse cardiovascular prognosis. Measurement of coronary flow velocity reserve by transthoracic Doppler echocardiography is a feasible and reproducible method for the evaluation of coronary microvascular function. This review provides a practical overview of the method in a clinical setting of angina and noobstructive CAD, including technical details and prognostic significance.

## 1. Introduction

The discrepancy between angina symptoms, positive stress tests, and no evidence of flow-limiting stenosis on invasive angiography is a common diagnostic challenge, more prevalent in women than in men [1–3]. No evidence of obstructive coronary artery disease (CAD) often results in no diagnosis and limited treatment options, yet follow-up has revealed an increased risk of cardiovascular events in these patients compared with an age- and sex-matched reference population [2, 4]. Over the last two decades, abnormalities of cardiac microvascular function have received increased attention, including coronary microvascular dysfunction (CMD), as the possible explanation for the continued symptoms and adverse cardiovascular prognosis in these patients [5, 6]. CMD is a dysfunction of the coronary resistance vessels, causing a mismatch between coronary blood supply and myocardial oxygen demand. Transthoracic Doppler echocardiography (TTDE) is an established method of assessment of coronary microvascular function with a

well-documented prognostic significance [7]. The main focus of this review is to provide a practical overview of the TTDE-guided evaluation of coronary microvascular function, including technical details and common pitfalls.

## 2. The Concept of Coronary Flow Velocity Reserve

The coronary arterial system comprises a network of vessels with distinct functional properties. Epicardial arteries are conductance vessels with capacitance function offering little resistance to coronary blood flow. Prearterioles and arterioles are resistance vessels sensitive to changes in shear stress and perfusion pressure, responsible for the regulation and distribution of coronary blood flow. Their main function is to prevent myocardial ischemia by matching the oxygen supply with the dynamics of myocardial oxygen demand. The energy production in the normal heart primarily depends on oxidative phosphorylation; thus, an increase in cardiac activity demands for an adequate increase in oxygen

supply. Because the myocardium already extracts more than 70% of the oxygen delivered, this can only be met by an increase in coronary blood flow. Under physiological conditions, the mechanism of autoregulation allows for up to a 5-fold increase in coronary blood flow to meet the oxygen demand with increased cardiac activity [8].

Coronary microvascular vessels are beyond the resolution of the current angiographic systems; however, their function can be assessed indirectly, e.g., through measurements of steady-state coronary blood flow velocities during rest and pharmacologically induced hyperemia using TTDE. In the absence of significant obstructive CAD, the ratio of hyperemic to resting coronary flow velocities (m/s), coronary flow velocity reserve (CFVR), is an established physiological estimate of coronary microvascular function (Figure 1) [9]. The measured increase in coronary flow velocity equals the increase in total myocardial flow if epicardial vessel diameter is constant. TTDE CFVR is measured on a continuous scale, and cutoffs of 2 or 2.5 have been used and are associated with adverse cardiovascular outcomes in angina patients with no obstructive CAD [10].

### 3. Technical Considerations

TTDE assessment of coronary microvascular function is summarized in Table 1. Coronary flow velocities can be measured in all three major coronary arteries, and the choice of the vessel is often determined by feasibility. There are no large-scale studies comparing CFVR in all three vessels in unselected patient cohorts; however, the existing literature suggests the highest CFVR feasibility rates (up to 100%) in the left anterior descending artery (LAD), followed by the right and circumflex coronary arteries [11, 12]. The following review is, therefore, focused on the LAD-CFVR evaluation.

Proximal to distal segments of LAD can be visualized by a 2D color Doppler in a modified parasternal short-axis view, parasternal long-axis view, and foreshortened apical four- or two-chamber views, using a 2.7–8 MHz transducer, with the patient laid in a stable left lateral decubitus position [13]. The color Doppler velocity range is set between 10 and 25 cm/s, and the baseline color scale is set between 1.00 and 2.50 kHz, depending on low or high flow velocities, respectively [11, 14, 15].

Several factors may affect the quality and validity of a CFVR assessment. Use of adenosine, dipyridamole, or regadenoson as a stressor requires 24-hour abstinence from drinks and food containing significant amount of methylxanthines (e.g., coffee, tea, soda, energy drinks, chocolate, and banana) which block adenosine receptors. [16] Medications containing dipyridamole should be paused for at least 48 hours, and medications affecting myocardial perfusion or myocardial metabolic activity (e.g., nitrates,  $\beta$ -blockers, and antihypertensives) should be paused for at least 24 hours. Thorough patient preparations, including breathing exercises and comfortable positioning, are of essence to prevent probe displacement due to body movements or increased breathing activity during hyperemia.

Identification, alignment, and fixation of the vessel are the most important and time-consuming steps in the process

(Figure 2). The artery is identified using Doppler flow mapping. Color gain can be adjusted to obtain the optimal image quality. Moreover, if visualization is challenging, intravenous contrast enhancement in refracted doses can be used. Coronary flow velocity is measured by using a pulsed-wave Doppler as a laminar flow signal directed toward the transducer. The ultrasound beam should be aligned as parallel to the coronary flow as technically possible. Angle correction for coronary flow velocity measurements is not routinely applied due to CFVR being a ratio; however, it is essential that the ultrasound beam is kept under the same angle during both rest and hyperemia to avoid measurement errors. The pattern of coronary flow is biphasic with the highest flow during diastole. Both 2D color Doppler and pulsed-wave Doppler images should be stored frequently throughout the examination to document probe positioning and sampling angle and to capture the peak flow velocities during rest and hyperemia. In addition, heart rate and blood pressure should be documented frequently during rest, hyperemia, and once after discontinuation of the vasodilator.

**3.1. Vasodilators.** The most common vasodilators used for TTDE CFVR evaluation are adenosine, dipyridamole, and regadenoson. Adenosine (0.14 mg/kg/minute; infusion) induces microvascular dilatation through activation of A2A receptors [17]. This results in a 3- to 4-fold increase in coronary blood flow in a normal epicardial vessel. Due to the short half-life of adenosine (<10 seconds), there is no need for an antidote and most side effects resolve in a few seconds after discontinuation of the adenosine infusion. The most common side effects are flushing, chest tightness, and shortness of breath. Less common but more serious side effects are AV block and bronchospasm [18]. In some patients, shortness of breath during adenosine infusion can be dominating, leading to an increased chest movement and higher risk of probe dispositioning and measure error. Dipyridamole (0.84 mg/kg; infusion) inhibits reuptake of endogenous adenosine and has a similar effect on coronary microcirculation. The side effect profile is, however, slightly different. The most common side effects are dizziness, chest and abdominal discomfort, and headache [19]. Dipyridamole has a significantly longer half-life, and administration of an antidote (aminophylline; 50–250 mg) is often necessary. Like adenosine, the selective A2A receptor agonist regadenoson (0.4 mg; rapid injection) dilates the coronary microvasculature by acting on the smooth muscle cells. The most common side effects are shortness of breath, headache, and flushing, which resolve within 15 minutes of administration. Persisting adverse reactions can be attenuated using aminophylline. These three vasodilators assess the nonendothelial dependent pathway of coronary microvascular function in the absence of epicardial coronary stenosis, although the effect is also to some part mediated by endothelial release of nitric oxide [20]. Furthermore, adenosine and dipyridamole have previously been considered equal to achieve hyperemia and are used interchangeably in TTDE [21].

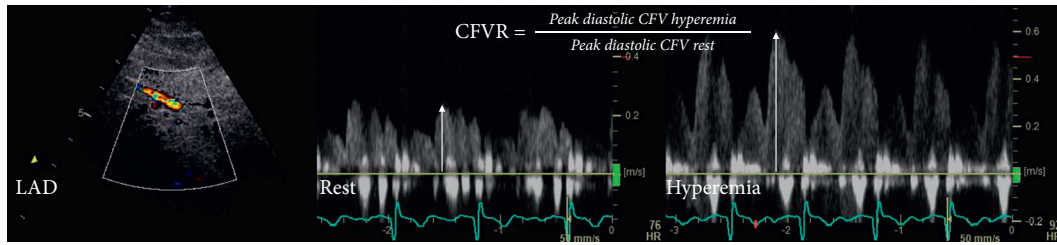


FIGURE 1: Coronary flow velocity reserve (CFVR) measured in the left anterior descending artery (LAD).

TABLE 1: Noninvasive assessment of coronary microvascular function by transthoracic Doppler echocardiography.

Summary of noninvasive assessment of coronary microvascular function by transthoracic Doppler echocardiography
Physiological pathway: nonendothelial dependent
Preferred coronary artery: left anterior descending artery
Measurement: coronary flow velocity reserve (CFVR) ratio of hyperemic to resting coronary flow velocities (m/s); continuous scale
Cutoff for coronary microvascular dysfunction: CFR <2.0
Common vasodilators: adenosine (0.14 mg/kg/minute; intravenous infusion); dipyridamole (0.84 mg/kg; intravenous infusion); and regadenoson (0.4 mg; intravenous injection)
Patient preparation: absence from methylxanthines and medications affecting myocardial perfusion or myocardial metabolic activity; breathing exercises
Examination steps:
(i) Identification of the coronary flow signal using a 2D color Doppler or intravenous contrast enhancement in case of poor visualization
(ii) Alignment of the coronary flow signal of the ultrasound beam as parallel to the coronary flow as possible
(iii) Maintenance of probe position and measuring angle throughout the examination
(iv) Documentation of characteristic flow curves during rest and hyperemia
(v) CFVR quality considerations [11]
Common pitfalls:
(i) Loss of coronary flow signal/change in measuring angle due to patient/probe displacement
(ii) Alternating peak flow velocities due to coronary tortuosity/multiple vessels
(iii) Noise artefacts mimicking/blurring coronary flow signal

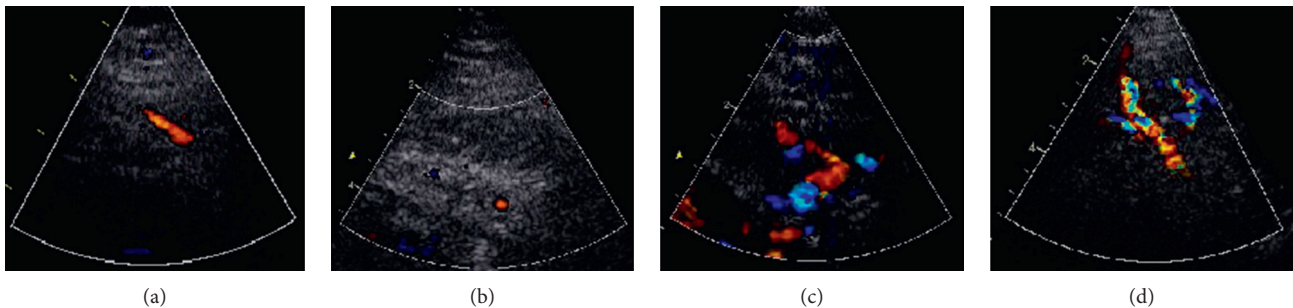


FIGURE 2: 2D color Doppler view of the left anterior descending artery (LAD) demonstrating the importance of artery identification and alignment for accurate CFVR estimation. (a) Optimal visualization of the LAD segment in a foreshortened two-chamber view. Suboptimal artery identification compromising quality of CFVR evaluation: (b) only a short segment of the artery visible; (c) tortuous artery; and (d) multiple vessels in the same frame.

Simultaneous assessment of left ventricular regional wall motion can be performed during dipyridamole and adenosine infusions [22].

**3.2. Feasibility and Variability.** Published reports show that TTDE CFVR in the LAD is highly reproducible in experienced hands. In a large study of angina patients with no obstructive CAD ( $n = 947$ ), CFVR of the LAD was feasible in 97% of patients, with only 6% of all examinations performed

using an intravenous contrast agent [11]. Smaller studies have reported feasibility rates between 66% and 100% [23–27]. The feasibility is lower in the circumflex and right coronary arteries. Common factors affecting feasibility are operator experience and patient-related factors (high BMI, diabetes, and presence of nonobstructive atherosclerosis) [11]. Good repeatability (repeated examinations) of CFVR in the LAD has previously been reported for both healthy volunteers and various patient populations [6, 23, 28–31]. Low intra- and interreader variations have been reported by

several research groups, suggesting good reproducibility (repeated readings) of CFVR [6, 28, 32]. The good repeatability and reproducibility of TTDE CFVR supports the use of CFVR in serial evaluations in both clinical and research settings, as well as an outcome measure.

TTDE CFVR in the LAD is closely correlated with CFVR measured using an intracoronary Doppler guidewire in patients undergoing angiography for suspected obstructive CAD [23, 25–27]. A few studies have explored the agreement between TTDE CFVR and the current noninvasive gold standard for the evaluation of coronary microvascular function, positron emission tomography, in various patient populations, reporting a wide range of correlation coefficients (ranging between 0.27 and 0.91), and there is no clear agreement between the methods [28, 30, 31]. However, also test-retest properties of positron emission tomography are suboptimal with a CoV of approximately 20% in healthy individuals [33]. Other noninvasive methods include cardiac magnetic resonance imaging and CT-perfusion. These have, however, not yet been standardized or validated for use in diagnosing coronary microvascular function. Small studies have found nonsignificant correlations between coronary microvascular function assessed using TTDE and cardiac magnetic resonance perfusion imaging, suggesting perhaps that techniques measuring coronary flow and myocardial perfusion are not interchangeable in the evaluation of coronary microvascular function [34, 35].

**3.3. Factors Affecting the Quality of Coronary Flow Velocity Measurement.** Several patient- and non-patient-related factors may influence the quality and validity of CFVR measurements (Figures 2–4). To date, there is no consensus on the quality score for TTDE CFVR. The iPOWER (Improve Diagnosis and Treatment of Women with Angina Pectoris and Microvessel Disease) research group has suggested a semiquantitative quality score, based on a large, unselected sample of women ( $n=947$ ) with angina and no obstructive disease [11]. The score (0 [nonfeasible], 1 [low quality], 2 [medium quality], and 3 [high quality]) was based on 4 main criteria, including (1) vessel identification, (2) maintenance of probe position throughout the examination, (3) visibility and configuration of coronary flow in the 2D color Doppler mode, and (4) characteristics of flow curves in the pulsed-wave mode [11]. Identification of a single vessel without confounding side branches, good visibility and parallel alignment of beam direction to the vessel flow, consistent probe positioning throughout the entire examination, and characteristic biphasic flow curves gradually increasing during hyperemia with well-defined peaks would classify as a high-quality examination.

The most common pitfall during CFVR assessment is the loss of coronary flow signal or significant shift in measurement angle due to patient or probe displacement (e.g., uncomfortable positioning) or increased chest movements due to side effects of the stress agent, underscoring the importance of proper patient preparation. Another pitfall is alternating peak flow velocities due to arterial tortuosity or multiple vessels measured by the pulsed wave (Figure 2).

Furthermore, noise from the pericardial space (fluid or fat) can sometimes mimic coronary flow, producing uncharacteristic flow curves. These errors lead to nonfeasible examinations and, if not recognized, to under- or overestimation of CFVR.

**3.4. Factors Associated with CFVR.** According to the current European guidelines, CFVR  $<2$  indicates impaired coronary microvascular function [36]. The current cutoff is based on studies investigating a broad spectrum of patients with various risk factor profiles and stages of CAD, ranging from normal epicardial arteries to obstructive CAD [15]. CFVR has previously been associated with several risk factors, including age, hypertension, diabetes, smoking status, resting heart rate, and dyslipidemia [37–43]. However, recent studies investigating women with angina and no obstructive CAD have come to a conclusion that conventional cardiovascular risk factors account for little of the variation in CFVR in these patients [37, 39, 44]. A CFVR cutoff of 2 has also been associated with significant CAD and regional myocardial ischemia [45–48]. A few studies have reported the usefulness of TTDE CFVR to assess the functional significance of intermediate coronary artery stenosis [48, 49]. Currently, there is a knowledge gap on the association between CFVR and plaque burden in patients with nonobstructive CAD.

## 4. Prognostic Value of CFVR

Increasing amount of literature suggests that CMD evaluated by TTDE CFVR predicts adverse cardiovascular outcomes in patients without obstructive CAD. In a meta-analysis performed by our group, including 4 prognostic studies evaluating patients with stable angina and no obstructive CAD (4,516 patients; 284 events), the pooled relative risk for cardiovascular events (incident fatal and nonfatal coronary heart disease) was 4.57 (95% CI 3.43–6.08) [7, 50–53]. A similar prognostic value of CFVR assessed by PET has been reported [7, 54].

## 5. Clinical Application of TTDE CFVR

Angina patients without obstructive CAD are often underdiagnosed and undertreated and at higher risk of hospital readmissions, repeated invasive diagnostic procedures, depression and vital exhaustion, reduced quality of life, and premature exit from the workforce [55–57]. Evaluation of coronary microvascular function using TTDE CFVR in these patients is recommended by ESC guidelines (Class IIb recommendation); however, despite TTDE being a noninvasive, low-cost, and radiation-free method, it is not routinely implemented in clinical practice due to its limited availability [36]. TTDE is an operator-dependent imaging modality; thus, the quality of CFVR largely depends on operator skills and experience. TTDE CFVR performed by an experienced operator is feasible, reproducible, and correlates well with the invasive gold standard. Increasing knowledge and awareness of the adverse prognosis associated with myocardial ischemia in the absence of flow-limiting CAD warrants a wider use of noninvasive diagnostic



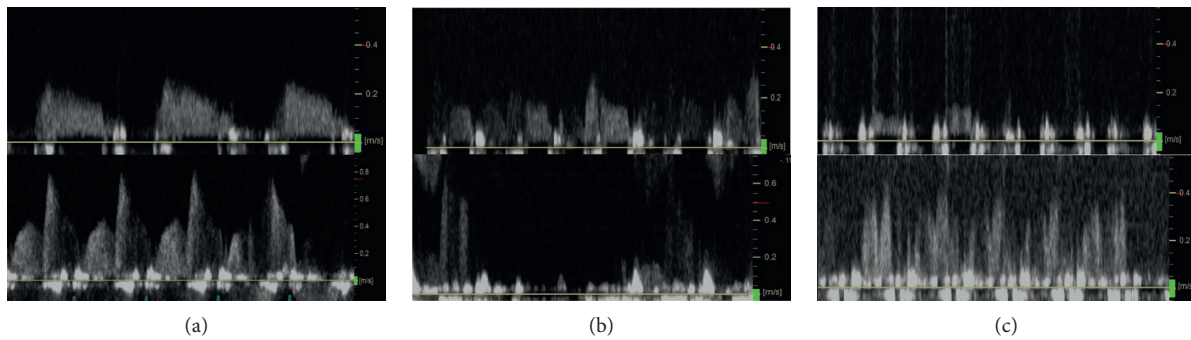


FIGURE 3: Examples of different qualities of coronary flow velocity curves at rest (upper level) and peak hyperemia (lower level). (a) Well-defined and reproducible flow curves. (b) Blurred and inconsistent flow curves (e.g., due to chest movements). (c) Poorly defined flow curves (e.g., due to probe displacement leading to partial loss of coronary flow signal).

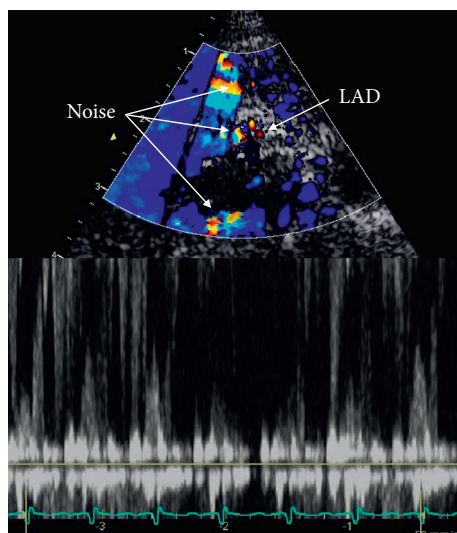


FIGURE 4: Example of noise artifact compromising coronary flow signal, making coronary flow velocity curves blurred and poorly reproducible. Noise artifacts can occur from surrounding structures (e.g., vessels, epicardial fat, and flow in the left ventricular cavity) and can sometimes mimic coronary flow as they usually increase during hyperemia.

techniques, including TTDE, in clinical evaluation of coronary microvascular function.

Evaluation of coronary microvascular function can benefit angina patients in terms of a diagnosis and symptom management. Currently, there is no evidence-based treatment of CMD; however, management of lifestyle factors and risk factors may have a beneficial effect [55]. According to the recent CorMica (Coronary Microvascular Angina) trial, a patient-centered approach, including evaluation of coronary microcirculation as an add-on procedure to diagnostic invasive angiography, linked together with medical therapy (antianginal and prevention therapies, including lifestyle modification), is feasible and improves angina in patients with no obstructive CAD [58]. Looking beyond angina patients with nonobstructive CAD, CMD can be present in other clinical settings, including myocardial diseases (e.g., hypertrophic or dilated cardiomyopathy and amyloidosis), aortic stenosis, and obstructive CAD [59]. However,

evidence on the effect of therapy on CMD associated with these conditions is largely lacking.

## 6. Conclusions

The noninvasive assessment of coronary microvascular function by TTDE CFVR in the LAD is an established method with documented prognostic significance. Compared with other noninvasive methods (e.g., cardiac magnetic resonance imaging or positron emission tomography), TTDE CFVR is an inexpensive, readily available, non-radiative procedure and can be performed simultaneously with diagnostic transthoracic echocardiography as an add-on examination. CFVR by TTDE is feasible and reproducible; however, the method is technically challenging and requires extensive operator experience. There is currently no agreement upon the quality score for CFVR. Large, multicenter trials are warranted to establish the value of TTDE CFVR in cardiovascular risk stratification in patients with no obstructive CAD. Furthermore, the role of TTDE CFVR in guiding symptom management and evaluation of prevention and potential treatment therapies is yet to be established.

## Data Availability

No data were used in this study.

## Conflicts of Interest

The authors declare no conflicts of interest.

## References

- [1] M. R. Patel, E. D. Peterson, D. Dai et al., "Low diagnostic yield of elective coronary angiography," *New England Journal of Medicine*, vol. 362, no. 10, pp. 886–895, 2010.
- [2] C. N. Bairey Merz, C. J. Pepine, M. N. Walsh, and J. L. Fleg, "Ischemia and No obstructive coronary artery disease (INOCA)," *Circulation*, vol. 135, no. 11, pp. 1075–1092, 2017.
- [3] M. R. Patel, D. Dai, A. F. Hernandez et al., "Prevalence and predictors of nonobstructive coronary artery disease identified with coronary angiography in contemporary clinical practice," *American Heart Journal*, vol. 167, no. 6, pp. 846–852, 2014.



- [4] L. Jespersen, A. Hvelplund, S. Z. Abildstrom et al., "Stable angina pectoris with no obstructive coronary artery disease is associated with increased risks of major adverse cardiovascular events," *European Heart Journal*, vol. 33, no. 6, pp. 734–744, 2012.
- [5] C. N. Merz, S. F. Kelsey, C. J. Pepine et al., "The women's ischemia syndrome evaluation (WISE) study: protocol design, methodology and feasibility report," *Journal of the American College of Cardiology*, vol. 33, no. 6, pp. 1453–1461, 1999.
- [6] E. Prescott, S. Z. Abildstrøm, A. Aziz et al., "Improving diagnosis and treatment of women with angina pectoris and microvascular disease: the iPOWER study design and rationale," *American Heart Journal*, vol. 167, no. 4, pp. 452–458, 2014.
- [7] P. Brainin, D. Frestad, and E. Prescott, "The prognostic value of coronary endothelial and microvascular dysfunction in subjects with normal or non-obstructive coronary artery disease: a systematic review and meta-analysis," *International Journal of Cardiology*, vol. 254, pp. 1–9, 2018.
- [8] F. Crea, G. A. Lanza, and P. G. Camici, *Coronary Microvascular Dysfunction*, Springer, New York, NY, USA, 2014.
- [9] K. L. Gould and K. Lipscomb, "Effects of coronary stenoses on coronary flow reserve and resistance," *The American Journal of Cardiology*, vol. 34, no. 1, pp. 48–55, 1974.
- [10] A. I. Löffler and J. M. Bourque, "Coronary microvascular dysfunction, microvascular angina, and management," *Current Cardiology Reports*, vol. 18, pp. 1–7, 2016.
- [11] M. M. Michelsen, A. Pena, N. D. Mygind et al., "Coronary flow velocity reserve assessed by transthoracic doppler: the iPOWER study: factors influencing feasibility and quality," *Journal of the American Society of Echocardiography*, vol. 29, no. 7, pp. 709–716, 2016.
- [12] J. Vegsundvåg, E. Holte, R. Wiseth, K. Hegbom, and T. Hole, "Coronary flow velocity reserve in the three main coronary arteries assessed with transthoracic Doppler: a comparative study with quantitative coronary angiography," *Journal of the American Society of Echocardiography*, vol. 24, no. 7, pp. 758–767, 2011.
- [13] M. Krzanowski, W. Bodzoń, and P. P. Dimitrow, "Imaging of all three coronary arteries by transthoracic echocardiography. An illustrated guide," *Cardiovascular Ultrasound*, vol. 1, no. 1, p. 16, 2003.
- [14] T. Wada, K. Hirata, Y. Shiono et al., "Coronary flow velocity reserve in three major coronary arteries by transthoracic echocardiography for the functional assessment of coronary artery disease: a comparison with fractional flow reserve," *European Heart Journal-Cardiovascular Imaging*, vol. 15, no. 4, pp. 399–408, 2014.
- [15] P. Meimoun and C. Tribouilloy, "Non-invasive assessment of coronary flow and coronary flow reserve by transthoracic doppler echocardiography: a magic tool for the real world," *European Journal of Echocardiography*, vol. 9, no. 4, pp. 449–457, 2008.
- [16] C. E. Müller and K. A. Jacobson, "Xanthines as adenosine receptor antagonists," *Handbook of Experimental Pharmacology*, vol. 200, pp. 151–199, 2011.
- [17] T. W. Hein, W. Wang, B. Zoghi, M. Muthuchamy, and L. Kuo, "Functional and molecular characterization of receptor subtypes mediating coronary microvascular dilation to adenosine," *Journal of Molecular and Cellular Cardiology*, vol. 33, no. 2, pp. 271–282, 2001.
- [18] R. Saab and F. G. Hage, "Vasodilator stress agents for myocardial perfusion imaging," *Journal of Nuclear Cardiology*, vol. 24, no. 2, pp. 434–438, 2017.
- [19] S.-D. Lee, W.-C. Huang, N.-J. Peng, and C. Hu, "Dipyridamole-induced adverse effects in myocardial perfusion scans: dynamic evaluation," *IJC Heart & Vasculature*, vol. 14, pp. 14–19, 2016.
- [20] P. Smits, S. B. Williams, D. E. Lipson, P. Banitt, G. A. Rongen, and M. A. Creager, "Endothelial release of nitric oxide contributes to the vasodilator effect of adenosine in humans," *Circulation*, vol. 92, no. 8, pp. 2135–2141, 1995.
- [21] H. E. Lim, W. J. Shim, H. Rhee et al., "Assessment of coronary flow reserve with transthoracic doppler echocardiography: comparison among adenosine, standard-dose dipyridamole, and high-dose dipyridamole," *Journal of the American Society of Echocardiography*, vol. 13, no. 4, pp. 264–270, 2000.
- [22] P. A. Pellikka, A. Arruda-Olson, F. A. Chaudhry et al., "Guidelines for performance, interpretation, and application of stress echocardiography in ischemic heart disease: from the American society of echocardiography," *Journal of the American Society of Echocardiography*, vol. 33, no. 1, pp. 1–41, 2020.
- [23] C. Caiati, C. Montaldo, N. Zedda et al., "Validation of a new noninvasive method (contrast-enhanced transthoracic second harmonic echo doppler) for the evaluation of coronary flow reserve," *Journal of the American College of Cardiology*, vol. 34, no. 4, pp. 1193–1200, 1999.
- [24] S. M. Kim, W. J. Shim, H. E. Lim et al., "Assessment of coronary flow reserve with transthoracic Doppler echocardiography: comparison with intracoronary Doppler method," *Journal of Korean Medical Science*, vol. 15, no. 2, pp. 139–145, 2000.
- [25] D. J. R. Hildick-Smith, R. Maryan, and L. M. Shapiro, "Assessment of coronary flow reserve by adenosine transthoracic echocardiography: validation with intracoronary doppler," *Journal of the American Society of Echocardiography*, vol. 15, no. 9, pp. 984–990, 2002.
- [26] T. Hozumi, K. Yoshida, T. Akasaka et al., "Noninvasive assessment of coronary flow velocity and coronary flow velocity reserve in the left anterior descending coronary artery by doppler echocardiography," *Journal of the American College of Cardiology*, vol. 32, no. 5, pp. 1251–1259, 1998.
- [27] H. Lethen, H. P. Tries, J. Brechtken, S. Kersting, and H. Lambertz, "Comparison of transthoracic doppler echocardiography to intracoronary doppler guidewire measurements for assessment of coronary flow reserve in the left anterior descending artery for detection of restenosis after coronary angioplasty," *The American Journal of Cardiology*, vol. 91, no. 4, pp. 412–417, 2003.
- [28] M. Saraste, J. W. Koskenvuo, J. Knuuti et al., "Coronary flow reserve: measurement with transthoracic Doppler echocardiography is reproducible and comparable with positron emission tomography," *Clinical Physiology*, vol. 21, no. 1, pp. 114–122, 2001.
- [29] M. Galderisi, S. Cicala, A. D'Errico, O. De Divitiis, and G. De Simone, "Nebivolol improves coronary flow reserve in hypertensive patients without coronary heart disease," *Journal of Hypertension*, vol. 22, no. 11, pp. 2201–2208, 2004.
- [30] M. M. Michelsen, N. D. Mygind, A. Pena et al., "Transthoracic doppler echocardiography compared with positron emission tomography for assessment of coronary microvascular dysfunction: the iPOWER study," *International Journal of Cardiology*, vol. 228, pp. 435–443, 2017.
- [31] R. H. Olsen, L. R. Pedersen, M. Snoer et al., "Coronary flow velocity reserve by echocardiography: feasibility, reproducibility and agreement with PET in overweight and obese

- patients with stable and revascularized coronary artery disease,” *Cardiovascular Ultrasound*, vol. 14, no. 1, p. 22, 2016.
- [32] M. Snoer, T. Monk-Hansen, R. H. Olsen et al., “Coronary flow reserve as a link between diastolic and systolic function and exercise capacity in heart failure,” *European Heart Journal-Cardiovascular Imaging*, vol. 14, no. 7, p. 677, 2012.
- [33] C. Byrne, A. Kjaer, N. E. Olsen, J. L. Forman, and P. Hasbak, “Test-retest repeatability and software reproducibility of myocardial flow measurements using rest/adenosine stress Rubidium-82 PET/CT with and without motion correction in healthy young volunteers,” *Journal of Nuclear Cardiology*, 2020.
- [34] L. E. J. Thomson, J. Wei, M. Agarwal et al., “Cardiac magnetic resonance myocardial perfusion reserve index is reduced in women with coronary microvascular dysfunction,” *Circulation: Cardiovascular Imaging*, vol. 8, no. 4, 2015.
- [35] N. D. Mygind, A. Pena, M. Mide Michelsen et al., “Myocardial first pass perfusion assessed by cardiac magnetic resonance and coronary microvascular dysfunction in women with angina and no obstructive coronary artery disease,” *Scandinavian Journal of Clinical and Laboratory Investigation*, vol. 79, no. 4, pp. 238–246, 2019.
- [36] J. Knuuti, W. Wijns, A. Saraste et al., “2019 ESC Guidelines for the diagnosis and management of chronic coronary syndromes,” *European Heart Journal*, vol. 41, no. 3, pp. 407–477, 2020.
- [37] N. D. Mygind, M. M. Michelsen, A. Pena et al., “Coronary microvascular function and cardiovascular risk factors in women with angina pectoris and no obstructive coronary artery disease: the iPOWER study,” *Journal of the American Heart Association*, vol. 5, no. 3, 2016.
- [38] C. J. Pepine, R. D. Anderson, B. L. Sharaf et al., “Coronary microvascular reactivity to adenosine predicts adverse outcome in women evaluated for suspected ischemia,” *Journal of the American College of Cardiology*, vol. 55, no. 25, pp. 2825–2832, 2010.
- [39] J. D. Sara, R. J. Widmer, Y. Matsuzawa, R. J. Lennon, L. O. Lerman, and A. Lerman, “Prevalence of coronary microvascular dysfunction among patients with chest pain and nonobstructive coronary artery disease,” *JACC: Cardiovascular Interventions*, vol. 8, no. 11, pp. 1445–1453, 2015.
- [40] R. Sicari, F. Rigo, L. Cortigiani, S. Gherardi, M. Galderisi, and E. Picano, “Additive prognostic value of coronary flow reserve in patients with chest pain syndrome and normal or near-normal coronary arteries,” *The American Journal of Cardiology*, vol. 103, no. 5, pp. 626–631, 2009.
- [41] S. A. L. Ahmari, T. J. Bunch, K. Modesto et al., “Impact of individual and cumulative coronary risk factors on coronary flow reserve assessed by dobutamine stress echocardiography,” *The American Journal of Cardiology*, vol. 101, no. 12, pp. 1694–1699, 2008.
- [42] B. Tuccillo, M. Accadia, S. Rumolo et al., “Factors predicting coronary flow reserve impairment in patients evaluated for chest pain: an ultrasound study,” *Journal of Cardiovascular Medicine*, vol. 9, no. 3, pp. 251–255, 2008.
- [43] D.-H. Lee, H.-J. Youn, Y.-S. Choi et al., “Coronary flow reserve is a comprehensive indicator of cardiovascular risk factors in subjects with chest pain and normal coronary angiogram,” *Circulation Journal*, vol. 74, no. 7, pp. 1405–1414, 2010.
- [44] T. R. Wessel, C. B. Arant, S. P. McGorray et al., “Coronary microvascular reactivity is only partially predicted by atherosclerosis risk factors or coronary artery disease in women evaluated for suspected ischemia: results from the NHLBI women’s ischemia syndrome evaluation (WISE),” *Clinical Cardiology*, vol. 30, no. 2, pp. 69–74, 2007.
- [45] M. Daimon, H. Watanabe, H. Yamagishi et al., “Physiologic assessment of coronary artery stenosis without stress tests: noninvasive analysis of phasic flow characteristics by transthoracic doppler echocardiography,” *Journal of the American Society of Echocardiography*, vol. 18, no. 9, pp. 949–955, 2005.
- [46] P. Voci, F. Pizzuto, E. Mariano, P. E. Puddu, P. A. Chiavari, and F. Romeo, “Measurement of coronary flow reserve in the anterior and posterior descending coronary arteries by transthoracic doppler ultrasound,” *The American Journal of Cardiology*, vol. 90, no. 9, pp. 988–991, 2002.
- [47] Y. Matsumura, T. Hozumi, H. Watanabe et al., “Cut-off value of coronary flow velocity reserve by transthoracic doppler echocardiography for diagnosis of significant left anterior descending artery stenosis in patients with coronary risk factors,” *The American Journal of Cardiology*, vol. 92, no. 12, pp. 1389–1393, 2003.
- [48] P. Meimoun, T. Benali, S. Sayah et al., “Evaluation of left anterior descending coronary artery stenosis of intermediate severity using transthoracic coronary flow reserve and dobutamine stress echocardiography,” *Journal of the American Society of Echocardiography*, vol. 18, no. 12, pp. 1233–1240, 2005.
- [49] H. Okayama, T. Sumimoto, G. Hiasa et al., “Assessment of intermediate stenosis in the left anterior descending coronary artery with contrast-enhanced transthoracic doppler echocardiography,” *Coronary Artery Disease*, vol. 14, no. 3, pp. 247–254, 2003.
- [50] K. Nakanish, S. Fukuda, K. Shimada et al., “Impaired coronary flow reserve as a marker of microvascular dysfunction to predict long-term cardiovascular outcomes, acute coronary syndrome and the development of heart failure,” *Circulation Journal*, vol. 76, no. 8, pp. 1958–1964, 2012.
- [51] E. Balázs, K. S. Pintér, Á. Egyed, M. Csanády, T. Forster, and A. Nemes, “The independent long-term prognostic value of coronary flow velocity reserve in female patients with chest pain and negative coronary angiograms (Results from the SZEGED study),” *International Journal of Cardiology*, vol. 146, no. 2, pp. 259–261, 2011.
- [52] J. A. Lowenstein, C. Caniggia, G. Rousse et al., “Coronary flow velocity reserve during pharmacologic stress echocardiography with normal contractility adds important prognostic value in diabetic and nondiabetic patients,” *Journal of the American Society of Echocardiography*, vol. 27, no. 10, pp. 1113–1119, 2014.
- [53] L. Cortigiani, F. Rigo, S. Gherardi et al., “Coronary flow reserve during dipyridamole stress echocardiography predicts mortality,” *JACC: Cardiovascular Imaging*, vol. 5, no. 11, pp. 1079–1085, 2012.
- [54] V. L. Murthy, M. Naya, C. R. Foster et al., “Improved cardiac risk assessment with noninvasive measures of coronary flow reserve,” *Circulation*, vol. 124, no. 20, pp. 2215–2224, 2011.
- [55] V. Kunadian, A. Chieffo, P. G. Camici et al., “An EAPCI expert consensus document on ischaemia with non-obstructive coronary arteries in collaboration with European society of cardiology working group on coronary pathophysiology & microcirculation endorsed by coronary vasomotor disorders international study group,” *European Heart Journal*, vol. 41, no. 37, pp. 3504–3520, 2020.
- [56] D. F. Bechsgaard, I. Gustafsson, M. M. Michelsen et al., “Vital exhaustion in women with chest pain and no obstructive coronary artery disease: the iPOWER study,” *Evidence Based Mental Health*, 2020.

- [57] L. Jespersen, S. Z. Abildstrom, A. Hvelplund et al., "Symptoms of angina pectoris increase the probability of disability pension and premature exit from the workforce even in the absence of obstructive coronary artery disease," *European Heart Journal*, vol. 34, no. 42, pp. 3294–3303, 2013.
- [58] T. J. Ford, B. Stanley, R. Good et al., "Stratified medical therapy using invasive coronary function testing in angina," *Journal of the American College of Cardiology*, vol. 72, no. 23, pp. 2841–2855, 2018.
- [59] F. Crea, P. G. Camici, and C. N. Bairey Merz, "Coronary microvascular dysfunction: an update," *European Heart Journal*, vol. 35, no. 17, pp. 1101–1111, 2014.

## Review Article

# Thermodilution-Based Invasive Assessment of Absolute Coronary Blood Flow and Microvascular Resistance: Quantification of Microvascular (Dys)Function?

Daniëlle C. J. Keulards <sup>1</sup>, Mohamed El Farissi <sup>1</sup>, Pim. A. L Tonino <sup>1,2</sup>, Koen Teeuwen,<sup>1</sup> Pieter-Jan Vlaar,<sup>1</sup> Eduard van Hagen,<sup>1</sup> Inge. F. Wijnbergen,<sup>1</sup> Annemiek de Vos,<sup>1</sup> Guus R. G. Brueren,<sup>1</sup> Marcel van't Veer,<sup>1,2</sup> and Nico H. J. Pijls<sup>1,2</sup>

<sup>1</sup>Catharina Hospital, Eindhoven, Netherlands

<sup>2</sup>Eindhoven University of Technology, 5612 AZ Eindhoven, Netherlands

Correspondence should be addressed to Daniëlle C. J. Keulards; [danielle.keulards@catharinaziekenhuis.nl](mailto:danielle.keulards@catharinaziekenhuis.nl)

Received 12 May 2020; Revised 9 October 2020; Accepted 23 October 2020; Published 18 November 2020

Academic Editor: Piotr Musialek

Copyright © 2020 Daniëlle C. J. Keulards et al. This is an open access article distributed under the Creative Commons Attribution License, which permits unrestricted use, distribution, and reproduction in any medium, provided the original work is properly cited.

During the last two decades, there has been a sharp increase in both interest and knowledge about the coronary microcirculation. Since these small vessels are not visible by the human eye, physiologic measurements should be used to characterize their function. The invasive methods presently used (coronary flow reserve (CFR) and index of microvascular resistance (IMR)) are operator-dependent and mandate the use of adenosine to induce hyperemia. In recent years, a new thermodilution-based method for measurement of absolute coronary blood flow and microvascular resistance has been proposed and initial procedural problems have been overcome. Presently, the technique is easy to perform using the Rayflow infusion catheter and the Coroventis software. The method is accurate, reproducible, and completely operator-independent. This method has been validated noninvasively against the current golden standard for flow assessment: Positron Emission Tomography-Computed Tomography (PET-CT). In addition, absolute flow and resistance measurements have proved to be safe, both periprocedurally and at long-term follow-up. With an increasing number of studies being performed, this method has great potential for better understanding and quantification of microvascular disease.

## 1. Invasive Diagnosis of Microvascular Disease: Time for a Leap Forward?

In the last two decades, there has been a sharp increase in publications about the coronary microcirculation with more than 200 new articles per year. It reflects a new interest for the microcirculation. It is fully accepted nowadays that epicardial coronary artery disease is not the only pathologic entity in ischemic heart disease and that the microcirculation has been underappreciated for years. It has been recognized that 25–50% of patients with chest pain visiting the catheterization laboratory do not present with significant epicardial stenosis: so-called Angina with Nonobstructive Coronary Artery (ANOCA) disease or

Myocardial Infarction with Nonobstructive Coronary Artery (MINOCA) disease [1]. Moreover, a considerable number of patients continue to have chest complaints even after successful percutaneous coronary intervention (PCI) of epicardial lesions [2]. Due to this mismatch between patients' symptoms and epicardial angiography, assessment of the coronary microcirculation or microvasculature has gained interest [3].

Coronary microvascular disease (CMVD) can be divided into roughly three categories: (1) CMVD in the absence of obstructive coronary artery disease (primary CMVD), (2) CMVD secondary to myocardial diseases, for example, left ventricular hypertrophy and Takotsubo, and (3) CMVD in the presence of obstructive coronary artery disease [4]. Most



likely, primary microvascular dysfunction is caused by a combination of factors being intimal thickening, smooth muscle cell proliferation, and molecular mechanisms [4]. The microcirculation is too small to be depicted by traditional invasive imaging methods. Therefore, only functional methods can be used to evaluate the microcirculation in the catheterization laboratory. There are several invasive and noninvasive methods focusing on microcirculatory pressure and flow. This review discusses a new and promising invasive method for easy and accurate assessment of absolute coronary blood flow and microvascular resistance using thermodilution and low rate infusion of saline.

## 2. When to Assess Microvascular Function and/or Coronary Vasospasm?

Due to the increased interest and recognition of microvascular coronary artery disease and coronary vasospasm, more of such patients present at the outpatient clinic or emergency ward. The question that remains is who should undergo further invasive analysis and which investigational methods can be used.

The diagnosis ANOCA, as mentioned, is used to characterize patients with chest pain but with normal/near-normal coronary arteries. Many different pathologies can cause ANOCA as previously mentioned. The first suspicion for the physician follows from the anamnesis and/or cardiac enzymes or functional testing. It is important to realize that patients presenting with "chest pain" are not always comparable and that patients with ANOCA often present with slightly different symptoms, that is, chest tightness after exercise or at rest, dyspnea, and so forth [5].

Some patients present with a myocardial infarction and marked elevated cardiac enzymes without coronary stenosis (MINOCA). Most of these patients with obvious chest/dyspnea complaints undergo some sort of additional noninvasive diagnostic test like bike-treadmill testing or coronary CT-angiography. When no abnormalities are found but clinical suspicion remains, an invasive coronary angiogram can be planned. In the cath lab, the endothelium-dependent and endothelium-independent causes of ANOCA can be distinguished. The current EAPCI consensus document on INOCA states that vasospastic coronary artery disease could, and sometimes should, be assessed within the invasive angiography session (class IIa recommendation) [5]. Coronary vasospasm is also called endothelium-dependent microvascular disease and can be assessed after the administration of increasing doses of intracoronary acetylcholine (ACH). ACH normally binds to the ACH-receptor and causes vasodilatation in the endothelial cell. ACH always causes slight simultaneous constriction of the vascular smooth muscle cell, but in healthy endothelium the net product is vasodilatation [6]. In case of abnormal endothelial cells, ACH binds to the ACH-receptor and does not cause vasodilatation and the slight simultaneous constriction of the smooth muscle cells leading to a net constriction. During ACH testing, a standard approach involves sequential infusion of ACH at concentrations approximating  $10^{-6}$ ,  $10^{-5}$ , and  $10^{-4}$  mol/L.

Epicardial spasm can be diagnosed when the epicardial coronary artery is narrowed >90% after administration of the ACH, accompanied by recognizable complaints and ECG changes corresponding to ischemia. The full protocol is also presented in the consensus document mentioned above [5].

Existing high microvascular resistance is called endothelium-independent microvascular disease. Maximal vasodilatory hyperemia is always caused by the intracoronary (or intravenous) administration of endothelium-independent vasodilators, that is, saline in the case of absolute flow and resistance measurement using the dedicated Rayflow catheter (but also adenosine/regadenoson when measuring IMR/CFR). The full description of the measurement method is explained in the chapter below. IMR and CFR measurement has already been explained extensively previously [7] and goes beyond the scope of this article. The overall diagnostic path that can be followed for ANOCA is displayed in Figure 1.

## 3. Measurement of Absolute Blood Flow and Resistance

To apply this technique, cardiac catheterization and/or FFR can be performed according to routine by either femoral or radial access. Guiding catheters should be advanced as usual and next a pressure/temperature wire (Pressure wire X™ Abbott, Saint Paul, MN, USA) is introduced in the ostium of the coronary artery. After intracoronary administration of 200 micrograms of nitroglycerin and proper equalization of pressures, the pressure wire can be further advanced into the coronary artery in addition to, if desired, assessment of epicardial abnormality using FFR or nonhyperemic pressure ratios (NHPR). Fractional flow reserve (FFR) is measured by intravenous administration of adenosine; RFR (available using the Coroventis software) does not require adenosine and is preferred in some centers. Following epicardial assessment, a dedicated monorail infusion catheter (Rayflow™, Hexacath, Paris) is advanced over the pressure wire and positioned with its tip in the proximal part of the coronary artery (Figure 2).

This infusion catheter has an outer diameter of 0.84 mm (2.5 French) and it consists of a 25 cm long rapid exchange inner monorail lumen for the 0.014" pressure wire and an infusion lumen along the complete length of the catheter. The catheter is equipped with 4 infusion holes at a distance of 7 mm from its tip mandatory for rapid and complete mixing of saline with blood in the coronary artery (Figure 3). In addition, the infusion catheter has two inner side holes approximately 1 cm from the tip between the infusion lumen and the monorail lumen to record precisely the temperature of saline at the spot where it enters the coronary artery. Before saline infusion starts, the temperature is calibrated and body temperature is set to "zero" (reference temperature, Figure 4, panel 1), where after all changes in temperature are related to this reference temperature. During the measurement, the sensor of the pressure/temperature wire is positioned in the distal part of the coronary artery.

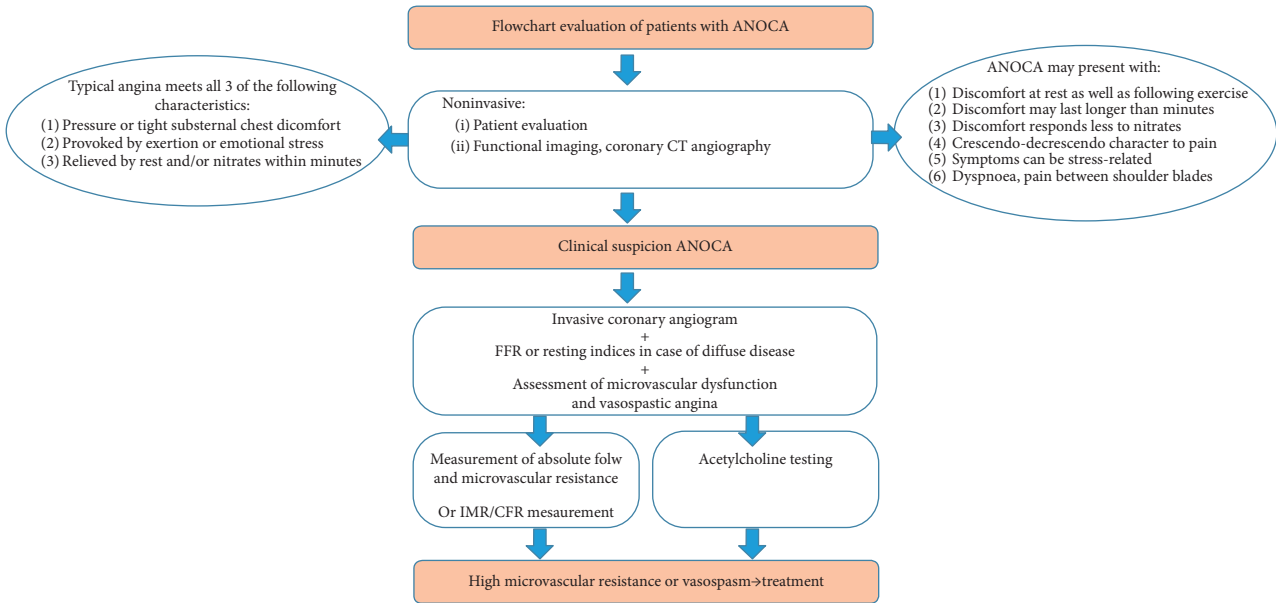


FIGURE 1: The evaluation of ANOCA patients in a flowchart. ANOCA: Angina with Nonobstructive Coronary Arteries, CT: computed tomography, FFR: fractional flow reserve, IMR: index of microvascular resistance, and CFR: coronary flow reserve.

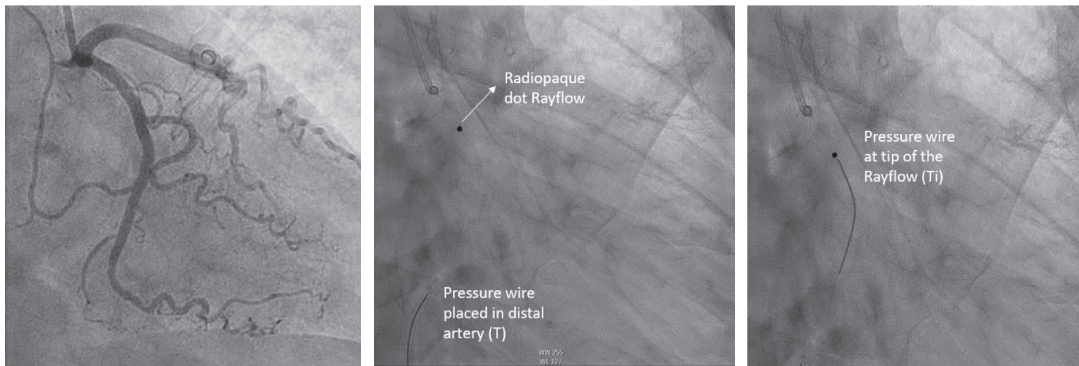


FIGURE 2: Pressure wire and infusion catheter position. In the left panel, a normal circumflex artery is shown. The middle panel shows the pressure wire X, which is placed in the distal coronary artery, and the Rayflow catheter in the proximal artery. The Rayflow is visible by a radiopaque dot at the tip. In this position, the measurement starts. The right panel shows the position of the pressure wire when it is pulled back towards the inner side holes of the Rayflow catheter; now the infusion temperature is assessed. T: the infusion temperature of the saline as measured at the infusion holes of the Rayflow catheter; T: the distal coronary temperature after complete mixing of blood and saline measured by the pressure wire after calibration to body temperature.

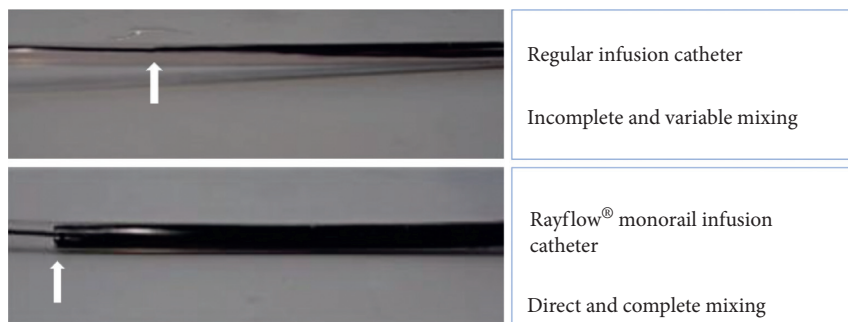


FIGURE 3: Difference in infusion between normal catheter and Rayflow. In the upper panel, an in vitro setup of a coronary artery is shown. The regular infusion catheter is placed in the “vessel” filled with saline and the infusate is dyed black with ink. It is visible that there is incomplete and variable mixing in case of the regular infusion catheter (arrow indicates tip of infusion catheter). In the lower panel, the Rayflow is used. Here immediate and complete mixing is shown, starting directly at the infusion holes (indicated by the arrow).

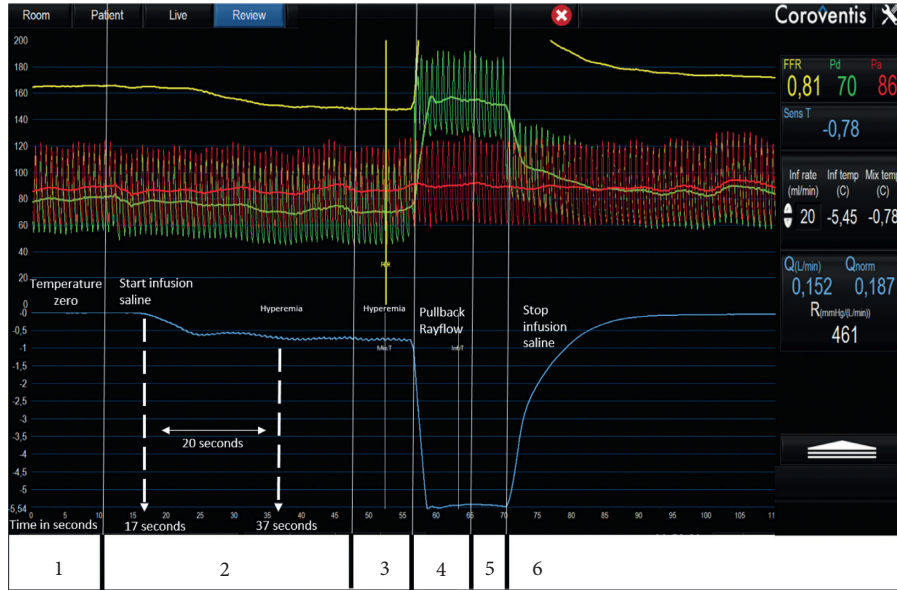


FIGURE 4: Measurement screen, step-by-step. This figure shows the software screen during the flow and resistance measurement. Panel 1: the temperature measured by the pressure wire is zeroed, which means it is calibrated at body temperature. Panel 2: the infusion of saline starts at 20 ml/min in this case; the fast decrease in temperature is visible here. Panel 3: steady-state maximum hyperemia has been reached here and  $T$  is recorded. Panel 4: the pressure wire is pulled back to the tip of the Rayflow to measure the infusion temperature of the saline. This pullback is indicated by the fast decrease in temperature and sudden increase in distal pressure. Panel 5: the infusion temperature measurement reaches steady state and  $T_i$  is calculated. Panel 6: the infusion pump is stopped and the temperature of the blood reaches starting values within 30 seconds. Further, the timeline in the figure indicates the time in seconds. Here, it can be appreciated that it takes approximately 20 seconds for hyperemia to occur. *Red tracing: aortic pressure; green tracing: distal coronary pressure; blue tracing: coronary temperature.* The numerical values of all relevant parameters are displayed in the right side of the Coroventis screen.  $T_i$ : the infusion temperature of the saline as measured at the infusion holes of the Rayflow catheter;  $T$ : the distal coronary temperature after complete mixing of blood and saline measured by the pressure wire after calibration to body temperature.

Next, saline infusion is started at a rate of 15–25 ml/min ( $Q_i$ ) and absolute blood flow in the coronary artery is calculated as previously described [8–10]. Maximum hyperemia in the respective coronary artery is induced by the saline infusion itself within 10–20 seconds [11, 12].

During steady-state infusion, the temperature of the completely mixed blood and saline ( $T$ ) is measured in the distal coronary artery after a steady state has been reached (Figure 4, panel 3); the pressure wire is pulled back in the Rayflow catheter to determine the infusion temperature of the saline ( $T_i$ ) (Figure 4, panel 4). Absolute blood flow is then calculated by the following equation:

$$Q_b = 1.08 \frac{T_i}{T} Q_i, \quad (1)$$

where  $Q_b$  is the hyperemic coronary blood flow in ml/min.  $T_i$  is the infusion temperature of the saline as measured at the infusion holes of the Rayflow catheter.  $T$  is the distal coronary temperature after complete mixing of blood and saline measured by the pressure wire. Both  $T$  and  $T_i$  are measured as a difference to body temperature (calibrated to 0).  $Q_i$  is the infusion rate of saline in ml/min. The constant value 1.08 relates to the difference between the specific heats and densities of blood and saline.

Because also distal coronary pressure ( $Pd$ ) is recorded simultaneously, the microvascular resistance ( $R$ ) can be calculated in analogy to Ohm's law by dividing the

distal pressure and flow by the following simplified equation:

$$R = \frac{Pd}{Q_b}. \quad (2)$$

All signals are instantaneously displayed on the regular cath lab monitor by dedicated software (Coroflow®, Coroventis, Uppsala, Sweden; Figures 4 and 5). This software displays not only all pressure parameters and fractional flow reserve but also absolute blood flow, the normal value of absolute blood flow (obtained by  $Q_b/FFR$ ), and microvascular resistance (in mmHg/L/min or WU).

#### 4. Advantages Compared to Present Methods

The first and most important advantage of the absolute flow and resistance measurement is the ability to measure absolute blood flow and microvascular resistance truly quantitatively. CFR reflects the ratio between basal and hyperemic coronary flows. This tells us something about both the epicardial and microcirculatory functions lumped together but does not enable distinguishing between these two compartments. CFR can be estimated by a ratio of flow velocities, measured by Doppler. CFR can also be approximated by thermodilution during an IMR measurement using a bolus of saline to measure mean transit time ( $T_{mn}$ ) at rest and during maximum hyperemia.  $CFR_{thermo}$  is



Equipment for absolute blood flow and resistance measurement

- (i) Physiological saline
- (ii) The Abbott pressure wire X
- (iii) The Rayflow catheter
- (iv) Infusion pump (heat element switched off and able to infuse at high pressure and in ml/min)
- (v) Coroventis software and radio receiver

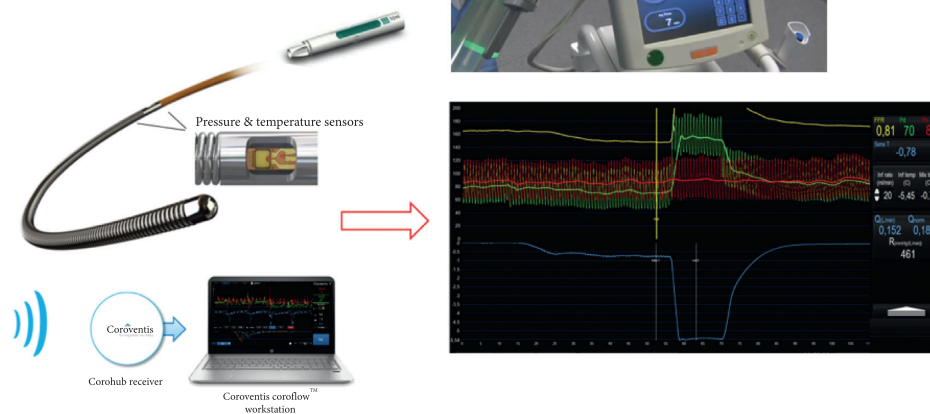


FIGURE 5: Equipment. All equipment needed for the thermodilution-based assessment of absolute blood flow and resistance is displayed here. The Rayflow catheter is shown in the upper panel, clearly indicating the 4 infusion holes at 0°, 90°, 180°, and 270°. The middle panel shows the infusion pump. The lower panel shows the pressure wire with the necessary software.

represented then by the ratio of mean transit times [7]. Use of CFR in clinical practice is limited because of its variability due to blood pressure, heart rate, vessel diameter, age, and others. This causes a large variation in “normal” values and values can vary significantly within the same patient over time. In addition, Doppler techniques are sensitive to slight motion of the patients, breathing, and minimal position changes of the sensor and as such are operator-dependent. IMR itself is not influenced by blood pressure, heart rate, or vessel diameter but is still operator-dependent due to the injection technique of boluses of saline. IMR software tries to limit variability by taking the mean of three measurements. In contrast, the absolute flow and resistance measurements are completely operator-independent: once the infusion of saline has started, the operator stands back, while steady-state measurements are performed. Measurements can be repeated quickly if desired.

Also, by infusing saline through the dedicated Rayflow catheter, maximum hyperemia occurs within 10–20 seconds after start of infusion and no additional hyperemic stimulus is necessary as tested extensively by De Bruyne et al. [11–13]. The absence of need for adenosine makes this method very patient-friendly, since hyperemia by the saline infusion itself is not causing chest discomfort in the vast majority of patients. In a large safety study in only 2% of the patients, mild chest discomfort was noticed [8, 14]. This is in contrast to the frequently observed (although innocent) chest pain observed during hyperemia induced by

intravenous adenosine [15, 16]. Therefore, although generally 30–60 seconds is sufficient to perform the flow and resistance measurements, these measurements can be safely continued for minutes if desired and without any side effect.

The safety of absolute flow and resistance method has been investigated, both periprocedurally and at long-term follow-up [14]. Except for short rapid transient conduction disturbances in 2.6% of measurements, no noticeable side effects were observed periprocedurally and at follow-up of 30 days and 1 year; no adverse event or index vessel related revascularization could be attributed to these measurements.

Reproducibility is excellent [8] and the complete measurement procedure takes only a few minutes in addition to FFR or RFR measurement. As such, a complete evaluation of both the epicardial and the microvascular compartments can be performed easily and quickly. Lastly, the method was validated against the current golden standard for flow assessment: the PET-CT [13].

## 5. Short Overview of the Necessary Equipment

In contrast to IMR, to perform the measurement as explained above, some specific equipment is needed in addition to the pressure wire. First, as a matter of fact the Rayflow multipurpose monorail infusion catheter is mandatory to infuse the saline and to guarantee complete mixing of blood and saline, a prerequisite for reliable measurement

(Figures 3 and 5). Second, a programmable infusion pump is used, which should be able to infuse saline at a rate of 15–25 ml/min at high pressure. Finally, for rapid and instantaneous recording of all relevant parameters and the calculations made, presence of Coroflow software and a radio receiver (Coroflow®, Coroventis, Uppsala, Sweden) is mandatory. All equipment is summarized in Figure 5.

## 6. Practical Issues

Like with every invasive imaging modality, there are some practical issues to keep in mind when using this technique. First, the Rayflow catheter is compatible with a 6F guiding and 6F introducer sheath. Next, the heating element of the infusion pump should be switched off. Next, it is to make sure there is enough saline in the infusion pump to complete the whole measurement. For one measurement, generally 50 cc of saline is needed. Further it is important to wait long enough till maximum hyperemia occurs and all values ( $P_a$ ,  $P_d$ , and  $T$ ) stabilize before pulling back the pressure wire into the Rayflow catheter for measurement of  $T_i$ . Such steady state is generally achieved within 20–30 seconds and this ensures correct values and high reproducibility.

In the event of an AV-block (sometimes seen in small RCA when using an infusion rate above 15 ml/min), the infusion pump should be stopped and AV-conduction recovers immediately. After several seconds, the pump can be adjusted to a lower infusion rate and the measurement can be repeated. All cases of AV-block in the aforementioned safety study disappeared immediately after stopping the infusion and medication was never required to recover AV-conduction [14]. Finally, it should be kept in mind that calculated flow refers to maximum flow distal to the tip of the Rayflow catheter and that resistance refers to minimal resistance of the myocardium corresponding to that position.

## 7. Studies Performed Previously, Limitations, and Future Applications

As a matter of fact, patients with ANOCA, MINOCA, syndrome X, mismatch between epicardial abnormalities and chest pain, and a multitude of primary myocardial diseases will be the focus for quantifying microvascular function. In that regard, and for any interindividual comparison, need for normal values is obvious. In a large recently performed study, ranges of normal values were defined and were as expected quite large due to dependency of resistance on the mass of the myocardial territory distal to the spot of measurement [17].

To exclude the extent of the myocardial territory as a variable, it is recommendable to express flow per gram of tissue (ml/min/g) and resistance as resistance  $\times$  gram of tissue (WU  $\times$  g). In that case, mass should be obtained from coronary CT and MRI. That has been done recently and when doing so, circumscribed narrow ranges of normal minimal resistance were obtained, equal for all 3 major perfusion territories [18].

For intraindividual follow-up of microvascular disease and effects of treatment, this methodology is extremely

suitable because every patient or myocardial territory has its own control. A number of studies have been performed or are presently performed in this respect. Already years ago, when equipment was less refined, Wijnbergen et al. [19] studied changes in myocardial resistance from directly after STEMI PPCI to days to weeks of follow-up. It was suggested that a normal or increased value of resistance measurement after PPCI, which restored considerably at follow-up, was associated with favorable outcome, whereas a persistent high resistance would be unfavorable [19]. Larger studies are mandatory to relate such measurements to outcome, in analogy to IMR studies [7, 20]. This method was also recently used to better understand the recovery of the microcirculation after PCI of chronic occlusions [21, 22]. Here flow and resistance measurements were performed directly after CTO PCI and at follow-up. Recovery of both absolute blood flow and myocardial resistance was observed over time.

Currently there are a couple of interesting trials using this technique. The ongoing IMPACT-CTO 2 trial (ClinicalTrials.gov Identifier: NCT03830853) combines absolute flow and resistance assessment, FFR, RFR, and IMR with intracoronary imaging within the same patient after CTO PCI and at long-term follow-up. These measurements might provide further insight into coronary physiology and anatomy after CTO PCI. Another study to be mentioned in this context is the prospective multicenter randomized placebo-controlled EDIT-CMD (EudraCT number: 2018-003518-41) study, where patients with chest pain of uncertain origin, microcirculation, and effects of calcium antagonists, are studied before treatment and after 6 weeks of calcium-antagonist treatment.

Finally, in case of attempted pharmacologic treatment or risk factor modification of microvascular disease, the measurements described in this paper may prove a suitable instrument for recording progression or regression of disease. Larger studies are required to draw more definite conclusions, especially in different clinical scenarios, without limiting ourselves to ANOCA/MINOCA. With the wide field of applications of this harmless technique, the studies mentioned are only the tip of the iceberg. Multiple areas of further research exist.

## 8. Absolute Flow and Resistance Measurement: the Future Invasive Standard for the Coronary Microcirculation?

Taking into account its ease of use, safety, accuracy, reproducibility, and the capability for specific and quantitative characterization of the coronary microvasculature, the measurement of absolute coronary blood flow and microvascular resistance can be proposed as the future standard for invasive assessment of microvascular (dys)function.

### Abbreviations

ANOCA:	Angina with Nonobstructive Coronary Arteries
CAG:	Coronary angiogram
CFR:	Coronary flow reserve
CMVD:	Coronary microvascular disease

FFR:	Fractional flow reserve
IMR:	Index of microvascular resistance ( $U$ )
LAD:	Left anterior descending
LCx:	Ramus circumflex
MINOCA:	Myocardial Infarction with Nonobstructive Coronary Arteries
PCI:	Percutaneous coronary intervention
$P_d$ :	Distal pressure (mmHg)
$Q$ :	Flow (ml/min)
$R$ :	Resistance (wood units)
RCA:	Right coronary artery
$T$ :	Distal coronary temperature ( $^{\circ}C$ )
$T_i$ :	Infusion temperature ( $^{\circ}C$ )
WU:	Wood units (mmHg/L/min).

## Conflicts of Interest

Nico H. J. Pijls reports institutional grant from Abbott and Hexacath, consulting for Abbott and Opsens, minor equities in Philips, GE, ASML, and Heartflow, and consulting for GE and personal fees for GE. All other authors report no conflicts of interest.

## References

- [1] M. R. Patel, E. D. Peterson, D. Dai et al., "Low diagnostic yield of elective coronary angiography," *New England Journal of Medicine*, vol. 362, no. 10, pp. 886–895, 2010.
- [2] S. V. Arnold, J.-S. Jang, F. Tang, G. Graham, D. J. Cohen, and J. A. Spertus, "Prediction of residual angina after percutaneous coronary intervention," *European Heart Journal—Quality of Care and Clinical Outcomes*, vol. 1, no. 1, pp. 23–30, 2015.
- [3] F. Crea and G. A. Lanza, "Angina pectoris and normal coronary arteries: cardiac syndrome X," *Heart*, vol. 90, no. 4, pp. 457–463, 2004.
- [4] V. R. Taqueti and M. F. Di Carli, "Coronary microvascular disease pathogenic mechanisms and therapeutic options: JACC state-of-the-art review," *Journal of the American College of Cardiology*, vol. 72, no. 21, pp. 2625–2641, 2018.
- [5] V. Kunadian, A. Chieffo, P. G. Camici et al., "An EAPCI expert consensus document on ischaemia with non-obstructive coronary arteries in collaboration with european society of cardiology working group on coronary pathophysiology & microcirculation endorsed by coronary vasomotor disorders international study group," *European Heart Journal*, vol. 41, no. 37, pp. 3504–3520, 2020.
- [6] H. Yasue, K. Matsuyama, K. Matsuyama, K. Okumura, Y. Morikami, and H. Ogawa, "Responses of angiographically normal human coronary arteries to intracoronary injection of acetylcholine by age and segment. Possible role of early coronary atherosclerosis," *Circulation*, vol. 81, no. 2, pp. 482–490, 1990.
- [7] W. F. Fearon, L. B. Balsam, H. M. O. Farouque et al., "Novel index for invasively assessing the coronary microcirculation," *Circulation*, vol. 107, no. 25, pp. 3129–3132, 2003.
- [8] P. Xaplanteris, S. Fournier, D. C. J. Keulards et al., "Catheter-based measurements of absolute coronary blood flow and microvascular resistance: feasibility, safety, and reproducibility in humans," *Circulation. Cardiovascular Interventions*, vol. 11, no. 3, Article ID e006194, 2018.
- [9] W. Aarnoudse, M. van't Veer, N. H. J. Pijls et al., "Direct volumetric blood flow measurement in coronary arteries by thermodilution," *Journal of the American College of Cardiology*, vol. 50, no. 24, pp. 2294–2304, 2007.
- [10] M. Veer, I. F. Wijnbergen, G. G. Toth et al., "Novel monorail infusion catheter for volumetric coronary blood flow measurement in humans: in vitro validation," *EuroIntervention*, vol. 12, no. 6, pp. 701–707.
- [11] B. De Bruyne, J. Adjedj, P. Xaplanteris et al., "Saline-induced coronary hyperemia: mechanisms and effects on left ventricular function," *Circulation. Cardiovascular Interventions*, vol. 10, no. 4, p. e004719, 2017.
- [12] J. Adjedj, F. Picard, C. Collet et al., "Intracoronary saline-induced hyperemia during coronary thermodilution measurements of absolute coronary blood flow: an animal mechanistic study," *Journal of the American Heart Association*, vol. 9, no. 15, p. e015793, 2020.
- [13] H. Everaars, G. A. de Waard, S. P. Schumacher et al., "Continuous thermodilution to assess absolute flow and microvascular resistance: validation in humans using [ $^{15}O$ ]  $H_2O$  positron emission tomography," *European Heart Journal*, vol. 40, no. 28, pp. 2350–2359, 2019.
- [14] D. C. J. Keulards, M. Van 't Veer, J. M. Zelis et al., "Safety of absolute coronary flow and microvascular resistance measurements by thermodilution," *EuroIntervention*, vol. 20, 2020, in Press.
- [15] V. Lachmann, M. Heimann, C. Jung et al., "Feasibility, safety and effectiveness in measuring microvascular resistance with regadenoson," *Clinical Hemorheology and Microcirculation*, vol. 71, no. 3, pp. 299–310, 2019.
- [16] N. Ahmed, J. Layland, D. Carrick et al., "Safety of guidewire-based measurement of fractional flow reserve and the index of microvascular resistance using intravenous adenosine in patients with acute or recent myocardial infarction," *International Journal of Cardiology*, vol. 202, pp. 305–310, 2016.
- [17] S. Fournier, D. C. J. Keulards, M. van't Veer et al., "Normal values of thermodilution-derived absolute coronary blood flow and microvascular resistance in humans," *EuroIntervention*, 2020.
- [18] D. C. J. Keulards, S. Fournier, I. Colaiori et al., "Computed tomographic myocardial mass compared to invasive myocardial perfusion measurement," *Haert BMI*, vol. 106, no. 19, pp. 1489–1494, 2020.
- [19] I. Wijnbergen, M. van't Veer, J. Lammers, J. Ubachs, and N. H. J. Pijls, "Absolute coronary blood flow measurement and microvascular resistance in ST-elevation myocardial infarction in the acute and subacute phase," *Cardiovascular Revascularization Medicine*, vol. 17, no. 2, pp. 81–87, 2016.
- [20] W. F. Fearon, M. Shah, M. Ng et al., "Predictive value of the index of microcirculatory resistance in patients with ST-segment elevation myocardial infarction," *Journal of the American College of Cardiology*, vol. 51, no. 5, pp. 560–565, 2008.
- [21] D. C. J. Keulards, F. M. Zimmermann, N. H. J. Pijls, and K. Teeuwen, "Recovery of absolute coronary flow and resistance one week after percutaneous coronary intervention of a chronic totally occluded coronary artery using the novel RayFlow $^{\circ}$  infusion catheter," *EuroIntervention*, vol. 14, no. 5, pp. e588–e589, 2018.
- [22] D. C. J. Keulards, G. V. Karamasis, O. Alsanjari et al., "Recovery of absolute coronary blood flow and microvascular resistance after chronic total occlusion percutaneous coronary intervention: an exploratory study," *Journal of the American Heart Association*, vol. 9, no. 9, p. e015669, 2020.

## Review Article

# Coronary Microcirculation in Aortic Stenosis: Pathophysiology, Invasive Assessment, and Future Directions

Jo M. Zelis,<sup>1</sup> Pim A. L. Tonino,<sup>1</sup> Nico H. J. Pijls,<sup>1,2</sup> Bernard De Bruyne,<sup>3,4</sup>  
Richard L. Kirkeeide,<sup>5</sup> K. Lance Gould,<sup>5</sup> and Nils P. Johnson <sup>5</sup>

<sup>1</sup>Department of Cardiology, Catharina Hospital, Eindhoven, Netherlands

<sup>2</sup>Department of Biomedical Engineering, Eindhoven University of Technology, Eindhoven, Netherlands

<sup>3</sup>Department of Cardiology, Cardiovascular Center Aalst OLV Hospital, Aalst, Belgium

<sup>4</sup>Department of Cardiology, Lausanne University Hospital, Lausanne, Switzerland

<sup>5</sup>Weatherhead PET Center, Division of Cardiology, Department of Medicine, McGovern Medical School at UTHealth and Memorial Hermann Hospital, Houston, Texas, USA

Correspondence should be addressed to Nils P. Johnson; [nils.johnson@uth.tmc.edu](mailto:nils.johnson@uth.tmc.edu)

Received 8 May 2020; Revised 22 June 2020; Accepted 1 July 2020; Published 22 July 2020

Academic Editor: Joseph Dens

Copyright © 2020 Jo M. Zelis et al. This is an open access article distributed under the Creative Commons Attribution License, which permits unrestricted use, distribution, and reproduction in any medium, provided the original work is properly cited.

With the increasing prevalence of aortic stenosis (AS) due to a growing elderly population, a proper understanding of its physiology is paramount to guide therapy and define severity. A better understanding of the microvasculature in AS could improve clinical care by predicting left ventricular remodeling or anticipate the interplay between epicardial stenosis and myocardial dysfunction. In this review, we combine five decades of literature regarding microvascular, coronary, and aortic valve physiology with emerging insights from newly developed invasive tools for quantifying microcirculatory function. Furthermore, we describe the coupling between microcirculation and epicardial stenosis, which is currently under investigation in several randomized trials enrolling subjects with concomitant AS and coronary disease. To clarify the physiology explained previously, we present two instructive cases with invasive pressure measurements quantifying coexisting valve and coronary stenoses. Finally, we pose open clinical and research questions whose answers would further expand our knowledge of microvascular dysfunction in AS. These trials were registered with NCT03042104, NCT03094143, and NCT02436655.

## 1. Introduction

The seminal 4-group classification of coronary microvascular dysfunction proposed in 2007 placed aortic stenosis (AS) into a category with other myocardial diseases, both primary and secondary [1]. The importance of microcirculatory dysfunction due to AS has become even more clear given the confluence of increasing prevalence due to demographic changes [2] and of expanding treatment since the development of transcatheter aortic valve implantation (TAVI) [3]. Nevertheless, clinical observations enabled by refined diagnostic testing and less invasive treatment have, if anything, exposed unresolved physiologic questions regarding how we should understand, assess, and manage microvascular dysfunction in the patient with AS. This review addresses this

practical need by summarizing the hemodynamic pathophysiology linking aortic stenosis and myocardial dysfunction, describing our invasive tools for quantifying microcirculatory function including its relationship with epicardial stenosis, and noting unresolved questions of clinical importance and how they might be answered. For clarity, we only focus on AS without coexisting myocardial pathology like amyloid or other infiltrative diseases.

## 2. Supply versus Demand

Uniquely among our organs, the heart must pump its own blood supply and cannot meaningfully augment oxygen extraction, implying that only increased supply can match increased need. Wall stress, contractility, and heart rate



account for most myocardial oxygen consumption. The law of Laplace informs us that wall stress is directly proportional to pressure and to radius but inversely proportional to thickness. AS increases wall stress through elevated afterload, and, in response, the heart compensates through increased wall thickness. In other words, left ventricular (LV) hypertrophy offsets pressure overload to reduce wall stress and thereby oxygen requirements. However, LV hypertrophy brings its own disadvantages, namely, diastolic dysfunction, insufficient capillary density [4], and diffuse fibrosis [5].

As a semiquantitative and practical metric of coronary supply versus myocardial demand, a unitless index has been proposed using pressure measurements [6]. The area under the aortic (or, in situations of aortic stenosis, LV) curve during systole (the so-called systolic pressure time integral or SPTI) has been shown in animal models to have a very high and direct correlation with myocardial oxygen demand, even superior to the pressure-rate product [7]. The area between the aortic (or, in situations of epicardial disease, distal coronary) and LV pressure curves during diastole (the so-called diastolic pressure time integral or DPTI) provides a more sophisticated but similarly motivated metric than “coronary perfusion pressure” (difference in end-diastolic pressures between the aorta and LV) and resembles the supply to the myocardium. DPTI/SPTI balances supply and demand into a single unitless ratio, although this formulation ignores other factors such as arterial oxygen content and relative LV mass and wall tension [6]. Directional changes in an individual patient signal dynamic shifts in supply versus demand, while its unitless adjustment for absolute heart rate and blood pressure variation enables cross-sectional comparison among patients.

Although commonly considered as a single “myocardium,” the subepicardial and subendocardial layers display distinct patterns of blood flow with differential sensitivity to pathology. On the one hand, the subepicardium faces generally low pressures from the pericardial space and thoracic cavity throughout the cardiac cycle, while, on the other hand, the subendocardium experiences generally low LV filling pressures during diastole that rise dramatically during systole. Even under normal conditions, the LV pressures during systole compress the subendocardium and redistribute flow to midmyocardial and subepicardial layers [8], a phenomenon explained by competing ‘vascular waterfall’ [9] and ‘intramyocardial pump’ [10] models. Consequently, after a 90-second coronary occlusion, the subepicardium reperfuses more quickly than the subendocardium [11]. Furthermore, during a wide range of pathologic perturbations, “the decrease in subendocardial and increase in subepicardial flow were often associated with normal or even elevated total coronary blood flows” [12], indicating that transmural maldistribution provides a unique guide for understanding many disease states. In animal models, a ratio below 0.8 has been demonstrated via microspheres to correlate with a reduction in subendocardial flow relative to the subepicardium; values  $>0.8$  have been associated with intact and relatively homogeneous perfusion among myocardial layers [6].

To apply these principles of supply versus demand to aortic stenosis, consider the animal model in Figure 1 [12]. Under control conditions, no gradient exists between the LV and the aorta, DPTI and SPTI have similar areas under their respective curves (for a supply/demand ratio close to unity), and coronary perfusion displays a diastolic dominant pattern. As constriction begins using a band around the ascending aorta, left atrial pressure (a surrogate for LV filling pressures) rises, reducing DPTI supply at the same time that an elevated systolic pressure increases SPTI demand. Coronary flow becomes more dependent on flow during systole. With progressive constriction, these changes continue with falling DPTI supply (through a combination of increasing left atrial pressure and tachycardia), rising SPTI demand (as the band creates an ever worse supra-avalvular aortic stenosis), and emerging systolic-dominant coronary flow pattern. This fall in DPTI/SPTI preferentially affects the subendocardium; other animal studies have demonstrated a uniform endocardial/epicardial ratio of 0.97 and flows above 6 cc/min/g under normal hyperemic conditions but an imbalanced ratio of 0.80 (less subendocardial flow) and fall in flow to below 4 cc/min/g with valvular AS [13].

In many ways, Figure 1 provides a conceptual template for what happens in humans, albeit over a different time scale. Progressive AS increases SPTI, while rising LV filling pressures decrease DPTI, leading to a net reduction in the supply/demand (DPTI/SPTI) ratio. However, acute banding in animals does not have time to produce LV hypertrophy as in humans, which further increases the vulnerability of our subendocardium. Also, note that the tachycardia from acute banding in an animal model does not occur in humans with slowly progressive disease, although it represents an additional mechanism for reducing DPTI. For example, in a human cohort, with normal angiograms but critical aortic stenosis (4 subjects, mean gradient 93 mmHg, and aortic valve area 0.48 cm<sup>2</sup>), undergoing invasive hemodynamic study, average DPTI/SPTI of 0.34 with net lactate extraction at baseline 85 beats/minute fell with isoproterenol stress to DPTI/SPTI of 0.16 and switched to net lactate production at 113 beats/minute [14]. These observations could explain why patients can have angina from AS even with normal coronary arteries [15].

### 3. Myocardial Resistance

Unfortunately, our intuitive notion of “resistance” gained from daily life and basic electrical circuits often provides a suboptimal analogy for understanding myocardial behavior. As a result, much of the literature on “myocardial resistance” must be reviewed with caution or at least through the lens of a more sophisticated understanding. This section discusses key points relevant to understanding the concept as it applies to AS since the general topic goes beyond the scope of this review.

During baseline or resting conditions, myocardial flow remains relatively stable over a wide range of perfusion pressures [16] via a large number of homeostatic control mechanisms referred to in aggregate as “autoregulation.” Consequently, basal myocardial resistance represents a

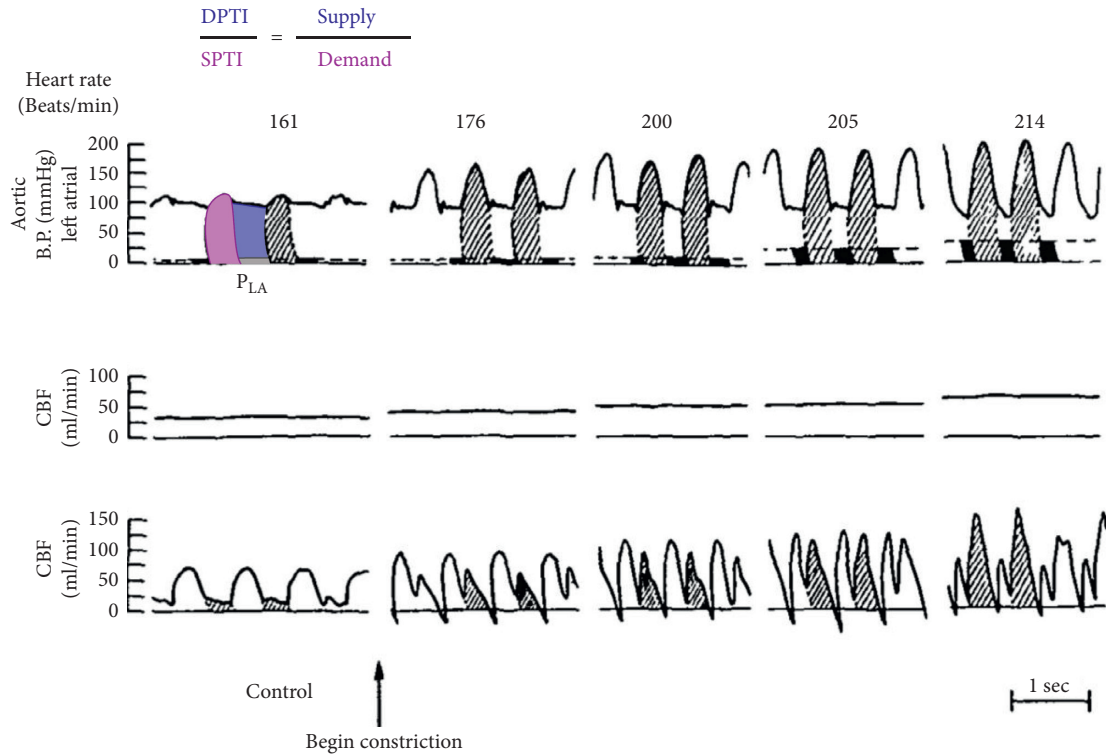


FIGURE 1: Animal aortic banding model that parallels the development of aortic valvular stenosis: at baseline, the systolic demand (shaded) and diastolic supply (not shaded) are well balanced when recording the aortic and left atrial pressures in this animal model of dynamic, supravalvular stenosis. With progressive banding demand rises (shaded area increases), supply falls (due to acute tachycardia in this animal model but also rising left atrial filling pressures marked as filled areas during diastole). Coronary blood flow (CBF, which corresponds to mean coronary blood flow) begins as diastolic dominant (unique to the normal heart) but concludes as systolic dominant (more typical of a peripheral organ bed) (reprinted from Figure 2 of a 1972 publication [12]).

dynamic phenomenon without unique value. Only under conditions of vasodilation does a largely linear relationship exist between perfusion pressure and flow, although somewhat curvilinear at very low perfusion pressures below the range of stable patients. The slope of this hyperemic relationship can be used to estimate resistance. However, in crucial distinction to an electrical resistor, coronary pressure does not fall to 0 mmHg with complete occlusion of the epicardial artery. Depending on how it is measured, this residual pressure has been termed the coronary “wedge pressure” or “zero-flow pressure” or “back pressure.” When accounting for venous and aortic pressures, the scaled wedge pressure quantifies relative maximum collateral blood flow [17].

Animal models of supravalvular aortic stenosis inform us about its effects on myocardial resistance. Compared to normal dogs, animals with LV hypertrophy after 8–10 months of aortic banding displayed a more shallow slope (less flow for the same coronary pressure) but also a higher wedge pressure [18] as depicted in Figure 2. More LV hypertrophy was associated with shallower slopes in that study, implying a dose-response relationship. Additionally, the wedge pressure was roughly twice as high in the setting of LV hypertrophy (24 mmHg versus 12 mmHg) and correlated with LV filling pressures (Pearson coefficient approximately

0.8, indicating that  $0.8^2 = 64\%$  of the variation can be explained).

Several aspects add further complexity to this vasodilated relationship between flow and pressure. First, inotropic (dobutamine and exercise) and chronotropic stimulation can change the slope by about 20% in addition to increasing the wedge pressure [19, 20]. This change in slope, corresponding to a higher resistance, might reflect the compressive effects of higher LV pressure and/or relatively more time spent in systole, indicating that a unique “minimum resistance” cannot be expected. Second, the myocardium displays capacitive and inductive effects necessitating the more general concept of impedance to account for phasic aspects in aortic pressure and flow. While many publications describe diastolic pressure/flow relationships [21], few account for these active effects that largely average out over the entire cardiac cycle. Third, the subepicardium and subendocardium display different pressure/flow relationships, generally with a similar slope but a lower zero-flow pressure in the subepicardium [22].

Before presenting existing resistance data in humans with AS, several points deserve to be mentioned. First, two main invasive techniques exist to measure coronary flow (Doppler flow velocity and bolus thermodilution), thereby introducing heterogeneity in the literature. Encouragingly,

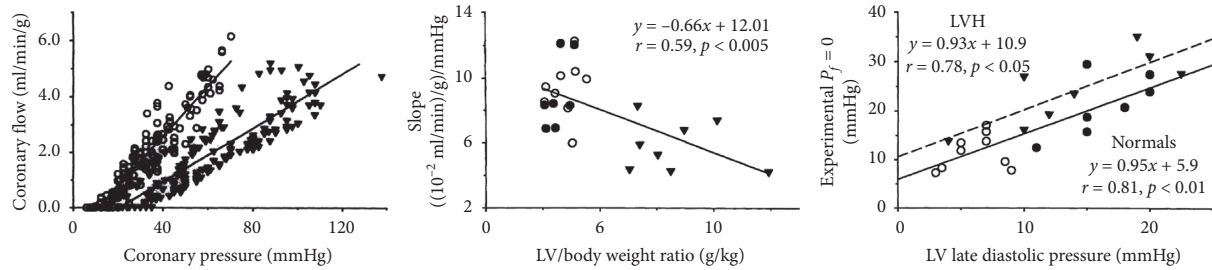


FIGURE 2: Myocardial resistance in an animal model of aortic stenosis: at about 2 months of age, a 20–25 mmHg peak systolic gradient is created in dogs who were then studied at 10–14 months of age and compared with normal animals. During intravenous adenosine infusion, coronary flow is measured as a function of coronary pressure with progressive coronary constriction. Open circles represent normal dogs, and closed triangles represent those with supra-aortic stenosis. The flow versus pressure relationship (left) shifts to the right and rotates clockwise when moving from normal to aortic stenosis. Its slope relates inversely to the amount of left ventricular hypertrophy (middle), indicating a dose-response relationship. Its intercept correlates directly with left ventricular filling pressures (right). In these ways, the decrease in slope corresponds to an increase in myocardial resistance and the change in intercept to a rising zero-flow pressure due to higher LV filling pressures (reprinted from Figures 1–3 of a 1993 publication [19]).

vasodilatory hyperemia to enable either technique appears safe in patients with severe AS based on 40 reports from 1820 patients over 3 decades as summarized in Table 1. Second, techniques using bolus thermodilution [62] and Doppler flow velocity [63] have demonstrated an important bias when quantifying resistance by neglecting wedge pressure assessment in situations when the wedge pressure is elevated. Since most patients with severe AS undergoing TAVI or surgical aortic valve replacement (SAVR) will have at least a moderate elevation in LV filling pressure, which tracks with wedge pressure [18, 19], resistance measurements without this correction should be viewed skeptically. Third, to our knowledge, no study has yet distinguished between changes in wedge pressure versus slope when studying myocardial pressure/flow relationships in human AS. However, continuous thermodilution with the added technique of proximal balloon inflation can create an almost continuous flow versus pressure curve that allows both parameters to be estimated [64].

Table 2 presents a summary of the literature that has reported resistance assessment in humans with AS, both before and after TAVI. Data from 7 studies with a total of 174 vessels either compared resistance between normal patients and those with severe AS and/or serial resistance measurements in the same patients with severe AS before and after TAVI. While limited by modest sample sizes, two different techniques for measuring resistance, and lack of separate slope and zero-flow pressures (apart from 1 study that did measure wedge pressure explicitly), the data suggest two key points in keeping with the animal work described previously: myocardial resistance in AS exceeds that in normal subjects, and resistance falls after TAVI, both acutely and in the longer-term.

#### 4. Epicardial Stenosis

While severe AS by itself can be sufficient to explain symptoms of heart failure or angina, due to a supply-demand mismatch discussed above, epicardial coronary disease of angiographic significance can be seen in 40% to

75% of these patients [65]. Due to near-ubiquitous coronary angiography before TAVI, either invasively or via computed tomography, frequently identified epicardial lesions pose an unresolved treatment dilemma. Rarely is a stenosis so proximal and critical as to require percutaneous coronary intervention (PCI) in order to perform TAVI safely. In most situations, a stenosis could be treated either before or after TAVI with tradeoffs among benefit (usually symptoms resolve with TAVI alone, and the impact of PCI on spontaneous myocardial infarction remains unclear in this older population with severe AS), ease of coronary access (more difficult after TAVI), periprocedural risk (potentially, complications are less well-tolerated with severe AS), and antiplatelet therapy (less flexible after PCI). Table 3 summarizes ongoing randomized trials in this area. In the interim, observational data using fractional flow reserve (FFR) suggested improved outcomes, defined as a composite of death, myocardial infarction, and stroke, versus angiographic selection, mainly through the avoidance of procedural complications in lesions lacking a large hyperemic pressure gradient [66].

Superimposing a coronary stenosis on severe AS exacerbates the supply/demand mismatch. A fixed epicardial stenosis produces a pressure loss that increases with flow but has separate contributions from viscous (friction, linear) and separation (expansion, quadratic) components. Figure 3 superimposes this net stenosis pressure/flow relationship on the description of myocardial performance during vasodilation. The intersection of the stenosis curve and the myocardial load line represents the observations at hyperemia with corresponding FFR and coronary flow reserve (CFR) values [69]. During resting conditions, coronary flow is controlled by autoregulation and does not change, translating into stable nonhyperemic pressure ratios over time as demonstrated in the literature summarized in Table 4. While constancy can be comforting, it overlooks that most patients remain asymptomatic at rest, and thus, only a hyperemic assessment could link with exertional symptoms, acknowledging that dedicated studies



TABLE 1: Literature review of vasodilator stress agents in severe aortic stenosis.

Authors	Citation	N	Drug	Technique	Safety issues
Roy et al. [23]	<i>Nucl Med Commun</i> 1998; 19: 789	12	Dipy	SPECT	No
Carpeggiani et al. [24]	<i>J CV Med</i> 2008; 9: 893	15	Dipy	PET	No
Liu et al. [25]	<i>Sci Rep</i> 2019; 9: 12443	15	Dipy	SPECT	No
Burwash et al. [26]	<i>Heart</i> 2008; 94: 1627	20	Dipy	PET	No but 16 excluded
Rajappan et al. [27]	<i>Circulation</i> 2002; 105: 470	20	Dipy	PET	No
Nemes et al. [28]	<i>Herz</i> 2002; 27: 780	21	Dipy	TTE	No
Baroni et al. [29]	<i>Heart</i> 1996; 75: 492	25	Dipy	TTE	No
Huikuri et al. [30]	<i>AJC</i> 1987; 59: 336	27	Dipy	SPECT	2 hypotension
Demirkol et al. [31]	<i>Cardiology</i> 2002; 97: 37	30	Dipy	SPECT	No
Nemes et al. [32]	<i>Clin Physiol Funct Imaging</i> 2009; 29: 447	49	Dipy	TTE	No
Avakian et al. [33]	<i>IJC</i> 2001; 81: 21	110	Dipy	SPECT	No
Camuglia et al. [34]	<i>JACC</i> 2014; 63: 1808	10	IC adeno	Doppler wire	No
Vendrik et al. [35]	<i>JAHA</i> 2020; 9:e015133	13	IC adeno	FFR	No
Wiegerinck et al. [36]	<i>Circ CV Int</i> 2015; 8:e002443	27	IC adeno	Combo	No
Ahmad et al. [37]	<i>JACC CV Int</i> 2018; 11: 2019	28	IC adeno	FFR	No
Scarsini et al. [38]	<i>EuroIntervention</i> 2018; 13: 1512	66	IC adeno	FFR	No
Di Gioia et al. [39]	<i>AJC</i> 2016; 117: 1511	106	IC adeno	FFR	No
Scarsini et al. [38]	<i>J Cardiovasc Transl Res</i> 2019; 12: 539	82	IC/IV adeno	FFR	No
Stähli et al. [40]	<i>Cardiology</i> 2012; 123: 234	4	IV adeno	FFR	No
Stundl et al. [41]	<i>Clin Res Cardiol</i> 2019; 109	13	IV adeno	FFR	No
Lumley et al. [42]	<i>JACC</i> 2016; 68: 688	19	IV adeno	FFR	No
Burgstahler et al. [43]	<i>IJ CV Img</i> 2008; 24: 195	20	IV adeno	CMR	No
Hildick-Smith and Shapiro [44]	<i>JACC</i> 2000; 36: 1889	27	IV adeno	TTE	1 “tolerated poorly”
Mahmod et al. [45]	<i>JCMR</i> 2014; 16: 29	28	IV adeno	CMR	No
Samuels et al. [46]	<i>JACC</i> 1995; 25: 99	35	IV adeno	SPECT	2 hypotension, 2 AV block
Gutiérrez-Barrios et al. [47]	<i>Int J Cardiol</i> 2017; 236: 370	36	IV adeno	FFR	No
Stoller et al. [48]	<i>EuroIntervention</i> 2018; 14: 166	40	IV adeno	FFR	No
Takemoto et al. [49]	<i>JASE</i> 2014; 27: 200	41	IV adeno	TTE/FFR	No
Patsilinos et al. [50]	<i>Angiology</i> 1999; 50: 309	50	IV adeno	TTE/SPECT	No
Stanojevic et al. [51]	<i>J Inv Card</i> 2016; 28: 357	72	IV adeno	FFR	No
Patsilinos et al. [52]	<i>JNC</i> 2004; 11: 20	75	IV adeno	SPECT	9 AV block
Yamanaka et al. [53]	<i>JACC CV Int</i> 2018; 11: 2032	95	IV adeno	FFR/SPECT	1 AV block, 10% SBP < 40 mmHg
Ahn et al. [54]	<i>JACC</i> 2016; 67: 1412	117	IV adeno	CMR	No
Banovic et al. [55]	<i>Echo</i> 2014; 31: 428	127	IV adeno	TTE	No
Singh et al. [56]	<i>EJH</i> 2017; 38: 1222	174	IV adeno	CMR	No
Nishi et al. [57]	<i>Coron Artery Dis</i> 2018; 29: 223	9	Mixed	FFR	No
Arashi et al. [58]	<i>Cardiovasc Interv Ther</i> 2019; 34: 269	13	Mixed	FFR	No
Hussain et al. [59]	<i>JNC</i> 2017; 24: 1200	95	Mixed	SPECT	No
Banovic et al. [60]	<i>Coron Artery Dis</i> 2020; 31: 166–73	4	NR	FFR	No
Cremer et al. [61]	<i>JNC</i> 2014; 21: 1001	50	Rega	PET	2 hypotension

AV = atrioventricular, adeno = adenosine, CMR = cardiac magnetic resonance, dipy = dipyridamole, FFR = fractional flow reserve, IC = intracoronary, IV = intravenous, N = number of subjects, NR = not reported, PET = positron emission tomography, rega = regadenoson, SBP = systolic blood pressure, SPECT = single-photon emission computed tomography, and TTE = transthoracic echocardiography.

in AS are currently lacking and would be confounded by valvular symptoms.

Based on the discussion of myocardial resistance in the prior section, the existing data support an increase in hyperemic flow after TAVI due to a change in the myocardial load line. This change occurs both via a reduction in wedge pressure, largely mediated by its direct correlation with LV filling pressures [18, 19] that fall after AS has been treated, and a counterclockwise rotation from increasing slope [18]. However, the existence, time course, and relative magnitude

of these changes after TAVI in humans have not been demonstrated.

In contrast to inferences regarding the mechanisms in Figure 3, the secondary effect on the intersection of a fixed stenosis curve but dynamic myocardial load line can be seen more directly from observations summarized in Table 4 from 12 publications and about 350 lesions [68]. Overall resting flow may decrease slightly in the first year as expected from reduced myocardial demand, although the data imply that this effect remains modest and has essentially no impact

TABLE 2: Literature review of hyperemic myocardial resistance with severe aortic stenosis.

Authors	Citation	Normal subjects			Aortic stenosis subjects						
		N	HMR	p value*	N	Mean $\Delta P$ (mmHg)	AVA (cm <sup>2</sup> )	HMR	After TAVI	p value	Long term
<i>Doppler flow velocity with HMR in mmHg/(cm/sec) units</i>											
Vendrik et al. [35]	JAHA 2020; 9: e015133				13		0.83	2.54	2.18	<0.001†	1.95
Lumley et al. [42]	JACC 2016; 68: 688	30	2.29	0.14	19	57	0.74	2.82			
Wiegerinck et al. [36]	Circ CV Int 2015; 8: e002443	28	1.80	0.096	27	43	0.78	2.10	1.83	0.072	
Ahmad et al. [37]	JACC CV Int 2018; 11: 2019				30	38	0.68	2.42	2.14	0.03	
<i>Bolus thermodilution with HMR in mmHg*sec units</i>											
Nishi et al. [57]	Coron Artery Dis 2018; 29: 223	30	16.2	0.14	9	54	0.70	20.4			
Gutiérrez-Barríos et al. [47]	Int J Cardiol 2017; 236: 370	10	17.8	0.01	36	53		32.7			
Stoller et al. [48]	EuroIntervention 2018; 14: 166				40	45 to 58‡	<1.0	26.6§	30.7	0.42	

\* = compares normal versus aortic stenosis subjects. † = for this study, the p value refers to both Friedman test comparing baseline, post-TAVI, and long term as well as each pairwise comparison. ‡ = averages reported separately for subjects with (N=26) and without (N=14) coronary artery disease, respectively. § = only study to correct HMR using an explicitly measured zero-flow pressure.  $\Delta P$  = pressure gradient, AVA = aortic valve area, HMR = hyperemic myocardial resistance, N = number of subjects, and TAVI = transcatheter aortic valve implantation.

TABLE 3: Review of ongoing trials of coronary revascularization in severe aortic stenosis.

Study acronym	Trial ID	Status	N	Description	Completion
FAVOR IV-QVAS	NCT03977129	Recruiting	792	Randomized comparison of QFR and angiography-guided revascularization	2022
NOTION-3	NCT03058627	Recruiting	452	Routine FFR-guided complete revascularization with PCI compared with conservative management in TAVI patients	2025
FAITAVI	NCT03360591	Recruiting	320	Comparison of angiography-guided versus physiology-guided PCI of patients with CAD undergoing TAVI	2021
TCW	NCT03424941	Recruiting	328	FFR-guided PCI and TAVI in severe AS and multivessel CAD vs. CABG and SAVR	2021
FORTUNA	NCT03665389	Not yet recruiting	25	Comparison of FFR derived from coronary computed tomography angiography before TAVR and FFR after TAVI	2022
None	NCT03442400	Recruiting	50	Comparison of pre- and post-TAVI iFR/FFR values and assessment of short-term outcomes	2019
TAVI-PCI	NCT04310046	Not yet recruiting	980	Comparison of FFR-guided PCI within 40 days before TAVI or within 40 days after TAVI	2023

on nonhyperemic pressure ratios. More clearly suggested by the data is an acute increase in peak hyperemic flow with concomitantly higher CFR and lower FFR. However, these studies were small or modestly sized, used a variety of measurement techniques for flow, and did not stratify changes based on properties of the myocardial load line or stenosis curve. In these studies, coronary hyperemia was appropriately induced by pharmacologic stress in order to focus on fixed epicardial disease emphasized by pure vasodilation (and appropriate for revascularization) as opposed to exercise stress that includes vasoconstriction whose treatment is fundamentally medical.

The proposed model in Figure 3 neglects the important physiologic differences between the subepicardium and the subendocardium. Thus, Figure 4 depicts two separate curves relating pressure and flow in distinct layers of the myocardial wall. Under conditions of vasodilation, the higher LV pressures reduce flow in the subendocardium, which becomes further exacerbated as diastolic perfusion time

decreases with exercise. While not possible to measure different FFR values in various layers of the myocardium, Figure 4 nevertheless provides an explanatory framework for understanding the differential impact of epicardial coronary lesions on the microvasculature.

Figure 5 provides a clinical example of applying the DPTI/SPTI concept to individual data from an 82-year-old man with exertional dyspnea and a severe in-stent lesion in the right coronary artery but also a mean aortic valve gradient of 51 mmHg. In this case, an already reduced DPTI/SPTI became radically diminished as a result of diastolic pressure loss from the epicardial lesion. During hyperemia, the FFR reached 0.54, and the DPTI/SPTI fell to 0.16, the same as the average value in the previously mentioned study in which patients with critical AS switched to lactate production [14]. While removing the coronary stenosis might have increased the DPTI/SPTI to 0.66, only treating both AS and the coronary lesion would produce a balanced DPTI/SPTI of 0.95. As noted earlier, we do not have randomized

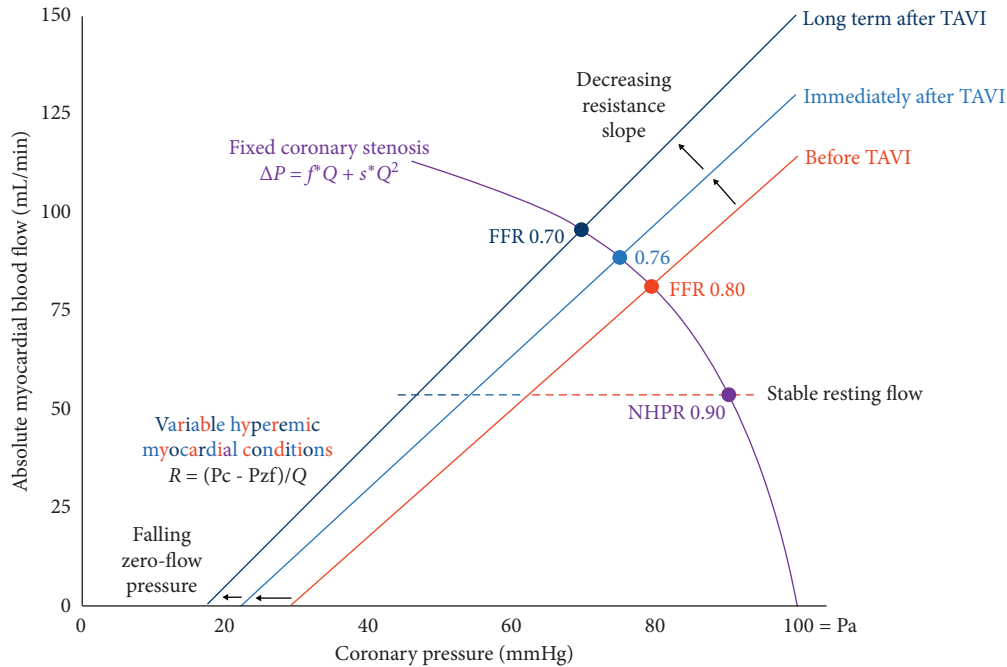


FIGURE 3: Myocardial flow versus coronary pressure relationships: during hyperemia, a linear relationship exists between absolute myocardial blood flow and coronary pressure (basically equal to aortic pressure in the absence of a stenosis). This so-called myocardial “load line” has both slope (how much extra flow for an increase in driving pressure) and offset (often referred to as the zero-flow or wedge pressure depending on how it is measured). The slope of the myocardial load line corresponds to the myocardial resistance which can be calculated through the formula  $R = (P_c - P_{zf})/Q$ , where  $R$  is the resistance,  $P_c$  is the coronary pressure,  $P_{zf}$  is the zero-flow, and  $Q$  is the flow. Under resting conditions (horizontal dashed line), the myocardium is capable of autoregulation to maintain a roughly constant flow over a wide range of perfusion pressures reflected by a constant nonhyperemic pressure ratio (NHPR). A fixed coronary stenosis produces both friction (“ $f$ ”) and separation (“ $s$ ”) components to net pressure loss as can be deduced from the well-known coronary stenosis formula  $\Delta P = f * Q + s * Q^2$ , where  $P$  is the pressure loss in mmHg and  $Q$  is the coronary flow in mL/min [67]. Its intersection with the myocardial load line represents the observations of FFR and maximum flow at peak hyperemia. Potential changes in the myocardial load line have been shown before versus after transcatheter aortic valve implantation (TAVI), although the relative magnitude and time course of a left shift (due to a fall in left ventricular filling pressures) and counterclockwise rotation (corresponding to more flow for the same driving pressure) have not yet been quantified (reprinted from the figure of recent 2020 editorial [68]).

trials demonstrating clinical advantages to treating coexisting coronary disease, but hemodynamically severe and focal lesions supplying large amounts of myocardium, as in this case, seem reasonable candidates for PCI based on using FFR in patients without AS.

## 5. Unanswered Questions

A review not only provides an opportunity to look backward and synthesize existing knowledge but also offers the possibility to identify gaps that remain and how they might be filled in the future. On a basic level, measuring in humans the changes seen in animal models [18] regarding myocardial load lines versus zero-flow pressure would provide us with a better appreciation for acute versus chronic benefits of TAVI. Perhaps, the immediate procedural impact of TAVI on the myocardium predominately affects zero-flow pressure (through a reduction in LV filling pressures as seen in animal work [18]), whereas chronic remodeling over months mainly changes the slope of the myocardial load line (through a regression in LV hypertrophy as seen in animal models [20]). Continuous thermodilution with the added technique of proximal balloon inflation provides perhaps the

most comprehensive yet practical examination in order to separate and quantify these effects in actual patients undergoing treatment [64].

Apart from a confirmation of translational animal physiology and conceptual insight, what clinical advantages might come from such data? Currently, we do not understand when to treat mixed coronary disease and AS, and in some cases, FFR values fall after TAVI, particularly when previously in the 0.75 to 0.85 range [68]. If we understood the degree and time course of myocardial changes after TAVI, then we could better predict which coronary lesions might take on added importance and benefit from revascularization versus those that would remain hemodynamically modest, even after longer-term remodeling. Additionally, some patients with valvular cardiomyopathy recover LV function after TAVI, whereas others remain depressed. Does the slope of the myocardial load line predict this potential reversibility? If yes, then it would permit better patient selection in order to optimize the TAVI risk/benefit. Finally, the changes in myocardial resistance should be expected to be linked to pretreatment severity of the AS as well as the hemodynamic efficacy of the TAVI device. Because myocardial resistance is

TABLE 4: Literature review of coronary physiology before versus after treatment of severe aortic stenosis.

Authors	Citation	N	Baseline	Immediate	p value	Long term	p value	Time	Treatment	Method	
Nemes et al. [28]	<i>Herz</i> 2002; 27: 780	21	62.2			40.1	<0.01	15 months	SAVR	Echo Doppler (diastolic)	
Hildick-Smith and Shapiro [44]	<i>JACC</i> 2000; 36: 1889	27	43			41	NS	6 months	SAVR	Echo Doppler (diastolic)	
Carpeggiani et al. [24]	<i>J CV Med</i> 2008; 9: 893	8	1.01			0.92	>0.05	12 months	SAVR	PET	
Rajappan et al. [70]	<i>Circulation</i> 2003; 107: 3170	22	1.08			1.01	0.27	12 months	SAVR	PET	
Camuglia et al. [34]	<i>JACC</i> 2014; 63: 1808	8	22	20	NS	18	NS	12 months	TAVI	Wire (Doppler)	
Vendrik et al. [35]	<i>JAHA</i> 2020; pending	13	19.98	19.7	NS	21.44	0.397	6 months	TAVI	Wire (Doppler)	
Ahmad et al. [37]	<i>JACC CV Int</i> 2018; 11: 2019	30	22.13	24.84	0.1				TAVI	Wire (Doppler)	
Wiegerinck et al. [36]	<i>Circ CV Int</i> 2015; 8: e002443	27	24.4	25.5	0.401				TAVI	Wire (Doppler)	
			Instantaneous wave-free ratio (iFR)								
Vendrik et al. [35]	<i>JAHA</i> 2020; pending	13	0.82	0.83	NS	0.83	0.735	6 months	TAVI		
Ahmad et al. [37]	<i>JACC CV Int</i> 2018; 11: 2019	30	0.88	0.88	0.94				TAVI		
Scarsini et al. [38]	<i>EuroIntervention</i> 2018; 13: 1512	145	0.89	0.89	0.66				TAVI		
			Hyperemic perfusion (cc/min/g) or Doppler velocity (cm/sec) or mean transit time (sec)								
Nemes et al. [28]	<i>Herz</i> 2002; 27: 780	21	117			91.5	<0.05	15 months	SAVR	Echo Doppler (diastolic)	
Hildick-Smith and Shapiro [44]	<i>JACC</i> 2000; 36: 1889	27	71			108	<0.01	6 months	SAVR	Echo Doppler (diastolic)	
Carpeggiani et al. [24]	<i>J CV Med</i> 2008; 9: 893	8	1.68			1.46	NS	12 months	SAVR	PET	
Rajappan et al. [27]	<i>Circulation</i> 2003; 107: 3170	22	2.17			2.27	0.61	12 months	SAVR	PET	
Camuglia et al. [34]	<i>JACC</i> 2014; 63: 1808	8	34	29	NS	39	NS	12 months	TAVI	Wire (Doppler)	
Vendrik et al. [35]	<i>JAHA</i> 2020; pending	13	26.36	30.78	<0.001	40.2	<0.001	6 months	TAVI	Wire (Doppler)	
Wiegerinck et al. [36]	<i>Circ CV Int</i> 2015; 8: e002443	27	44.5	51.1	0.027				TAVI	Wire (Doppler)	
Ahmad et al. [37]	<i>JACC CV Int</i> 2018; 11: 2019	30	33.44	40.33	0.004				TAVI	Wire (Doppler)	
Stoller et al. [48]	<i>EuroIntervention</i> 2018; 14: 166	40	0.44	0.48	0.53				TAVI	Wire (thermo)	
			Coronary flow reserve (CFR)								
Nemes et al. [32]	<i>Herz</i> 2002; 27: 780	21	1.96			2.37	<0.05	15 months	SAVR	Echo Doppler (diastolic)	
Hildick-Smith and Shapiro [44]	<i>JACC</i> 2000; 36: 1889	27	1.76			2.61	<0.01	6 months	SAVR	Echo Doppler (diastolic)	
Carpeggiani et al. [24]	<i>J CV Med</i> 2008; 9: 893	8	1.68			1.58	NS	12 months	SAVR	PET	
Rajappan et al. [70]	<i>Circulation</i> 2003; 107: 3170	22	2.02			2.28	0.17	12 months	SAVR	PET	
Camuglia et al. [34]	<i>JACC</i> 2014; 63: 1808	8	1.53	1.58	0.41	2.18	<0.01	12 months	TAVI	Wire (Doppler)	
Vendrik et al. [35]	<i>JAHA</i> 2020; pending	13	1.28	1.65	<0.001	1.94	<0.001	6 months	TAVI	Wire (Doppler)	
Wiegerinck et al. [36]	<i>Circ CV Int</i> 2015; 8: e002443	27	1.9	2.1	0.113				TAVI	Wire (Doppler)	
Stoller et al. [48]	<i>EuroIntervention</i> 2018; 14: 166	40	1.9	2	0.72				TAVI	Wire (thermo)	
			Fractional flow reserve (FFR)								
Stundl et al. [41]	<i>Clin Res Cardiol</i> 2019; Epub	13	0.77			0.76	0.11	2 months	TAVI		
Vendrik et al. [35]	<i>JAHA</i> 2020; pending	13	0.85	0.79	<0.001	0.71	<0.001	6 months	TAVI		
Ahmad et al. [37]	<i>JACC CV Int</i> 2018; 11: 2019	30	0.87	0.85	0.0008				TAVI		
Stoller et al. [48]	<i>EuroIntervention</i> 2018; 14: 166	40	0.9	0.93	0.0021				TAVI		
Pesarini et al. [71]	<i>Circ CV Int</i> 2016; 9: e004088	133	0.89	0.89	0.73				TAVI		

NS = not significant (actual p value not reported), PET = positron emission tomography, SAVR = surgical aortic valve replacement, TAVI = transcatheter aortic valve implantation, and thermo = bolus thermodilution (based on the table from 2020 editorial [68]).

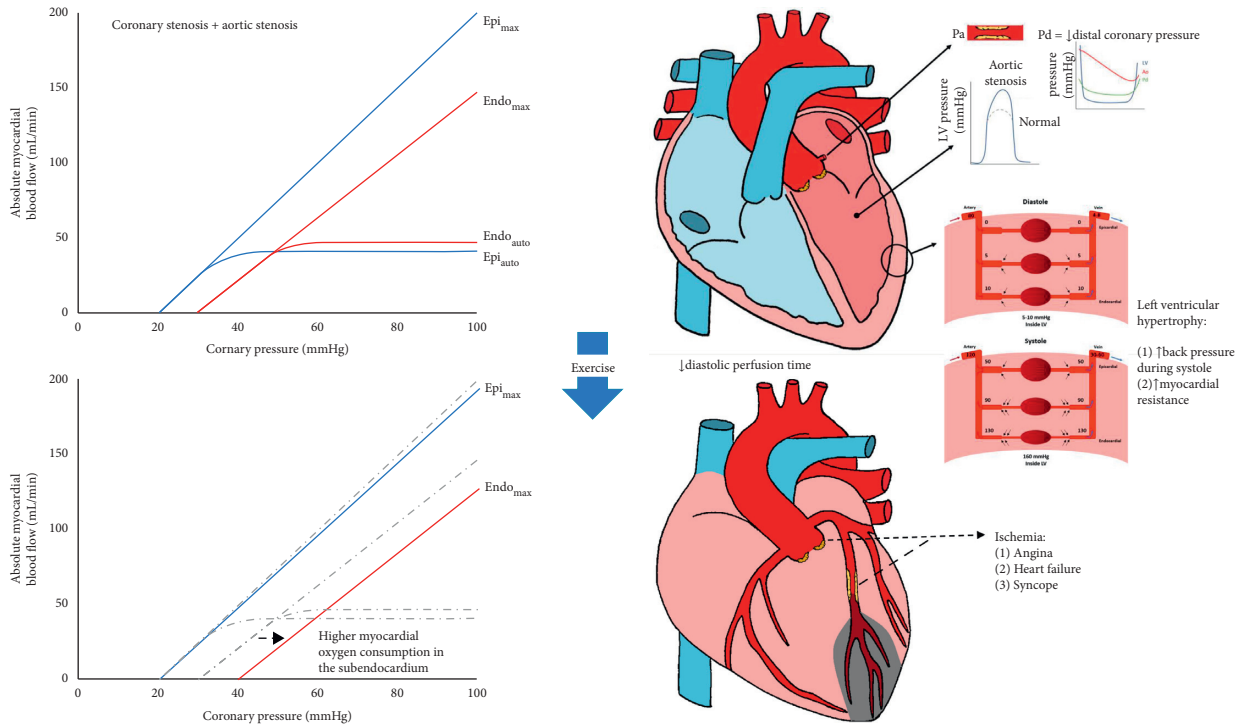


FIGURE 4: Transmural impact of aortic stenosis with coronary disease: reduced flow from aortic stenosis and coronary stenosis does not affect all layers of the myocardium equally. Under baseline conditions, autoregulation (“auto” subscript) maintains a relatively stable flow for most perfusion pressures. Vasodilation (“max” subscript) produces the net hyperemic myocardial load line from Figure 3 that is made up of a lower offset in the subepicardium (Epi) than the subendocardium (Endo), with potentially different slopes as well. Exercise reduces diastolic perfusion time and increases left ventricular pressures, preferentially affecting the subendocardium both through tachycardia and also increased oxygen consumption. The resulting hypoperfusion can produce the classic symptoms of valvular stenosis.

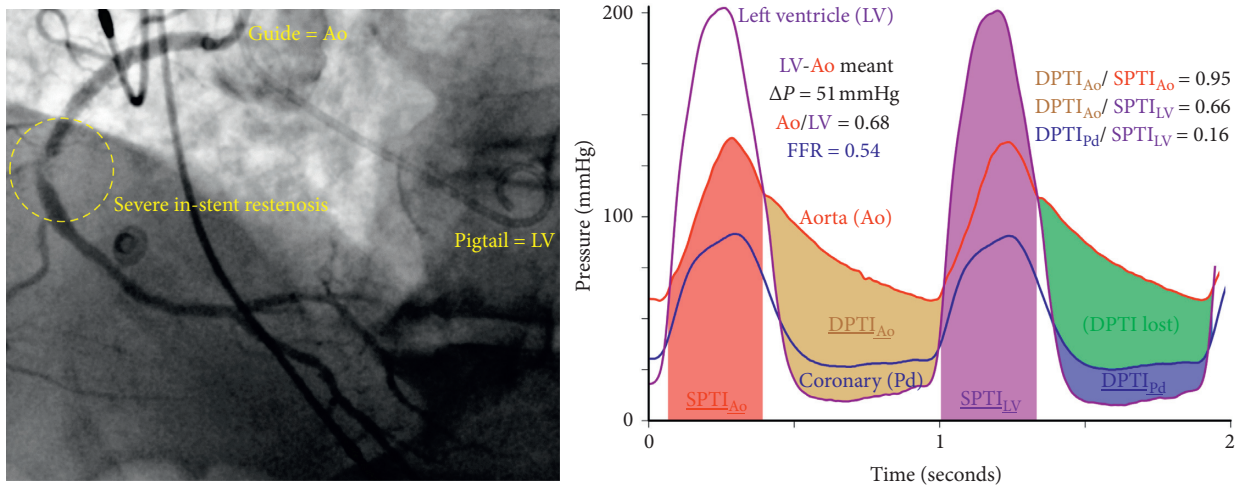


FIGURE 5: Clinical case of simultaneous aortic and coronary stenosis assessment: as detailed in the text, this 82-year-old man with exertional dyspnea underwent coronary evaluation before transcatheter aortic valve implantation. Three pressures were measured simultaneously: aortic (via the guide catheter), coronary (via a distal pressure wire), and left ventricular (via a pigtail catheter). Intravenous papaverine induced coronary hyperemia with a fractional flow reserve (FFR) of 0.54. Both the severe aortic stenosis (baseline mean gradient 51 mmHg) and the severe in-stent coronary lesion imbalance myocardial demand (systolic pressure time integral, or SPTI) and diastolic coronary supply (diastolic pressure time integral, or DPTI). This figure allows for a visual understanding of the additive effects of the tandem aortic valve and coronary stenosis.

inherently a hyperemic concept, do baseline parameters such as the resting valve gradient or aortic valve area perform worse than hyperemic parameters such as the

stress aortic valve index (SAVI) [72]? In that case, it would argue against relying solely on resting measurements when selecting patients for TAVI.



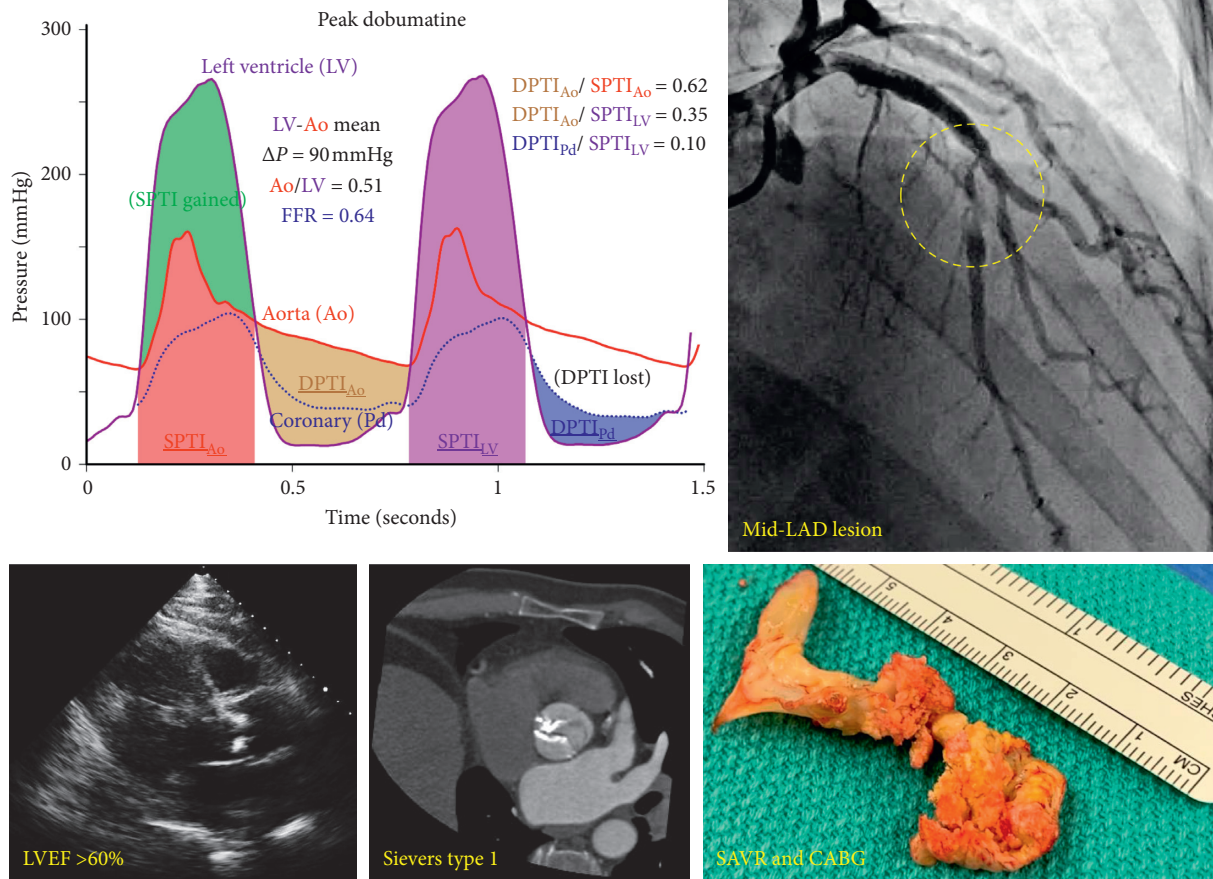


FIGURE 6: Clinical case of asymptomatic but severe stenosis: as detailed in the text, this 55-year-old asymptomatic man was referred for an incidental heart murmur on routine physical examination. A treadmill exercise test showed good functional capacity with no symptoms or abnormal responses, and echocardiography found normal ejection fraction. However, his bicuspid aortic valve had moderate-to-severe stenosis at baseline, rising to a mean gradient of 90 mmHg during intravenous dobutamine stress. Furthermore, his left anterior descending (LAD) coronary artery had an angiographically moderate-to-severe stenosis and fractional flow reserve (FFR) of 0.64 during intravenous adenosine infusion. When superimposing these curves (the distal coronary pressure tracing has been time-scaled to match the aortic pressure tracing), myocardial oxygen demand (systolic pressure time integral, or SPTI) greatly exceeds diastolic coronary supply (diastolic pressure time integral, or DPTI) due to increased SPTI from aortic stenosis and decreased DPTI due to coronary stenosis. Despite normal left ventricular function and a lack of symptoms, the patient underwent surgical aortic valve replacement (SAVR) and concomitant coronary artery bypass grafting (CABG) for extremely abnormal hemodynamics.

As a final sign of our yet incomplete knowledge of the coronary microcirculation in aortic stenosis, a clinical case is considered in Figure 6. This 55-year-old man was referred by his internist for an incidental murmur noted during a routine physical examination that was otherwise unremarkable. In daily life, he had no symptoms and performed 9:32 minutes of a standard Bruce treadmill protocol. Blood pressure, heart rate, and heart rhythm response were normal during the graded exercise; he denied angina and stopped due to leg fatigue. Echocardiography revealed normal LV function with an ejection fraction over 60%. Therefore, we have an asymptomatic patient with no evidence of sub-clinical cardiomyopathy.

However, extensive workup revealed a calcified bicuspid aortic valve with moderate-to-severe stenosis at baseline, rising to a mean gradient of 90 mmHg during intravenous dobutamine infusion with a SAVI of 0.51 (indicating that peak valvular flow is reduced by the stenotic valve to 51% of

maximum). A calcified mid-LAD stenosis had an FFR of 0.64 during intravenous adenosine with a focal pressure jump. An analysis of DPTI/SPTI (although not direct in this case since the valve and coronary stenoses were interrogated sequentially using different pharmacologic agents) showed a potential drop to 0.10 during peak stress, entering the region that has been associated with net lactate production in a small human study [14]. Therefore, we have coexisting and severe aortic and coronary stenoses confirmed by objective hemodynamic data.

Should we understand this case as a profound challenge to the relevance of hemodynamic physiology reviewed in this article? Or does it indicate that patient symptoms (or their lack) as well as standard noninvasive testing often tell us at most a modest amount regarding physiologic severity, thereby necessitating routine quantification? While awaiting the results of ongoing randomized controlled trials of TAVI in severe yet asymptomatic AS (clinicaltrials.gov, NCT03042104, NCT03094143, and NCT02436655), what

should we currently do with such patients who nevertheless exhibit extreme hemodynamic derangements? Can we expect that the reduction in sudden death seen in a small trial of SAVR for asymptomatic yet severe AS (mean gradient 63 mmHg) [73] will be confirmed in larger, ongoing trials? While these vital questions cannot be answered definitively at this moment, they serve as humble reminders regarding the profound capacity of the human coronary microcirculation in some patients to withstand a severe assault on multiple fronts.

### Conflicts of Interest

JMZ reports no support or industry relationships. PALT, NHJP, RLK, KLG, and NPJ have a patent pending on diagnostic methods for quantifying aortic stenosis and TAVI physiology. PALT reports no additional support or industry relationships. NHPJ receives institutional grant support from Abbott, serves as a consultant for Abbott and Opsens, and possesses equity in Philips, GE, ASML, and Heartflow. BDB has received institutional research grants and consulting fees from Abbott Vascular (formerly St. Jude Medical), Boston Scientific, and Opsens. BDB, RLK, KLG, and NPJ have a patent pending on correcting pressure signals from fluid-filled catheters. RLK reports no additional support or industry relationships. KLG is the 510(k) applicant for CFR Quant (K113754) and HeartSee (K143664 and K171303), software packages for cardiac positron emission tomography image processing, analysis, and absolute flow quantification. NPJ receives internal funding from the Weatherhead PET Center for Preventing and Reversing Atherosclerosis, has an institutional licensing and consulting agreement with Boston Scientific for the smart minimum FFR algorithm (commercialized under 510(k) K191008), and has received significant institutional research support from St. Jude Medical (CONTRAST, NCT02184117) and Philips Volcano Corporation (DEFINE-FLOW, NCT02328820), studies using intracoronary pressure and flow sensors.

### References

- [1] P. G. Camici and F. Crea, "Coronary microvascular dysfunction," *New England Journal of Medicine*, vol. 356, no. 8, pp. 830–840, 2007.
- [2] A. P. Durko, R. L. Osnabrugge, N. M. Van Mieghem et al., "Annual number of candidates for transcatheter aortic valve implantation per country: current estimates and future projections," *European Heart Journal*, vol. 39, no. 28, pp. 2635–2642, 2018.
- [3] H. R. Andersen, L. L. Knudsen, and J. M. Hasenkam, "Transluminal implantation of artificial heart valves. description of a new expandable aortic valve and initial results with implantation by catheter technique in closed chest pigs," *European Heart Journal*, vol. 13, no. 5, pp. 704–708, 1992.
- [4] E. A. Breisch, S. R. Houser, R. A. Carey, J. F. Spann, and A. A. Bove, "Myocardial blood flow and capillary density in chronic pressure overload of the feline left ventricle," *Cardiovascular Research*, vol. 14, no. 8, pp. 469–475, 1980.
- [5] B. Schwartzkopff, H. Frenzel, J. Diekerhoff et al., "Morphometric investigation of human myocardium in arterial hypertension and valvular aortic stenosis," *European Heart Journal*, vol. 13, no. suppl D, pp. 17–23, 1992.
- [6] J. I. E. Hoffman and G. D. Buckberg, "The myocardial oxygen supply:demand index revisited," *Journal of the American Heart Association*, vol. 3, no. 1, Article ID e000285, 2014.
- [7] D. Baller, H. J. Bretschneider, and G. Hellige, "Validity of myocardial oxygen consumption parameters," *Clinical Cardiology*, vol. 2, no. 5, pp. 317–327, 1979.
- [8] P. Libby, R. O. Bonow, D. L. Mann, and D. P. Zipes, *Braunwald's Heart Disease: A Textbook of Cardiovascular Medicine*, Elsevier, Amsterdam, Netherlands, 8th edition, 2007.
- [9] J. M. Downey and E. S. Kirk, "Inhibition of coronary blood flow by a vascular waterfall mechanism," *Circulation Research*, vol. 36, no. 6, pp. 753–760, 1975.
- [10] J. A. Spaan, N. P. Breuls, and J. D. Laird, "Diastolic-systolic coronary flow differences are caused by intramyocardial pump action in the anesthetized dog," *Circulation Research*, vol. 49, no. 3, pp. 584–593, 1981.
- [11] H. F. Downey, G. J. Crystal, and F. A. Bashour, "Asynchronous transmural perfusion during coronary reactive hyperaemia," *Cardiovascular Research*, vol. 17, no. 4, pp. 200–206, 1983.
- [12] G. D. Buckberg, D. E. Fixler, J. P. Archie, and J. I. E. Hoffman, "Experimental subendocardial ischemia in dogs with normal coronary arteries," *Circulation Research*, vol. 30, no. 1, pp. 67–81, 1972.
- [13] D. Alyono, R. W. Anderson, D. G. Parrish, X. Z. Dai, and R. J. Bache, "Alterations of myocardial blood flow associated with experimental canine left ventricular hypertrophy secondary to valvular aortic stenosis," *Circulation Research*, vol. 58, no. 1, pp. 47–57, 1986.
- [14] G. Buckberg, L. Eber, M. Herman, and R. Gorlin, "Ischemia in aortic stenosis: hemodynamic prediction," *The American Journal of Cardiology*, vol. 35, no. 6, pp. 778–784, 1975.
- [15] K. L. Gould and B. A. Carabello, "Why angina in aortic stenosis with normal coronary arteriograms?" *Circulation*, vol. 107, no. 25, pp. 3121–3123, 2003.
- [16] R. Rubio and R. M. Berne, "Regulation of coronary blood flow," *Progress in Cardiovascular Diseases*, vol. 18, no. 2, pp. 105–122, 1975.
- [17] N. H. Pijls, J. A. Van Son, R. L. Kirkeeide, B. De Bruyne, and K. L. Gould, "Experimental basis of determining maximum coronary, myocardial, and collateral blood flow by pressure measurements for assessing functional stenosis severity before and after percutaneous transluminal coronary angioplasty," *Circulation*, vol. 87, no. 4, pp. 1354–1367, 1993.
- [18] D. J. Duncker, J. Zhang, and R. J. Bache, "Coronary pressure-flow relation in left ventricular hypertrophy. importance of changes in back pressure versus changes in minimum resistance," *Circulation Research*, vol. 72, no. 3, pp. 579–587, 1993.
- [19] D. J. Duncker, J. Zhang, T. J. Pavlek, M. J. Crampton, and R. J. Bache, "Effect of exercise on coronary pressure-flow relationship in hypertrophied left ventricle," *American Journal of Physiology-Heart and Circulatory Physiology*, vol. 269, no. 1, pp. H271–H281, 1995.
- [20] D. J. Duncker and R. J. Bache, "Effect of chronotropic and inotropic stimulation on the coronary pressure-flow relation in left ventricular hypertrophy," *Basic Research in Cardiology*, vol. 92, no. 4, pp. 271–286, 1997.
- [21] F. J. Klocke, R. E. Mates, J. M. Canty, and A. K. Ellis, "Coronary pressure-flow relationships. controversial issues and probable implications," *Circulation Research*, vol. 56, no. 3, pp. 310–323, 1985.

- [22] D. J. Duncker and R. J. Bache, "Regulation of coronary blood flow during exercise," *Physiological Reviews*, vol. 88, no. 3, pp. 1009–1086, 2008.
- [23] S. Roy, T. Hawkins, and J. P. Bourke, "The safety of dipyridamole-thallium imaging in patients with critical aortic valve stenosis and angina," *Nuclear Medicine Communications*, vol. 19, no. 8, pp. 789–794, 1998.
- [24] C. Carpeggiani, D. Neglia, U. Paradossi, L. Pratali, M. Glauber, and A. L'Abbate, "Coronary flow reserve in severe aortic valve stenosis: a positron emission tomography study," *Journal of Cardiovascular Medicine*, vol. 9, no. 9, pp. 893–898, 2008.
- [25] F. S. Liu, S. Y. Wang, Y. C. Shiau, and Y. W. Wu, "The clinical value and safety of ECG-gated dipyridamole myocardial perfusion imaging in patients with aortic stenosis," *Scientific Reports*, vol. 9, p. 12443, 2019.
- [26] I. G. Burwash, M. Lortie, P. Pibarot et al., "Myocardial blood flow in patients with low-flow, low-gradient aortic stenosis: differences between true and pseudo-severe aortic stenosis. Results from the multicentre TOPAS (Truly or pseudo-severe aortic stenosis) study," *Heart*, vol. 94, no. 12, pp. 1627–1633, 2008.
- [27] K. Rajappan, O. E. Rimoldi, D. P. Dutka et al., "Mechanisms of coronary microcirculatory dysfunction in patients with aortic stenosis and angiographically normal coronary arteries," *Circulation*, vol. 105, no. 4, pp. 470–476, 2002.
- [28] A. Nemes, T. Forster, Z. Kovács, A. Thury, I. Ungi, and M. Csanády, "The effect of aortic valve replacement on coronary flow reserve in patients with a normal coronary angiogram," *Herz*, vol. 27, no. 8, pp. 780–784, 2002.
- [29] M. Baroni, S. Maffei, M. Terrazzi, C. Palmieri, F. Paoli, and A. Biagini, "Mechanisms of regional ischaemic changes during dipyridamole echocardiography in patients with severe aortic valve stenosis and normal coronary arteries," *Heart*, vol. 75, no. 5, pp. 492–497, 1996.
- [30] H. V. Huikuri, U. R. Korhonen, M. J. Ikäheimo, J. Heikkilä, and J. T. Takkunen, "Detection of coronary artery disease by thallium imaging using a combined intravenous dipyridamole and isometric handgrip test in patients with aortic valve stenosis," *The American Journal of Cardiology*, vol. 59, no. 4, pp. 336–340, 1987.
- [31] M. O. Demirkol, B. Yaymaci, H. Debeş, Y. Başaran, and F. Turan, "Dipyridamole myocardial perfusion tomography in patients with severe aortic stenosis," *Cardiology*, vol. 97, no. 1, pp. 37–42, 2002.
- [32] A. Nemes, E. Balázs, M. Csanády, and T. Forster, "Long-term prognostic role of coronary flow velocity reserve in patients with aortic valve stenosis—insights from the SZEGED Study," *Clinical Physiology and Functional Imaging*, vol. 29, no. 6, pp. 447–452, 2009.
- [33] S. D. Avakian, M. Grinberg, J. C. Meneguetti, J. A. F. Ramires, and A. d. P. Mansur, "SPECT dipyridamole scintigraphy for detecting coronary artery disease in patients with isolated severe aortic stenosis," *International Journal of Cardiology*, vol. 81, no. 1, pp. 21–27, 2001.
- [34] A. C. Camuglia, J. Syed, P. Garg et al., "Invasively assessed coronary flow dynamics improve following relief of aortic stenosis with transcatheter aortic valve implantation," *Journal of the American College of Cardiology*, vol. 63, no. 17, pp. 1808–1809, 2014.
- [35] J. Vendrik, Y. Ahmad, A. Eftekhari et al., "Long-term effects of transcatheter aortic valve implantation on coronary hemodynamics in patients with concomitant coronary artery disease and severe aortic stenosis," *Journal of the American Heart Association*, vol. 9, no. 5, Article ID e015133, 2020.
- [36] E. M. A. Wiegerinck, T. P. Van De Hoef, M. C. Rolandi et al., "Impact of aortic valve stenosis on coronary hemodynamics and the instantaneous effect of transcatheter aortic valve implantation," *Circulation: Cardiovascular Interventions*, vol. 8, no. 8, Article ID e002443, 2015.
- [37] Y. Ahmad, M. Göteborg, C. Cook et al., "Coronary hemodynamics in patients with severe aortic stenosis and coronary artery disease undergoing transcatheter aortic valve replacement," *JACC: Cardiovascular Interventions*, vol. 11, no. 20, pp. 2019–2031, 2018.
- [38] R. Scarsini, G. Pesarini, C. Zivelonghi et al., "Physiologic evaluation of coronary lesions using instantaneous wave-free ratio (iFR) in patients with severe aortic stenosis undergoing transcatheter aortic valve implantation," *EuroIntervention*, vol. 13, no. 13, pp. 1512–1519, 2018.
- [39] G. Di Gioia, M. Pellicano, G. G. Toth et al., "Fractional flow reserve-guided revascularization in patients with aortic stenosis," *The American Journal of Cardiology*, vol. 117, no. 9, pp. 1511–1515, 2016.
- [40] B. E. Stähli, W. Maier, R. Corti, T. F. Lüscher, and L. A. Altwegg, "Fractional flow reserve evaluation in patients considered for transfemoral transcatheter aortic valve implantation: a case series," *Cardiol*, vol. 123, pp. 234–239, 2013.
- [41] A. Stundl, J. Shamekhi, S. Bernhardt et al., "Fractional flow reserve in patients with coronary artery disease undergoing TAVI: a prospective analysis," *Clinical Research in Cardiology*, vol. 109, no. 6, pp. 746–754, 2019.
- [42] M. Lumley, R. Williams, K. N. Asrress et al., "Coronary physiology during exercise and vasodilation in the healthy heart and in severe aortic stenosis," *Journal of the American College of Cardiology*, vol. 68, no. 7, pp. 688–697, 2016.
- [43] C. Burgstahler, M. Kunze, M. P. Gawaz et al., "Adenosine stress first pass perfusion for the detection of coronary artery disease in patients with aortic stenosis: a feasibility study," *The International Journal of Cardiovascular Imaging*, vol. 24, no. 2, pp. 195–200, 2008.
- [44] D. J. R. Hildick-Smith and L. M. Shapiro, "Coronary flow reserve improves after aortic valve replacement for aortic stenosis: an adenosine transthoracic echocardiography study," *Journal of the American College of Cardiology*, vol. 36, no. 6, pp. 1889–1896, 2000.
- [45] M. Mahmud, S. K. Piechnik, E. Levelt et al., "Adenosine stress native T1 mapping in severe aortic stenosis: evidence for a role of the intravascular compartment on myocardial T1 values," *Journal of Cardiovascular Magnetic Resonance*, vol. 16, no. 1, p. 92, 2014.
- [46] B. Samuels, H. Kiat, J. D. Friedman, and D. S. Berman, "Adenosine pharmacologic stress myocardial perfusion tomographic imaging in patients with significant aortic stenosis," *Journal of the American College of Cardiology*, vol. 25, no. 1, pp. 99–106, 1995.
- [47] A. Gutiérrez-Barrios, S. Gamaza-Chulián, A. Agarrado-Luna et al., "Invasive assessment of coronary flow reserve impairment in severe aortic stenosis and echocardiographic correlations," *International Journal of Cardiology*, vol. 236, pp. 370–374, 2017.
- [48] M. Stoller, S. Gloekler, R. Zbinden et al., "Left ventricular afterload reduction by transcatheter aortic valve implantation in severe aortic stenosis and its prompt effects on comprehensive coronary haemodynamics," *EuroIntervention*, vol. 14, no. 2, pp. 166–173, 2018.



- [49] K. Takemoto, K. Hirata, N. Wada et al., "Acceleration time of systolic coronary flow velocity to diagnose coronary stenosis in patients with microvascular dysfunction," *Journal of the American Society of Echocardiography*, vol. 27, no. 2, pp. 200–207, 2014.
- [50] S. Patsilnakos, S. Spanodimos, F. Rontoyanni et al., "Adenosine stress myocardial perfusion tomographic imaging in patients with significant aortic stenosis," *Journal of Nuclear Cardiology*, vol. 11, no. 1, pp. 20–25, 2004.
- [51] D. Stanojevic, P. Gunasekaran, P. Tadros et al., "Intravenous adenosine infusion is safe and well tolerated during coronary fractional flow reserve assessment in elderly patients with severe aortic stenosis," *The Journal of Invasive Cardiology*, vol. 28, no. 9, pp. 357–361, 2016.
- [52] S. P. Patsilnakos, I. P. Antonelis, G. Filippatos et al., "Detection of coronary artery disease in patients with severe aortic stenosis with noninvasive methods," *Angiology*, vol. 50, no. 4, pp. 309–317, 1999.
- [53] F. Yamanaka, K. Shishido, T. Ochiai et al., "Instantaneous wave-free ratio for the assessment of intermediate coronary artery stenosis in patients with severe aortic valve stenosis," *JACC: Cardiovascular Interventions*, vol. 11, no. 20, pp. 2032–2040, 2018.
- [54] J.-H. Ahn, S. M. Kim, S.-J. Park et al., "Coronary microvascular dysfunction as a mechanism of angina in severe AS," *Journal of the American College of Cardiology*, vol. 67, no. 12, pp. 1412–1422, 2016.
- [55] M. Banovic, V.-T. Bosiljka, B. Voin et al., "Prognostic value of coronary flow reserve in asymptomatic moderate or severe aortic stenosis with preserved ejection fraction and non-obstructed coronary arteries," *Echocardiography*, vol. 31, no. 4, pp. 428–433, 2014.
- [56] K. Singh, A. S. Bhalla, M. A. Qutub, K. Carson, and M. Labinaz, "Systematic review and meta-analysis to compare outcomes between intermediate- and high-risk patients undergoing transcatheter aortic valve implantation," *European Heart Journal-Quality of Care and Clinical Outcomes*, vol. 3, no. 4, pp. 289–295, 2017.
- [57] T. Nishi, H. Kitahara, Y. Saito et al., "Invasive assessment of microvascular function in patients with valvular heart disease," *Coronary Artery Disease*, vol. 29, no. 3, pp. 223–229, 2018.
- [58] H. Arashi, J. Yamaguchi, T. Ri et al., "Evaluation of the cut-off value for the instantaneous wave-free ratio of patients with aortic valve stenosis," *Cardiovascular Intervention and Therapeutics*, vol. 34, no. 3, pp. 269–274, 2019.
- [59] N. Hussain, W. Chaudhry, A. W. Ahlberg et al., "An assessment of the safety, hemodynamic response, and diagnostic accuracy of commonly used vasodilator stressors in patients with severe aortic stenosis," *Journal of Nuclear Cardiology*, vol. 24, no. 4, pp. 1200–1213, 2017.
- [60] M. Banovic, B. Lung, V. Brkovic et al., "Silent coronary artery disease in asymptomatic patients with severe aortic stenosis and normal exercise testing," *Coronary Artery Disease*, vol. 31, no. 2, pp. 166–173, 2020.
- [61] P. C. Cremer, S. Khalaf, J. Lou, L. Rodriguez, M. D. Cerqueira, and W. A. Jaber, "Stress positron emission tomography is safe and can guide coronary revascularization in high-risk patients being considered for transcatheter aortic valve replacement," *Journal of Nuclear Cardiology*, vol. 21, no. 5, pp. 1001–1010, 2014.
- [62] W. Aarnoudse, W. F. Fearon, G. Manoharan et al., "Epicardial stenosis severity does not affect minimal microcirculatory resistance," *Circulation*, vol. 110, no. 15, pp. 2137–2142, 2004.
- [63] B.-J. Verhoeff, T. P. van de Hoef, J. A. E. Spaan, J. J. Piek, and M. Siebes, "Minimal effect of collateral flow on coronary microvascular resistance in the presence of intermediate and noncritical coronary stenoses," *American Journal of Physiology-Heart and Circulatory Physiology*, vol. 303, no. 4, pp. H422–H428, 2012.
- [64] S. Fournier, I. Colaïori, G. Di Gioia, T. Mizukami, and B. De Bruyne, "Hyperemic pressure-flow relationship in a human," *Journal of the American College of Cardiology*, vol. 73, no. 10, pp. 1229–1230, 2019.
- [65] S. S. Goel, M. Ige, E. M. Tuzcu et al., "Severe aortic stenosis and coronary artery disease-implications for management in the transcatheter aortic valve replacement era," *Journal of the American College of Cardiology*, vol. 62, no. 1, pp. 1–10, 2013.
- [66] M. Lunardi, R. Scarsini, G. Venturi et al., "Physiological versus angiographic guidance for myocardial revascularization in patients undergoing transcatheter aortic valve implantation," *Journal of the American Heart Association*, vol. 8, no. 22, Article ID e012618, 2019.
- [67] K. L. Gould, "Pressure-flow characteristics of coronary stenoses in unsedated dogs at rest and during coronary vasodilation," *Circulation Research*, vol. 43, no. 2, pp. 242–253, 1978.
- [68] J. M. Zelis, P. A. L. Tonino, and N. P. Johnson, "Why can fractional flow reserve decrease after transcatheter aortic valve implantation?" *Journal of the American Heart Association*, vol. 9, Article ID e04905, 2020.
- [69] R. L. Kirkeeide, K. L. Gould, and L. Parsel, "Assessment of coronary stenoses by myocardial perfusion imaging during pharmacologic coronary vasodilation. VII. validation of coronary flow reserve as a single integrated functional measure of stenosis severity reflecting all its geometric dimensions," *Journal of the American College of Cardiology*, vol. 7, no. 1, pp. 103–113, 1986.
- [70] K. Rajappan, O. E. Rimoldi, P. G. Camici, N. G. Bellenger, D. J. Pennell, and D. J. Sheridan, "Functional changes in coronary microcirculation after valve replacement in patients with aortic stenosis," *Circulation*, vol. 107, no. 25, pp. 3170–3175, 2003.
- [71] G. Pesarini, R. Scarsini, C. Zivelonghi et al., "Functional assessment of coronary artery disease in patients undergoing transcatheter aortic valve implantation: influence of pressure overload on the evaluation of lesions severity," *Circulation: Cardiovascular Interventions*, vol. 9, no. 11, Article ID e004088, 2016.
- [72] N. P. Johnson, J. M. Zelis, P. A. L. Tonino et al., "Pressure gradient vs. flow relationships to characterize the physiology of a severely stenotic aortic valve before and after transcatheter valve implantation," *European Heart Journal*, vol. 39, no. 28, pp. 2646–2655, 2018.
- [73] D.-H. Kang, S.-J. Park, S.-A. Lee et al., "Early surgery or conservative care for asymptomatic aortic stenosis," *New England Journal of Medicine*, vol. 382, no. 2, pp. 111–119, 2020.

## Research Article

# Rate Pressure Products Affect the Relationship between the Fractional Flow Reserve and Instantaneous Wave-Free Ratio

**Suguru Ebihara, Hisao Otsuki, Hiroyuki Arashi , Junichi Yamaguchi, and Nobuhisa Hagiwara**

*Department of Cardiology, The Heart Institute of Japan, Tokyo Women's Medical University, Tokyo, Japan*

Correspondence should be addressed to Hiroyuki Arashi; [arashi.hiroyuki@twmu.ac.jp](mailto:arashi.hiroyuki@twmu.ac.jp)

Received 7 April 2020; Accepted 29 June 2020; Published 22 July 2020

Guest Editor: William Fearon

Copyright © 2020 Suguru Ebihara et al. This is an open access article distributed under the Creative Commons Attribution License, which permits unrestricted use, distribution, and reproduction in any medium, provided the original work is properly cited.

The rate pressure product (RPP) is an index of myocardial metabolism that correlates closely with myocardial hemodynamics. The relationship between the RPP and the fractional flow reserve (FFR) and instantaneous wave-free ratio (iFR) is not known. In this study, we investigated the effects of the RPP on the FFR and iFR. We retrospectively enrolled 195 patients (259 lesions) who had undergone invasive coronary angiography and both the iFR and FFR examinations between 2012 and 2017. The RPP was defined as systolic blood pressure multiplied by the heart rate, measured prior to the iFR evaluation. The study population was divided into the low-RPP ( $n = 129$ , mean RPP:  $6981 \pm 1149$ ) and high-RPP ( $n = 130$ , mean RPP:  $10391 \pm 1603$ ) groups according to the median RPP. Correlations and biases between the iFR and FFR were compared. The diagnostic performance of the iFR in the groups was calculated, using FFR as the gold standard. The correlation between the iFR and FFR was higher in the high-RPP group than in the low-RPP group. The bias between the iFR and FFR in the high-RPP group was smaller than that in the low-RPP group. The best cutoff value of the iFR for predicting an FFR of 0.8 was 0.90 for all lesions, 0.93 for the low-RPP group, and 0.82 for the high-RPP group. The iFR and RPP showed a weak but a statistically significant negative correlation ( $R = 0.14$ ;  $p = 0.029$ ). This was not observed for the relationship between the FFR and RPP. In conclusion, the RPP affects the relationship between the FFR and iFR. With FFR as the gold standard, the iFR may underestimate and overestimate the functionality of ischemia in the low- and high-RPP groups, respectively.

## 1. Introduction

Several studies have shown that reducing myocardial ischemia with coronary artery intervention improves both quality of life and clinical outcomes [1, 2]. The fractional flow reserve (FFR) is a hyperemic pressure-derived ratio that is considered the reference standard method for evaluating the functional severity of coronary artery stenosis based on substantial clinical outcome data [3–5]. The instantaneous wave-free ratio (iFR) is a nonhyperemic pressure-derived ratio; randomized controlled trials have demonstrated that the iFR-guided revascularization is not inferior to FFR-guided revascularization [6, 7].

The FFR and iFR correlate well and are similar coronary functional indexes, although they differ in some respects;

specifically, FFR is calculated by the pressure ratio during the entire cardiac cycle period under hyperemia, while the iFR is calculated by the pressure ratio during the diastolic cardiac cycle under resting conditions. The rate pressure product (RPP) is calculated as systolic blood pressure multiplied by the heart rate, which is an index of myocardial metabolism that is closely correlated with myocardial hemodynamics [8]. Previous reports suggested that the coronary blood flow at resting condition was easily affected by the fluctuation in blood pressure or heart rate, but the coronary blood flow under hyperemia was not [9, 10]. No studies, to date, have reported on the effects of the RPP on the relationship between the FFR and iFR. Therefore, the aim of this study was to evaluate the effects of the RPP on the FFR and iFR relationship. We also determined how the diagnostic

performance of the iFR is affected by the RPP when FFR is set as the gold standard.

## 2. Materials and Methods

**2.1. Patient Population.** In this study, we enrolled patients who had undergone clinically indicated invasive coronary angiography as well as both the iFR and FFR examinations between 2012 and 2017. Because we examined how the RPP affect the relationship between the FFR and iFR, we limited our analysis to patients who had undergone blood pressure and heart rate measurements just prior to the iFR and FFR evaluations. It is difficult to accurately assess the RPP in patients with atrial fibrillation. We, therefore, excluded patients who had had atrial fibrillation. Hemodialysis patients characteristically exhibit specific hemodynamic conditions; therefore, such patients were excluded. We also excluded patients with lesions in the left main trunk and those with bypass grafts. Finally, we excluded patients with ST segment elevation myocardial infarction, non-ST-segment elevation myocardial infarction, or New York Heart Association class IV heart failure. We included the patients with unstable angina pectoris, but the stenoses interrogated were the nonculprit lesions.

**2.2. Measurement of Rate Pressure Products.** The RPP was defined as the systolic blood pressure multiplied by the heart rate. Blood pressure and heart rate measurements taken just prior to the iFR measurement were used for the calculation. Blood pressure data were extracted from hemodynamic records taken during cardiac catheterization and had been measured using either invasive monitoring of the arterial catheter or a sphygmomanometer. Heart rate was recorded from the electrocardiography monitor or the oxygen saturation monitor. We divided lesions into two groups based on whether the RPP just prior to the iFR measurement for each lesion was greater or lesser than the median RPP; thus, patients in the low- and high-RPP groups had lesions with the RPP  $<8512$  and  $\geq 8512$ , respectively. Lesion characteristics were compared between the groups as were the correlations and biases between the FFR and iFR.

**2.3. Coronary Angiography, Quantitative Coronary Angiography, and Echocardiography.** Coronary angiography was performed according to standard clinical methods via the radial or femoral arterial approach. Quantitative coronary angiography (QCA) was performed by an independent physician using a computer-assisted automated edge detection algorithm [11]; the physician was blinded to the results of the iFR and FFR. The external diameter of the contrast-filled catheter (5-Fr or 6-Fr) was used as the calibration standard. The percentage of the stenosis diameter during end-diastole was measured using the worst-view trace. Echocardiography measurements were performed according to American Society of Echocardiography guidelines by an independent physician who was blinded to the results of the FFR and iFR. The left ventricular mass index and  $E/e'$  ratio were added to the analysis.

**2.4. Standard iFR and FFR Measurements.** Both the iFR and FFR examinations were performed using either diagnostic or interventional guiding catheters. After administering an intracoronary bolus of nitroglycerin, a coronary pressure wire (Prime Wire Prestige; Philips Volcano Corporation, San Diego, CA, USA) was calibrated outside of the body and advanced such that the sensor was positioned at the tip of the guiding catheter where the two pressures were equalized and recorded. After completion of the pressure equalization at the tip of the guide catheter, the guidewire was advanced to a point distal to the stenosis. First, the iFR was directly and automatically measured online using the Volcano Core system (Philips Volcano). Second, the FFR was measured during maximal hyperemia. Hyperemia in the target coronary artery was achieved either with an intracoronary bolus injection of 8–12 mg papaverine or with continuous intravenous administration of adenosine at  $150 \mu\text{g}/\text{kg}/\text{min}$ . At the end of each measurement, the pressure sensor was retracted to the tip of the guide catheter to avoid pressure drift.

**2.5. Statistical Analysis.** Continuous data were expressed as means  $\pm$  standard deviations. Categorical data were expressed as absolute values and percentages. The comparisons were made using Welch's *t*-test for normally distributed continuous variables, the Mann–Whitney *U* test for nonnormally distributed continuous variables, and Pearson's chi-squared test for categorical variables. Correlations between parameters were tested using Pearson's correlation coefficients. Fisher's *r*-to-*z* transformation was used to assess the significance of the difference between two correlation coefficients. Bland–Altman analysis was conducted to evaluate the bias and limits of agreement between each parameter. ROC curves were used to evaluate the diagnostic performance of the iFR when identifying a positive FFR measurement using the area under the curve (AUC). Multivariable regression analysis was performed to determine predictors of the FFR and iFR. Variables were included in the multivariable model if they reached  $p < 0.20$  after univariable regression analysis. *p* values  $< 0.05$  were considered to indicate statistical significance. Statistical analyses were performed using JMP statistical software (JMP Pro 14.0; SAS Institute Inc., Cary, NC, USA).

**2.6. Compliance with Ethical Standards.** The study protocol was based on the regulations of the hospital's ethics committee. All participating patients provided written informed consent. The study was conducted according to the principles of the 1975 Declaration of Helsinki.

## 3. Results

We enrolled 195 consecutive patients with 259 lesions in this study. The study patient characteristics are shown in Table 1. The mean patient age was  $68.8 \pm 10.4$  years; 57.9% of patients had diabetes mellitus, 72.3% had hypertension, and 67.2% had hypercholesterolemia. The mean left ventricular ejection fraction was 51.3%, and the mean glomerular filtration rate was  $60.4 \text{ mL}/\text{min}/1.73 \text{ m}^2$ .

TABLE 1: Patients' characteristics.

Patients' variables	n = 195
Age	68.8 ± 10.4
Men	45 (23.1%)
Body mass index (kg/m <sup>2</sup> )	23.9 ± 3.5
Diabetes mellitus	113 (57.9%)
Hypertension	141 (72.3%)
Hyperlipidemia	131 (67.2%)
Smoking	69 (35.4%)
Prior myocardial infarction	58 (29.7%)
Revascularization	105 (53.8%)
Left ventricular ejection fraction (%)	51.3 ± 9.7
Chronic kidney disease (>stage II)	102 (52.3%)
Glomerular filtration rate (mL/min/1.73 m <sup>2</sup> )	60.4 ± 16.4

\*Data are expressed as mean ± standard deviation or as number (percentage).

The median RPP was 8512 (interquartile range: 7200, 10220) (Supplemental Figure 1). A total of 129 (49.8%) lesions were classified as belonging to the low-RPP group (mean RPP: 6981 ± 1149) and 130 (50.2%) to the high-RPP group (mean RPP: 10391 ± 1603) according to the median RPP. Lesion characteristics of the low-RPP and high-RPP groups are shown in Table 2.

In comparison with the lesions in the low-RPP group, the lesions in the high-RPP group tended to be in older patients, females, nonsmokers, and patients with a history of myocardial infarction. The E/e' ratio in the high-RPP group was higher than that in the low-RPP group (14.1 ± 6.4 vs. 12.5 ± 4.5, respectively,  $p = 0.045$ ). No significant difference was observed in the QCA parameters.

The correlation between the FFR and iFR in the high-RPP group was significantly higher than that of the low-RPP group (Pearson's correlation:  $r = 0.82$  vs.  $r = 0.63$ , respectively,  $z = 3.3$ ,  $p = 0.001$ , Figure 1).

According to Bland-Altman analysis, the bias between the FFR and iFR in the high-RPP group was 0.058 (95% confidence interval (CI): 0.042–0.074) and that of the low-RPP group was 0.097 (95% CI: 0.079–0.115) (Figure 2).

The best cutoff value of the iFR for predicting an FFR of 0.80 was 0.90 for all lesions (AUC 0.79, sensitivity 0.74, specificity 0.67, and  $p < 0.0001$ ), with 0.93 for the low-RPP group (AUC 0.83, sensitivity 0.87, specificity 0.62, and  $p < 0.0001$ ), and 0.82 for the high-RPP group (AUC 0.79, sensitivity 0.57, specificity 0.93, and  $p < 0.0001$ ) (Figure 3) (Supplemental Figure 2).

Using the current iFR cutoff values of  $\leq 0.89$ , 26.4% of lesions in the low-RPP group would be underestimated, while 16.9% of lesions in the high-RPP group would be overestimated (Supplemental Figure 3).

Though there was no significant correlation between the RPP and FFR, the RPP and iFR showed a weak but significant inverse correlation (Pearson's correlation:  $r = 0.14$ ;  $p = 0.029$ ) (Figure 4).

Table 3 shows the variables which were associated with the iFR or FFR. In the univariable analysis, female sex ( $p = 0.11$ ) and the presence of diabetes mellitus ( $p = 0.04$ ) were potential predictors of FFR. The age ( $p = 0.02$ ),

presence of diabetes mellitus ( $p < 0.0001$ ), prior revascularization ( $p = 0.05$ ), left ventricular mass index ( $p = 0.19$ ), E/e' ( $p = 0.01$ ), glomerular filtration rate ( $p = 0.01$ ), and RPP ( $p = 0.04$ ) were potential predictors of the iFR. Presence of diabetes mellitus was the independent predictor of FFR in multivariable analysis ( $p = 0.04$ ;  $\beta = 0.13$ ). The presence of diabetes mellitus ( $p = 0.002$ ;  $\beta = 0.23$ ) and the RPP ( $p = 0.04$ ;  $\beta = -0.15$ ) were independent predictors of the iFR.

The best cutoff value of the RPP to predict discordance of the iFR  $\leq 0.89$  and FFR  $> 0.8$  was 10950 and 6572 for discordance of the iFR  $> 0.89$  and FFR  $\leq 0.8$  (Figure 5).

#### 4. Discussion

The RPP is an index that reflects myocardial metabolism and greatly affects the hemodynamics of the heart [8], suggesting that coronary artery pressure-derived indexes could be influenced by the RPP. No previous study has reported the influence of the RPP on the relationship between the FFR and iFR.

The primary findings in the present study were as follows: (1) the correlation between the FFR and iFR in the high-RPP group was higher than that of the low-RPP group; (2) the best cutoff value of the iFR for predicting an FFR of 0.8 was 0.90 for all lesions, 0.93 for the low-RPP group, and 0.82 for the high-RPP group; and (3) the iFR and RPP showed a weak but a statistically significant negative correlation. No similar result was found for the FFR and RPP. Moreover, multivariable analysis revealed that the RPP was independently associated with the iFR.

The reason for the higher correlation between the iFR and FFR in the high-RPP group might be that the oxygen consumption of the myocardium was increased, resulting in increased coronary blood flow to maintain the oxygen supply in the high-RPP group. If one simply considers the amount of blood flow in the coronary arteries, coronary blood flow under resting conditions in the high-RPP group may increase and be closer to that of the hyperemic condition. Hence, the correlation between the iFR and FFR in the high-RPP group is likely to be increased. The question remains as to whether FFR would be affected in a high-RPP environment. A previous study reported that coronary blood flow under hyperemia did not correlate with the RPP, while coronary blood flow under resting conditions had a significant positive correlation with the RPP [9]. Similarly, although we did not observe a significant correlation between the RPP and FFR, the RPP and iFR showed a weak but a significant negative correlation. de Bruyne et al. reported that the FFR was almost independent of hemodynamic changes including heart rate and blood pressure [10]. Kollit et al. reported that fluctuations in the heart rate had no significant influence on the measured values of FFR in a porcine model [12]. By contrast, a study reported that hyperemic coronary flow decreased, and resting coronary flow was maintained in an environment where coronary circulation compensated for microvascular resistance [13]. However, if the FFR is measured when the coronary microcirculation is optimally dilated using the correct method



TABLE 2: Lesion characteristics divided by the median of the rate pressure products.

	Low-RPP group ( <i>n</i> = 129)	High-RPP group ( <i>n</i> = 130)	<i>p</i> value
Age	67.8 ± 11.4	70.8 ± 9.0	0.02
Female	23 (17.8%)	40 (30.8%)	0.02
Body mass index (kg/m <sup>2</sup> )	23.7 ± 3.8	23.9 ± 3.6	0.74
Diabetes mellitus	68 (52.7%)	83 (63.9%)	0.08
Hypertension	92 (71.3%)	98 (75.4%)	0.48
Hyperlipidemia	95 (73.6%)	83 (63.9%)	0.11
Smoking	59 (45.7%)	37 (28.5%)	0.005
Prior myocardial infarction	33 (25.6%)	49 (37.7%)	0.045
Revascularization	78 (60.5%)	68 (52.3%)	0.21
LVEF (%)	49.9 ± 10.6	51.9 ± 8.7	0.10
LVMI (g/m <sup>2</sup> )	98.7 ± 29.8	91.5 ± 30.6	0.11
<i>E/e'</i>	12.5 ± 4.5	14.1 ± 6.4	0.048
Chronic kidney disease (>stage II)	69 (53.5%)	71 (54.6%)	0.9
GFR (mL/min/1.73 m <sup>2</sup> )	60.9 ± 17.1	58.0 ± 17.2	0.18
Percent diameter stenosis	63.6 ± 17.4	63.0 ± 18.3	0.77
Left anterior descending artery	78 (60.5%)	69 (53.1%)	0.26
Circumflex artery	24 (18.6%)	30 (23.1%)	0.44
Right coronary artery	27 (20.9%)	31 (23.9%)	0.66
FFR	0.77 ± 0.11	0.78 ± 0.12	0.51
iFR	0.87 ± 0.13	0.84 ± 0.16	0.09
Percent diameter stenosis	64 ± 17	63 ± 18	0.77
Lesion diameter (mm)	17.7 ± 6.9	18.5 ± 6.9	0.32
Reference diameter (mm)	2.7 ± 0.5	2.6 ± 0.5	0.06
Diffuse/tandem lesion	37 (28.7%)	37 (28.7%)	0.89
Rate pressure products	6981 ± 123	10392 ± 122	<0.0001
Systolic blood pressure (mmHg)	111 ± 19.0	138 ± 19.9	<0.0001
Heart rate (beats/minute)	63.3 ± 8.4	76.0 ± 12.2	<0.0001

RPP, rate pressure products; LVEF, left ventricular ejection fraction; LVMI, left ventricular mass index; GFR, glomerular filtration rate; FFR, fractional flow reserve; iFR, instantaneous wave-free ratio. \*Data are expressed as mean ± standard deviation or as number (percentage).

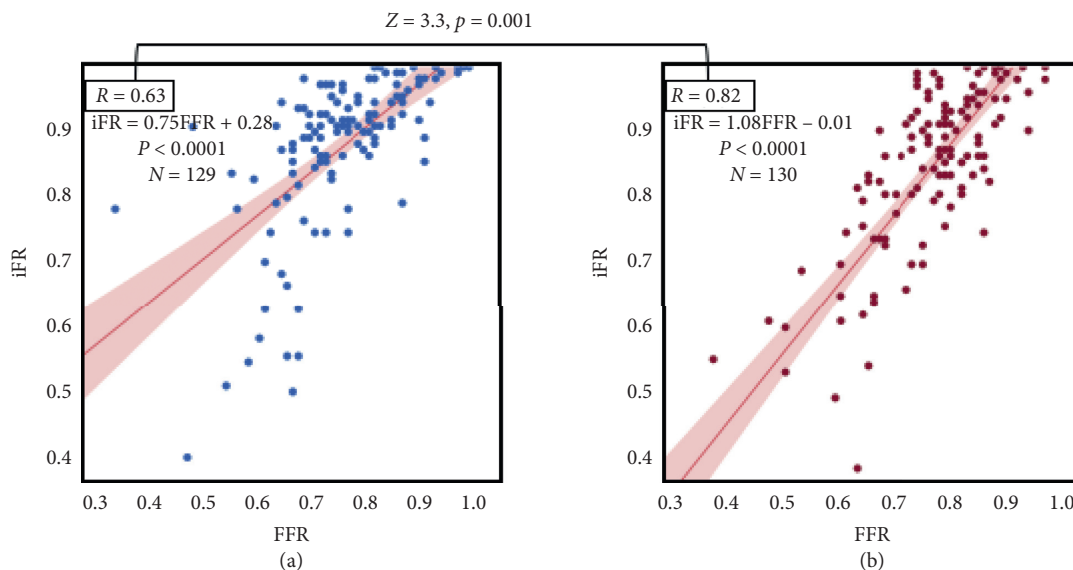


FIGURE 1: Scatter plots of the FFR and iFR in the low-RPP group (a) and the high-RPP group (b). RPP, rate pressure product; iFR, instantaneous wave-free ratio; FFR, fractional flow reserve.

and correct hyperemic agent, the FFR value might not be affected by the RPP value.

As regards the patient characteristics in our study, a total of 58% patients had diabetes mellitus, which is an important covariate for microvascular dysfunction. There are also

numerous reports which have suggested that the higher left ventricular mass index and higher *E/e'* ratio are associated with microvascular dysfunction [14, 15]. When adding the variables including the presence of diabetes mellitus, left ventricular mass index, and *E/e'* ratio to the multivariable



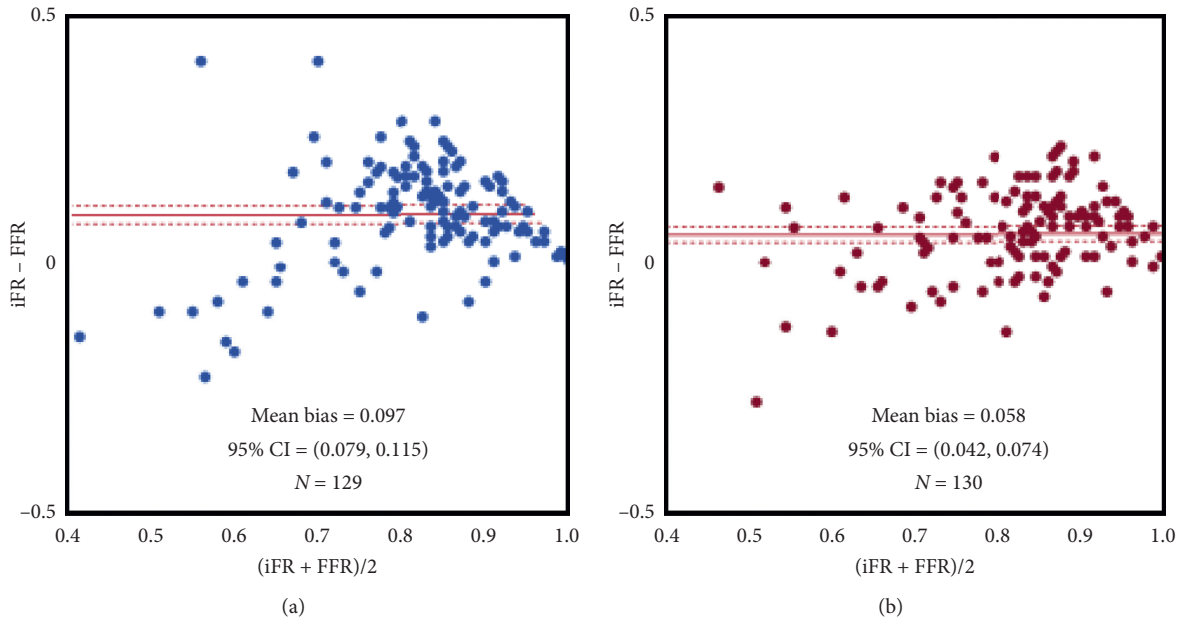


FIGURE 2: Bland–Altman plot comparing the FFR and iFR in the low-RPP group (a) and the high-RPP group (b). RPP, rate pressure products; iFR, instantaneous wave-free ratio; FFR, fractional flow reserve.

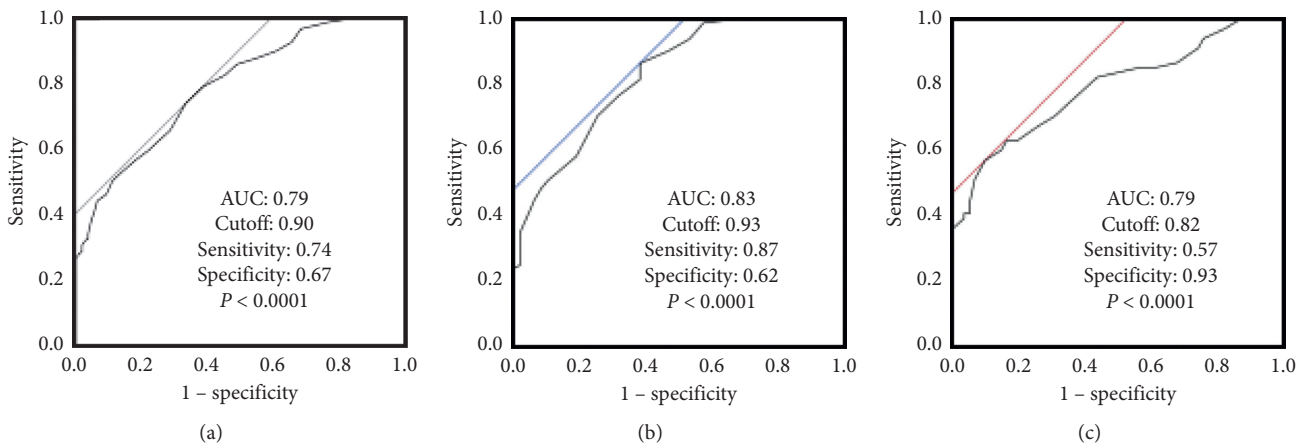


FIGURE 3: Receiver-operating characteristic curves of the iFR values for an FFR of 0.8 in all lesions (a), the low-RPP group (b), and high-RPP group (c). RPP, rate pressure products; AUC, area under the curve.

analysis to clarify the predictor of the iFR, the RPP was independently associated with the iFR. These data suggest that the iFR might be affected by the RPP regardless of microvascular dysfunction.

In this study, the best cutoff value of the iFR for predicting an FFR of 0.8 was 0.90 for all lesions. This value agrees with previously reported values. The best cutoff value for the low-RPP group was 0.93, higher than the standard predictive value of the iFR. The best cutoff value for the high-RPP group was 0.82, lower than the standard predictive value of the iFR. When using the corrected iFR cutoff values of  $\leq 0.93$  for the low-RPP group and  $\leq 0.82$  for the high-RPP group, a total of 23 (17.8%) lesions should be reclassified as “ischemic” in the low-RPP group and a total of 16 (12.3 %) lesions should be reclassified as “nonischemic” in the high-RPP group.

The FFR has hemodynamic independence through dilating and maximizing the coronary microcirculation in hyperemia. The iFR value is sensitive to the RPP fluctuations, while the FFR is less susceptible to the RPP fluctuations. Jain et al. reported that mental stress increased the RPP [16]. In this study, the stressful condition may have the greatest effect on the RPP value because the comorbidity of hypertension did not change between the high-RPP group and the low-RPP group. When examining the iFR, it may also be necessary to make this as stress-free as possible. Then, the difference between low- vs. high-RPP is more likely associated with patient hemodynamics at the time of physiologic assessment, further suggesting the stability of hyperemic measurements as opposed to resting measurements. Even if the iFR is positive, there is a possibility of false positive if the

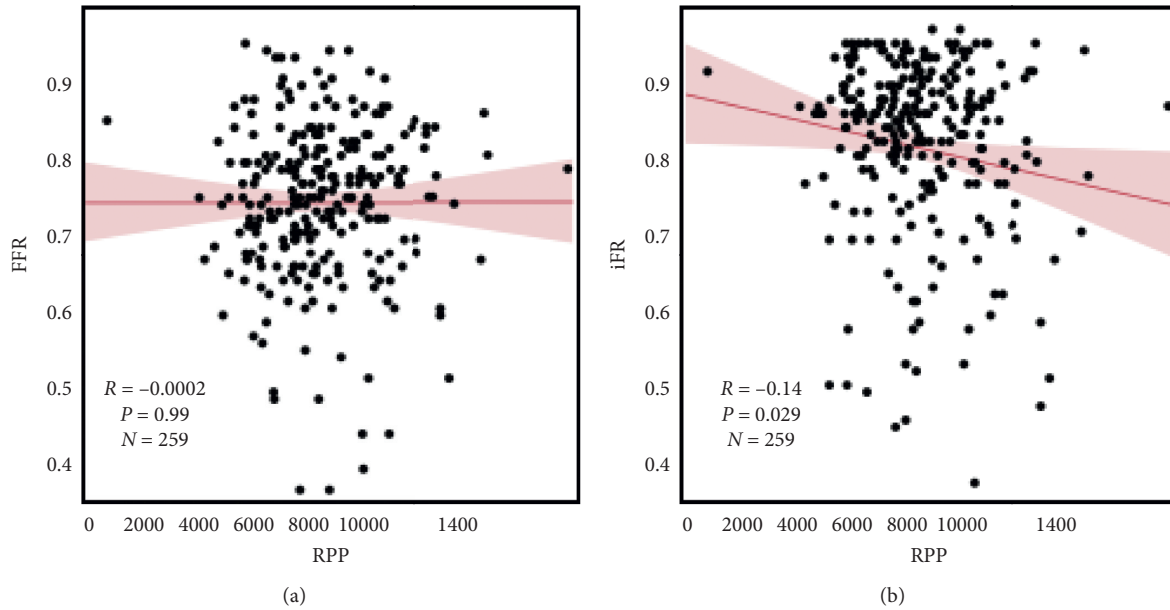


FIGURE 4: Scatter plots comparing the RPP with the FFR (a) and iFR (b). RPP, rate pressure products; iFR, instantaneous wave-free ratio; FFR, fractional flow reserve.

TABLE 3: The variables associated with the FFR and iFR.

	FFR				iFR			
	Univariable		Multivariable		Univariable		Multivariable	
	$\beta$	<i>p</i> value	$\beta$	<i>p</i> value	$\beta$	<i>p</i> value	$\beta$	<i>p</i> value
Age	0.04	0.52			-0.15	0.02	-0.01	0.87
Female	-0.1	0.11	-0.1	0.12	0.03	0.59		
Body mass index	-0.07	0.25			0.02	0.77		
Diabetes mellitus	0.13	0.04	0.13	0.04	0.24	<0.0001	0.23	0.002
Hypertension	0.005	0.94			0.02	0.7		
Dyslipidemia	0.03	0.61			-0.07	0.24		
Smoking	0.07	0.28			-0.05	0.47		
Prior myocardial infarction	-0.04	0.50			0.02	0.77		
Prior revascularization	-0.07	0.29			-0.12	0.05	-0.1	0.21
LVEF	0.02	0.79			0.04	0.52		
LVMI	-0.04	0.60			-0.1	0.19	-0.06	0.49
<i>E/e'</i>	-0.07	0.35			-0.18	0.01	-0.05	0.58
GFR	0.08	0.21			0.16	0.01	0.13	0.13
Rate pressure products	-0.001	0.99			-0.14	0.03	-0.15	0.04

LVEF, left ventricular ejection fraction; LVMI, left ventricular mass index; GFR, glomerular filtration rate; FFR, fractional flow reserve; iFR, instantaneous wave-free ratio.

RPP is 10950 or more at the time of the iFR measurement. Further, if the iFR is negative, there is a possibility of false negative if the RPP is 6572 or less at the time of the iFR measurement. Additional studies with a prospective study design and larger numbers of patients are necessary to validate the relation between the rate pressure products and iFR and FFR.

There are several limitations to this study. First, this was a retrospective observational cohort study conducted at a single center, and the number of study patients was relatively small. Second, there were no data on the changes in the iFR values at rest and during exercise in the same patients, and there were also no data on the clinical

endpoints. Third, the prevalence of diabetes mellitus and hypertension was higher than those of previous studies. These comorbidities induce structural changes in the myocardium and reduce coronary capacity, possibly influencing the relationship between the iFR and FFR. Fourth, analyses vary depending on which indicator is considered the gold standard. There is, however, abundant evidence in favor of using the FFR, and it is currently the most reliable index recommended in the guidelines. Furthermore, the FFR has customarily been the benchmark for evaluating other nonhyperemic indices. Fifth, there are no data on medication (i.e., calcium-channel blocker and beta-blocker), which might influence the results.

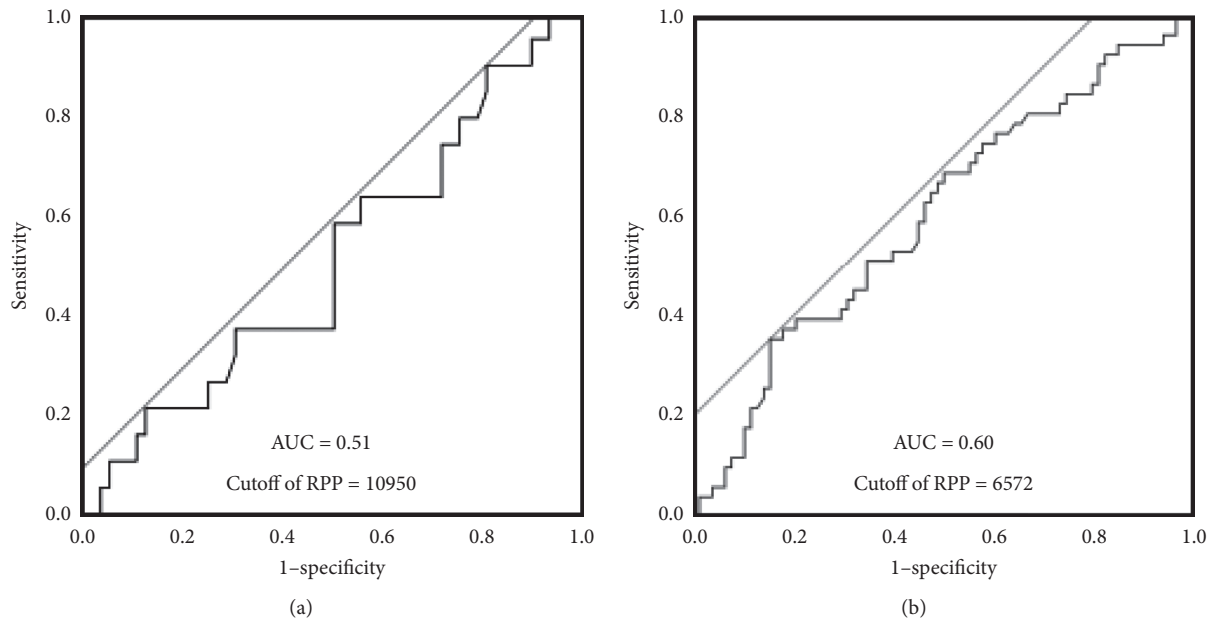


FIGURE 5: The best cutoff value of rate pressure products to predict discordance of the  $iFR \leq 0.89$  and  $FFR > 0.8$  (a) and discordance of the  $iFR > 0.89$  and  $FFR \leq 0.8$  (b). RPP, rate pressure products;  $iFR$ , instantaneous wave-free ratio; FFR, fractional flow reserve.

## 5. Conclusion

Rate pressure products may affect the relationship between the FFR and  $iFR$ . Setting FFR as the reference gold standard, the  $iFR$  may underestimate the functionality of ischemia in the low-RPP group and overestimate it in the high-RPP group.

## Data Availability

Clinical data used to support the findings of this study are restricted by the Tokyo Women's Medical University (TWMU) Ethics Committee in order to protect patient privacy. Data are available from the clinical research support center TWMU for researchers who meet the criteria for access to confidential data. Researchers can contact the corresponding author by e-mail.

## Conflicts of Interest

Arashi has received lecture fees from Abbot Vascular, Philips Volcano, and Boston Scientific. Yamaguchi reports that he is associated with a division (Clinical Research Division for Cardiovascular Catheter Intervention) financially maintained by donations from Abbott Vascular and Boston Scientific. No other authors have relationships relevant to the contents of this paper to disclose. This study does not have any relationship with industry.

## Authors' Contributions

SE and HO collected data and enrolled patients. SE, HO, and HA analyzed and wrote the manuscript. JY and NH reviewed the manuscript. HA conceptualized and designed the study. All authors have approved the final article.

## Acknowledgments

The authors would like to thank all staff including cardiology nurses, radiology technicians, and medical engineering technologists for their continuous and warm support. Moreover, the authors thank Midori Yasuoka who undertook the administrative tasks of their catheter laboratory team. The authors wish to thank Editage (<http://www.editage.com>) for English language editing and publication support.

## Supplementary Materials

Supplemental Figure 1: distribution of the rate pressure products. Supplemental Figure 2: diagnostic ability of the  $iFR$  in the high-RPP and low-RPP groups with respect to the FFR. Supplemental Figure 3: correlation between the FFR and  $iFR$  in the high-RPP and low-RPP groups. (*Supplementary Materials*)

## References

- [1] R. Hachamovitch, S. W. Hayes, J. D. Friedman, I. Cohen, and D. S. Berman, "Comparison of the short-term survival benefit associated with revascularization compared with medical therapy in patients with no prior coronary artery disease undergoing stress myocardial perfusion single photon emission computed tomography," *Circulation*, vol. 107, no. 23, pp. 2900–2907, 2003.
- [2] L. J. Shaw, D. S. Berman, D. J. Maron et al., "Optimal medical therapy with or without percutaneous coronary intervention to reduce ischemic burden: results from the Clinical Outcomes Utilizing Revascularization and Aggressive Drug Evaluation (COURAGE) trial nuclear substudy," *Circulation*, vol. 117, no. 10, pp. 1283–1291, 2008.

- [3] P. A. L. Tonino, B. De Bruyne, N. H. J. Pijls et al., "Fractional flow reserve versus angiography for guiding percutaneous coronary intervention," *New England Journal of Medicine*, vol. 360, no. 3, pp. 213–224, 2009.
- [4] B. De Bruyne, N. H. J. Pijls, B. Kalesan et al., "Fractional flow reserve-guided PCI versus medical therapy in stable coronary disease," *New England Journal of Medicine*, vol. 367, no. 11, pp. 991–1001, 2012.
- [5] B. De Bruyne, W. F. Fearon, N. H. J. Pijls et al., "Fractional flow reserve-guided PCI for stable coronary artery disease," *New England Journal of Medicine*, vol. 371, no. 13, pp. 1208–1217, 2014.
- [6] J. E. Davies, S. Sen, H. M. Dehbi et al., "Use of the instantaneous wave-free ratio or fractional flow reserve in PCI," *The New England Journal of Medicine*, vol. 376, no. 19, pp. 1824–1834, 2017.
- [7] M. Götberg, E. H. Christiansen, I. J. Gudmundsdottir et al., "Instantaneous wave-free ratio versus fractional flow reserve to guide PCI," *New England Journal of Medicine*, vol. 376, no. 19, pp. 1813–1823, 2017.
- [8] F. L. Gobel, L. A. Norstrom, R. R. Nelson, C. R. Jorgensen, and Y. Wang, "The rate pressure product as an index of myocardial oxygen consumption during exercise in patients with angina pectoris," *Circulation*, vol. 57, no. 3, pp. 549–556, 1978.
- [9] J. Czernin, P. Müller, S. Chan et al., "Influence of age and hemodynamics on myocardial blood flow and flow reserve," *Circulation*, vol. 88, no. 1, pp. 62–69, 1993.
- [10] B. de Bruyne, J. Bartunek, S. U. Sys, N. H. J. Pijls, G. R. Heyndrickx, and W. Wijns, "Simultaneous coronary pressure and flow velocity measurements in humans," *Circulation*, vol. 94, no. 8, pp. 1842–1849, 1996.
- [11] N. Suzuki, T. Asano, G. Nakazawa et al., "Clinical expert consensus document on quantitative coronary angiography from the Japanese Association of Cardiovascular Intervention and Therapeutics," *Cardiovascular Intervention and Therapeutics*, vol. 35, no. 2, pp. 105–116, 2020.
- [12] K. K. Kolli, R. K. Banerjee, S. V. Peelukhana et al., "Influence of heart rate on fractional flow reserve, pressure drop coefficient, and lesion flow coefficient for epicardial coronary stenosis in a porcine model," *American Journal of Physiology-Heart and Circulatory Physiology*, vol. 300, no. 1, pp. H382–H387, 2011.
- [13] S. S. Nijjer, G. A. de Waard, S. Sen et al., "Coronary pressure and flow relationships in humans: phasic analysis of normal and pathological vessels and the implications for stenosis assessment: a report from the Iberian-Dutch-English (IDEAL) collaborators," *European Heart Journal*, vol. 37, no. 26, pp. 2069–2080, 2016.
- [14] V. R. Taqueti, S. D. Solomon, A. M. Shah et al., "Coronary microvascular dysfunction and future risk of heart failure with preserved ejection fraction," *European Heart Journal*, vol. 39, no. 10, pp. 840–849, 2018.
- [15] H. Arashi, J. Yamaguchi, T. Ri et al., "The impact of tissue Doppler index E/e' ratio on instantaneous wave-free ratio," *Journal of Cardiology*, vol. 71, no. 3, pp. 237–243, 2018.
- [16] D. Jain, S. M. Shaker, M. Burg, F. J. T. Wackers, R. Soufer, and B. L. Zaret, "Effects of mental stress on left ventricular and peripheral vascular performance in patients with coronary artery disease," *Journal of the American College of Cardiology*, vol. 31, no. 6, pp. 1314–1322, 1998.